Sensitivity analysis of the dynamic response of floating wind turbines

Rouzbeh Siavashi

Submission date: June 2018

Supervisor: Finn Gunnar Nielsen, UiB

Co-supervisor: Mostafa Bakhoday Paskyabi, NERSC

Joachim Reuder, UiB

Geophysical Institute

University of Bergen

Preface

This master thesis is a part of Master's Programme in Renewable Energy at Geophysical Institute, University of Bergen (UiB).

I would like to express my deepest appreciation to all those who provided me the possibility to complete this report. I would like to express my special gratitude and thanks to my supervisor, Professor Finn Gunnar Nielsen, and my co-supervisors, Mostafa Bakhoday Paskyabi and Joachim Reuder, whose support, guidance, stimulating suggestions and encouragement helped me a lot to coordinate my thesis.

My thanks and appreciations also go to Marte Godvik and all people who have willingly helped me out with their comments and advices and given me such attention and time.

Bergen, June 2018

Rouzbeh Siavashi

Abstract

Development of offshore wind turbines shows a clear shift from the fixed-bottom turbines to the floating turbines. The reason for such tendency is due to the fact that moving towards the deep ocean will substantially limit the feasibility of using fixed-bottom wind turbines because of several significant operational and environmental constraints. For such conditions, the floating turbine concepts, adopted from the offshore oil and gas industries, will be able to maximize the wind power extraction by increasing the structural reliability and decreasing the construction cost.

Difficulties of structural design and development in the offshore wind energy industry, due to complex nature of offshore loading and structural responses (rotating mass, mooring tension, etc.), can be substantially reduced by utilizing accurate and reliable hydro- and aerodynamic numerical models.

In this master thesis, focus is on investigating the structural responses of two spar-buoy floating offshore wind turbines, i.e. Hywind Demo (2.3 MW) and OC3-Hywind (5 MW). The dynamic responses of Hywind Demo and OC3-Hywind due to the combined action of wind and waves are numerically simulated by the computational tool SIMA (Simulation of Marine Operations).

To ensure the performance of numerical simulations in order to capture efficiently the physical behaviour of the offshore wind turbines, model simulation results are required to be verified against the available reliable structural measurements.

The numerical model of Hywind Demo has previously been compared to full scale measurements. In this master thesis to extend the previous study, by using the measured environmental and dynamic responses as a reference, a sensitivity study is performed to better understand the sensitivity of various structural responses, such as e.g. platform pitch, as function of the various environmental parameters, such as e.g. turbulence intensity.

Moreover, the same sensitivity study will be applied to OC3-Hywind to better understand of the responses of bigger wind turbine compared to the smaller one, i.e. Hywind Demo.

The results show a high sensitivity of the investigated structural responses to the wave characteristics and turbulence intensity variations. Moreover, the analyses show more sensitivity of the local structural responses than global structural responses to alpha variation in wind shear profile power law. Also, the sensitivity to spatial variation of numerical wind field has a fluctuation pattern.

Furthermore, OC3-Hywind has greater structural responses because of bigger rotor diameter and more weight than Hywind Demo.

Co-coherence of longitudinal wind velocity fluctuation (u´) shows higher correlation between nodes for lower frequency than higher frequency for one realization.

Table of Contents

CHAPTER 1 INTRODUCTION 11

1.1 PROBLEM STATEMENT 11
1.2 THESIS ORGANIZATION 12

CHAPTER 2 BACKGROUND 13

2.1 FLOATING OFFSHORE WIND TURBINE 13
2.2 HYWIND DEMO 21
2.3 OC3-HYWIND 25
2.4 COHERENCE OF THE NUMERICAL WIND FIELD 29

CHAPTER 3 METHODS 33

3.1 ENVIRONMENTAL PARAMETERS VARIATION 34
3.1.1 Wave characteristics variation 34
3.1.2 Turbulence intensity variation 35
3.1.3 Alpha variation 35
3.1.4 Spatial resolution variation 36
3.2 EVALUATED STRUCTURAL RESPONSES 37
3.2.1 Electrical power 37
3.2.2 Platform pitch 37
3.2.3 Tip out-of-plane deflection for one blade 38

CHAPTER 4 ENVIRONMENT COMPONENTS MODELING 41

4.1 ENVIRONMENT COMPONENTS 42
4.1.1 Wind 42
4.1.2 Wave 44
4.1.3 Current 45

CHAPTER 5 RESULTS 47

5.1 HYWIND DEMO RESULTS 47
5.1.1 Below-rated wind speed *47*
5.1.2 Above-rated wind speed *53*
5.2 OC3-HYWIND RESULTS 58
5.2.1 Below-rated wind speed *58*
5.2.2 Above-rated wind speed *63*
5.3 COHERENCE OF THE NUMERICAL WIND FIELD 69

CHAPTER 6 DISCUSSION 73

6.1 THE DYNAMIC RESPONSES OF THE STRUCTURES 73
6.1.1 Wave characteristics *73*
6.1.2 Turbulence intensity *77*
6.1.3 Alpha in wind shear profile power law *79*
6.1.4 Spatial resolution of the numerical wind field *83*
6.2 COHERENCE OF THE NUMERICAL WIND FIELD 85

CONCLUSION 87

RECOMMENDATIONS FOR FURTHER WORK 89

BIBLIOGRAPHY 90

APPENDIX 1 SCATTER DIAGRAM I

APPENDIX 2 COMPLETE STRUCTURAL RESPONSES I

2.1 HYWIND DEMO RESULTS I
2.1.1 Below-rated wind speed ..... *I*
2.1.2 Above-rated wind speed ..... *XIV*
2.2 OC3-HYWIND RESULTS XXVI
2.2.1 Below-rated wind speed ..... *XXVI*
2.2.2 Above-rated wind speed ..... *XXXVIII*

List of Tables

TABLE 1. MAIN SPECIFICATION OF HYWIND DEMO STRUCTURE. [19] 25
TABLE 2. CHARACTERISTIC DATA FOR THE SIEMENS WIND TURBINE. [19] 25
TABLE 3. MAIN SPECIFICATIONS OF NREL 5 MW BASELINE WIND TURBINE. [23] 26
TABLE 4. FLOATING PLATFORM STRUCTURAL PROPERTIES. [24] 27
TABLE 5. ENVIRONMENTAL CONDITIONS FOR BELOW-RATED WIND SPEED BASE CASE. [19] 33
TABLE 6. ENVIRONMENTAL CONDITIONS FOR ABOVE-RATED WIND SPEED BASE CASE. [19] 33
TABLE 7. WAVE CHARACTERISTICS CASES IN THE BELOW-RATED WIND SPEED (CASE2 IS THE BASE CASE) 34
TABLE 8. WAVE CHARACTERISTICS CASES IN THE ABOVE-RATED WIND SPEED (CASE3 IS THE BASE CASE). 34
TABLE 9. TURBULENCE INTENSITY (TI) CASES (CASE_TI2 IS THE BASE CASE). 35
TABLE 10. ALPHA A CASES (CASE_ALPHA4 IS THE BASE CASE). 36
TABLE 11. SPATIAL RESOLUTION OF THE NUMERICAL WIND FIELD CASES WHERE CASE_SP1 IS THE BASE CASE. .. 36
TABLE 12. MEAN AND STANDARD DEVIATION OF PLATFORM PITCH. 48
TABLE 13. MEAN AND STANDARD DEVIATION OF ELECTRICAL GENERATOR OUTPUT. 50
TABLE 14. MEAN AND STANDARD DEVIATION OF TIP OUT-OF-PLANE DEFLECTION OF ONE BLADE. 50
TABLE 15. MEAN AND STANDARD DEVIATION OF ELECTRICAL GENERATOR OUTPUT. 52
TABLE 16. MEAN AND STANDARD DEVIATION OF TIP OUT-OF-PLANE DEFLECTION OF ONE BLADE. 53
TABLE 17. MEAN AND STANDARD DEVIATION OF PLATFORM PITCH. 55
TABLE 18. MEAN AND STANDARD DEVIATION OF TIP OUT-OF-PLANE DEFLECTION OF ONE BLADE. 57
TABLE 19. MEAN AND STANDARD DEVIATION OF ELECTRICAL GENERATOR OUTPUT. 58
TABLE 20. MEAN AND STANDARD DEVIATION OF PLATFORM PITCH. 58
TABLE 21. MEAN AND STANDARD DEVIATION OF MECHANICAL POWER. 60
TABLE 22. MEAN AND STANDARD DEVIATION OF TIP OUT-OF-PLANE DEFLECTION OF ONE BLADE. 62
TABLE 23. MEAN AND STANDARD DEVIATION OF MECHANICAL POWER. 62
TABLE 24. MEAN AND STANDARD DEVIATION OF TIP OUT-OF-PLANE DEFLECTION OF ONE BLADE. 65
TABLE 25. MEAN AND STANDARD DEVIATION OF PLATFORM PITCH. 66
TABLE 26. MEAN AND STANDARD DEVIATION OF TIP OUT-OF-PLANE DEFLECTION OF ONE BLADE. 67

TABLE 27. MEAN AND STANDARD DEVIATION OF MECHANICAL POWER. 69
TABLE 28. THE MAXIMUM AND MINIMUM VALUES OF THE HYWIND DEMO RESPONSES WHEN WAVE CHARACTERISTICS WERE VARIED. 74
TABLE 29. THE MAXIMUM AND MINIMUM VALUES OF THE OC3-HYWIND RESPONSES WHEN WAVE CHARACTERISTICS WERE VARIED. 74
TABLE 30. THE MAXIMUM AND MINIMUM VALUES OF THE HYWIND DEMO RESPONSES WHEN TURBULENCE INTENSITY WAS VARIED. 78
TABLE 31. THE MAXIMUM AND MINIMUM VALUES OF THE OC3-HYWIND RESPONSES WHEN TURBULENCE INTENSITY WAS VARIED. 79
TABLE 32. THE MAXIMUM AND MINIMUM VALUES OF THE HYWIND DEMO RESPONSES WHEN ALPHA WAS VARIED. 80
TABLE 33. THE MAXIMUM AND MINIMUM VALUES OF THE OC3-HYWIND RESPONSES WHEN ALPHA WAS VARIED. 80
TABLE 34. THE MAXIMUM AND MINIMUM VALUES OF THE HYWIND DEMO RESPONSES WHEN SPATIAL RESOLUTIONS WERE VARIED. 83
TABLE 35. THE MAXIMUM AND MINIMUM VALUES OF THE OC3-HYWIND RESPONSES FOR WHEN SPATIAL RESOLUTIONS WERE VARIED. 84

List of Figures

FIGURE 1. WIND TURBINE DEVELOPMENT FROM ONSHORE TOWARD DEEPER WATER. [3]..... 14
FIGURE 2. THE RELATION BETWEEN COST OF OFFSHORE WIND TURBINE SUBSTRUCTURES AND WATER DEPTH. [3] 15
FIGURE 3. OFFSHORE WIND TURBINE FOUNDATIONS FOR SHALLOW WATER. [3]..... 16
FIGURE 4. SOME FOUNDATIONS FOR TRANSITIONAL WATERS. [3]..... 17
FIGURE 5. FLOATING SUBSTRUCTURE CONCEPTS FOR DEEP WATERS. [4]..... 18
FIGURE 6. VARIOUS FLOATER CONCEPTS. [17] 19
FIGURE 7. LOADS ON AN OFFSHORE WIND TURBINE. [18] 20
FIGURE 8. THE HYWIND CONCEPT. [19]..... 22
FIGURE 9. HYWIND DEMO SCHEMATIC. [20] 23
FIGURE 10. OVERHEAD VIEW OF THE HULL AND THE MOORING SYSTEM. [20] 24
FIGURE 11. ONE MOORING LINE SCHEMATIC OF HYWIND DEMO. [20]..... 24
FIGURE 12. DIMENSIONAL COMPARISON BETWEEN HYWIND DEMO CONCEPT AND OC3-HYWIND CONCEPT. THE ILLUSTRATION IS TAKEN FROM MALHOTRA [25]. 28
FIGURE 13. THE SPATIAL RESOLUTION OF THE NUMERICAL WIND FIELD..... 36
FIGURE 14. DEGREES OF FREEDOM OF A FLOATING OFFSHORE WIND TURBINE. [5]..... 38
FIGURE 15. ILLUSTRATION OF TIP OUT-OF-PLANE DEFLECTION OF ONE BLADE. THE ILLUSTRATION IS TAKEN FROM MARINTEK [21]. 39
FIGURE 16. THE ILLUSTRATION OF THE NUMERICAL WIND FIELD. 42
FIGURE 17. AVERAGE LONGITUDINAL WIND VELOCITY FLUCTUATION (U´) FOR THE ABOVE-RATED WIND SPEED BASE CASE IN Y-Z PLANE..... 43
FIGURE 18. STD OF LONGITUDINAL WIND VELOCITY FLUCTUATION (U´) FOR THE ABOVE-RATED WIND SPEED BASE CASE ALONG Z-AXIS. 44
FIGURE 19. JONSWAP WAVE SPECTRUM USED IN THE ABOVE-RATED WIND SPEED BASE CASE. 45
FIGURE 20. MEAN AND STANDARD DEVIATION OF PLATFORM PITCH FOR DIFFERENT WAVE CHARACTERISTICS IN THE BELOW-RATED WIND SPEED. 48

FIGURE 21. MEAN AND STANDARD DEVIATION OF ELECTRICAL GENERATOR OUTPUT FOR DIFFERENT TURBULENCE INTENSITIES IN THE BELOW-RATED WIND SPEED. 49
FIGURE 22. MEAN AND STANDARD DEVIATION OF TIP OUT-OF-PLANE DEFLECTION OF ONE BLADE FOR DIFFERENT ALPHAS IN WIND SHEAR POWER LAW IN THE BELOW-RATED WIND SPEED. 51
FIGURE 23. MEAN AND STANDARD DEVIATION OF ELECTRICAL GENERATOR OUTPUT FOR DIFFERENT SPATIAL RESOLUTIONS IN THE BELOW-RATED WIND SPEED 52
FIGURE 24. MEAN AND STANDARD DEVIATION OF TIP OUT-OF-PLANE DEFLECTION OF ONE BLADE FOR DIFFERENT WAVE CHARACTERISTICS IN THE ABOVE-RATED WIND SPEED. 54
FIGURE 25. MEAN AND STANDARD DEVIATION OF PLATFORM PITCH FOR THREE TURBULENCE INTENSITIES IN ABOVE-RATED WIND SPEED. 55
FIGURE 26. MEAN AND STANDARD DEVIATION OF TIP OUT-OF-PLANE DEFLECTION OF ONE BLADE FOR DIFFERENT ALPHAS IN WIND SHEAR POWER LAW IN THE ABOVE-RATED WIND SPEED 56
FIGURE 27. MEAN AND STANDARD DEVIATION OF ELECTRICAL GENERATOR OUTPUT FOR DIFFERENT SPATIAL RESOLUTIONS IN THE ABOVE-RATED WIND SPEED. 57
FIGURE 28. MEAN AND STANDARD DEVIATION OF PLATFORM PITCH FOR DIFFERENT WAVE CHARACTERISTICS IN THE BELOW-RATED WIND SPEED. 59
FIGURE 29. MEAN AND STANDARD DEVIATION OF MECHANICAL POWER FOR DIFFERENT TURBULENCE INTENSITIES IN THE BELOW-RATED WIND SPEED. 60
FIGURE 30. MEAN AND STANDARD DEVIATION OF TIP OUT-OF-PLANE DEFLECTION OF ONE BLADE FOR DIFFERENT ALPHAS IN WIND SHEAR POWER LAW IN THE BELOW-RATED WIND SPEED. 61
FIGURE 31. MEAN AND STANDARD DEVIATION OF MECHANICAL POWER FOR DIFFERENT SPATIAL RESOLUTIONS IN THE BELOW-RATED WIND SPEED. 63
FIGURE 32. MEAN AND STANDARD DEVIATION OF TIP OUT-OF-PLANE DEFLECTION OF ONE BLADE FOR DIFFERENT WAVE CHARACTERISTICS IN THE ABOVE-RATED WIND SPEED. 64
FIGURE 33. MEAN AND STANDARD DEVIATION OF PLATFORM PITCH FOR DIFFERENT TURBULENCE INTENSITIES IN THE ABOVE-RATED WIND SPEED 66
FIGURE 34. MEAN AND STANDARD DEVIATION OF TIP OUT-OF-PLANE DEFLECTION OF ONE BLADE FOR DIFFERENT ALPHAS IN WIND SHEAR POWER LAW IN THE ABOVE-RATED WIND SPEED 67
FIGURE 35. MEAN AND STANDARD DEVIATION OF MECHANICAL POWER FOR DIFFERENT SPATIAL RESOLUTIONS IN THE ABOVE-RATED WIND SPEED 68
FIGURE 36. NUMERICAL WIND FIELD. 69
FIGURE 37. CO-COHERENCE OF LONGITUDINAL WIND VELOCITY FLUCTUATION (U´) BETWEEN EACH POINT AND MID-POINT FOR FREQUENCY OF 0.2 HZ. 70
FIGURE 38. AVERAGE CO-COHERENCE OF LONGITUDINAL WIND VELOCITY FLUCTUATION (U´) IN A RADIUS AROUND MID-NODE FOR FREQUENCY OF 0.2 HZ. 70
FIGURE 39. CO-COHERENCE OF LONGITUDINAL WIND VELOCITY FLUCTUATION (U´) BETWEEN EACH POINT AND MID-POINT FOR FREQUENCY OF 0.04 HZ. 71

FIGURE 40. AVERAGE CO-COHERENCE OF LONGITUDINAL WIND VELOCITY FLUCTUATION (U´) IN A RADIUS AROUND MID-NODE FOR FREQUENCY OF 0.04 HZ. 71
FIGURE 41. TYPICAL WIND TURBINE POWER OUTPUT CURVE. 75
FIGURE 42. THRUST FORCE ON THE HYWIND DEMO WIND TURBINE. [19] 76
FIGURE 43. THRUST FORCE ON THE 5 MW NREL BASELINE WIND TURBINE. [34] 76
FIGURE 44. MEAN BELOW- AND ABOVE-RATED WIND SPEED PROFILES WITH DIFFERENT ALPHA WITHIN SWEPT AREA OF BLADES OF HYWIND DEMO. 81
FIGURE 45. MEAN BELOW- AND ABOVE-RATED WIND SPEED PROFILES WITH DIFFERENT ALPHA WITHIN SWEPT AREA OF BLADES OF OC3-HYWIND. 81
FIGURE 46. STANDARD DEVIATION OF TIP OUT-OF-PLANE DEFLECTION OF ONE BLADE FOR VARIOUS ALPHAS FOR THE ABOVE-RATED WIND SPEED BASE CASE FOR HYWIND DEMO WITH TURBULENCE INTENSITY OF 11%. ... 82
FIGURE 47. STANDARD DEVIATION OF TIP OUT-OF-PLANE DEFLECTION OF ONE BLADE FOR VARIOUS ALPHAS FOR THE ABOVE-RATED WIND SPEED BASE CASE FOR HYWIND DEMO WITH TURBULENCE INTENSITY OF 1%. 82
FIGURE 48. FLATTEN VIEW OF CO-COHERENCE OF LONGITUDINAL WIND VELOCITY FLUCTUATION (U´) BETWEEN EACH POINT AND MID-POINT FOR FREQUENCY OF 0.2 HZ. 85
FIGURE 49. FLATTEN VIEW OF CO-COHERENCE OF LONGITUDINAL WIND VELOCITY FLUCTUATION (U´) BETWEEN EACH POINT AND MID-POINT FOR FREQUENCY OF 0.04 HZ. 86

CHAPTER 1 Introduction

This report is the result of the master thesis in Renewable Energy program with specialization of Wind Energy at University of Bergen (UiB).

The problem investigated in this report and thesis organization are mentioned in following sections.

1.1 Problem Statement

Offshore wind turbines have some clear advantages compared to the onshore wind turbines, such as e.g. stronger wind and less visual impact. This is why there is a trend toward offshore wind turbines in recent years, although unique challenges are introduced by offshore wind turbines. The expansion of offshore wind turbines industry is requiring installations in deeper water. As the offshore wind turbines develop toward deeper water, conventional substructures, such as e.g. monopiles, jackets and tripods, are not economically feasible. The best economical solution for deep water is floating wind turbines.

Therefore, the development of floating offshore wind turbines is required. Numerical models are the key part of this development. In order to ensure that a numerical model represent the real physical behaviour of a structure, verification of the computer model is required. One part of the verification of the computer model is performing a sensitivity study. By conducting the sensitivity study, the results from the analysis may contribute in the improvement of existing knowledge in optimizing the design of floating offshore wind turbines.

Keeping the importance of the sensitivity study in mind, the main purpose of this master thesis was set to better understand the sensitivity of the selected floating wind turbines' responses to various environmental parameters.

1.2 Thesis Organization

The importance and necessity of this study as well as presenting the thesis organization is introduced in CHAPTER 1.

An overview of the offshore wind turbines, Hywind Demo, OC3-Hywind and coherence of numerical wind field will be presented in CHAPTER 2.

In CHAPTER 3, the variation of environmental parameters in the sensitivity study and evaluation of structural responses will be described in detail.

A brief introduction to modeling of environmental components, i.e. wind, wave and current, will be presented in CHAPTER 4.

All the results will be presented without any interpretation in CHAPTER 5.

The interpretations and discussions about the results will be presented in CHAPTER 6.

The conclusions of the work in this thesis will be presented in CONCLUSION chapter.

Finally, proposal of further investigation to approach more accurate results will be presented in RECOMMENDATION FOR FURTHER WORK chapter.

.

CHAPTER 2 Background

There has been a drive towards renewable energy in recent years. Pollution, exhaustibility of fossil fuels and global warming are the main reasons for this tendency to renewable energy. There are various sources of renewable energy, such as solar energy, wind energy, biofuel, etc.

2.1 Floating Offshore Wind Turbine

One of the abundant renewable energy resources is wind. Although wind energy is applied by humans to grind grain or sail ships since thousands of years ago, first attempts to harness wind energy to produce electricity back to the late nineteenth centuries [1]. A wind turbine is a device that converts kinetic energy of wind into electricity.

A wind turbine is made up of different components, such as rotor blades, nacelle, tower, support structure, etc. Wind turbines are categorized to horizontal- and vertical-axis based on their rotation axis. However, most of modern wind turbines are horizontal-axis turbines.

A wind turbine can be located both onshore and offshore. Furthermore, offshore wind turbines are divided to three categories based on water depth where they are installed in [2],

- Shallow water, if the water depth is less than 30 meters,
- Transitional water, if the water depth is between 30 to 60 meters,
- Deep water, if the water depth is more than 60 meters.

Figure 1 shows the progression of wind turbines from onshore to offshore.

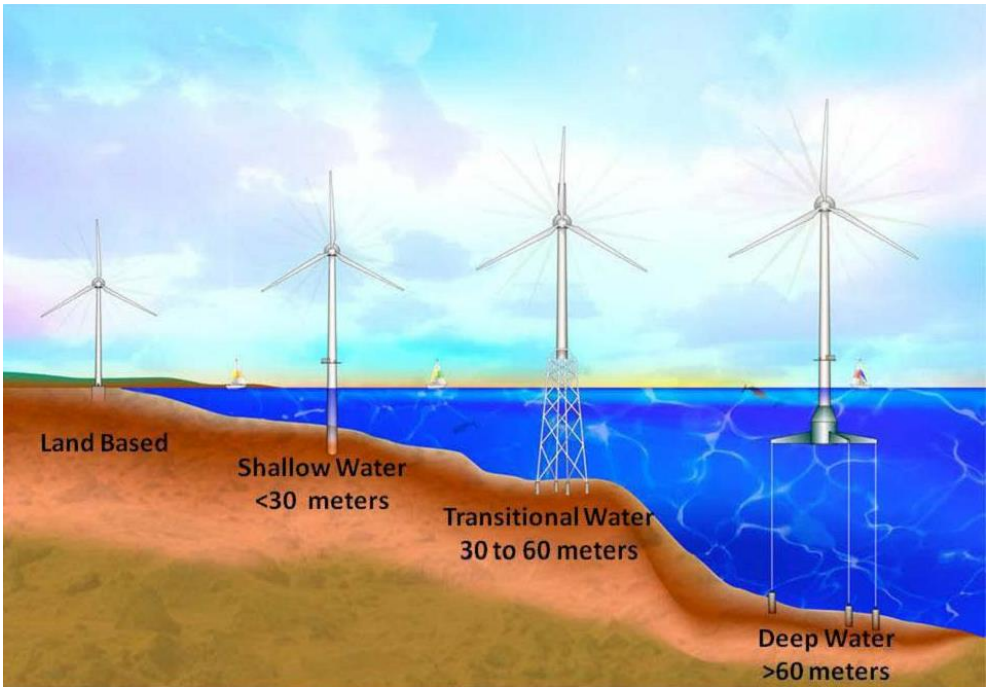

Figure 1. Wind turbine development from onshore toward deeper water. [3]

Although onshore wind energy for generating electricity is now competitive in cost with fossil fuels, further technology development of offshore wind turbines is needed [3]. Therefore, a lot of researches have been done in recent years. The most important reasons for the upward trend in use of offshore wind energy are [4]:

- Stronger and more steady wind with less turbulence intensity and smaller shear in offshore than onshore,
- No limitation to the size of an offshore wind turbine if it can be manufactured near the coastline, i.e. no dealing with road or rail logistical constraints,
- Vast availability of sea surface and no dealing with land occupation,
- No dealing with noise pollution and visual impact.

On the other hand, offshore wind turbines introduce exceptional problems, such as a higher capital investment, more challenging structural design, less accessibility, higher costs relating to maintenance issues and electric power transmission to shore [1]. Moreover, floating offshore wind turbines introduce more unique difficulties, such as dealing with large inertia loading on

the tower and nacelle caused by induced accelerations due to floater motions and also requiring more advanced blade control due to the floating motions. [5]

Substructure is the most critical part of offshore wind turbine development and must be opted mainly with respect to the water depth. Due to more complexity and equipment needed below the sea surface, cost of offshore substructures will increase as water depth increases. Figure 2 shows the relation between water depth and cost of offshore wind turbine substructure. [3]

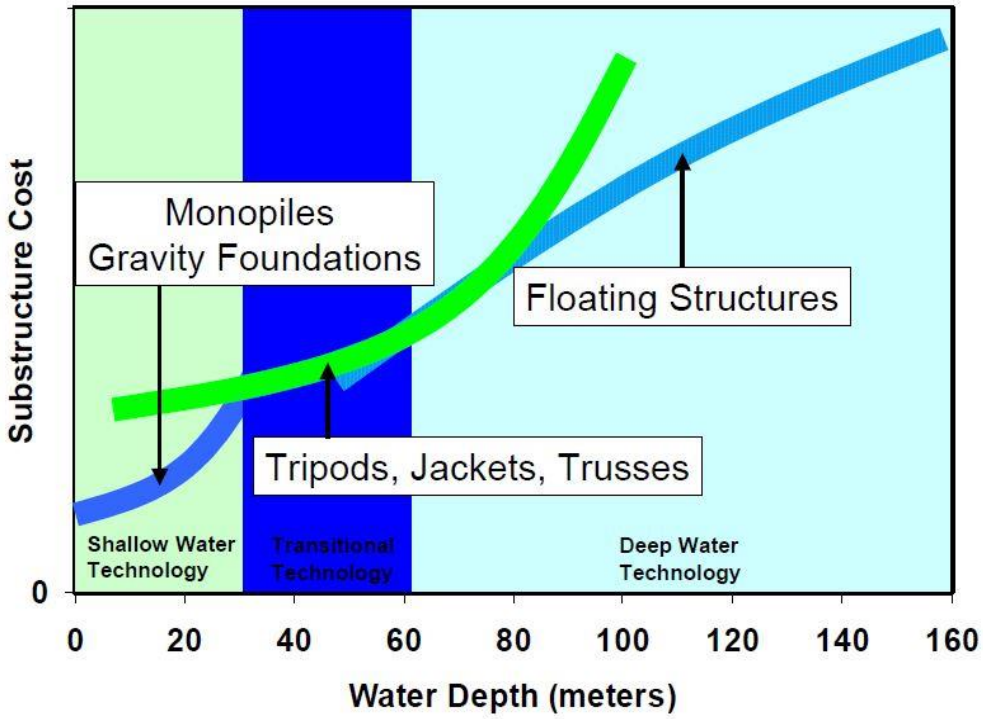

Figure 2. the relation between cost of offshore wind turbine substructures and water depth. [3]

Thus far most of offshore wind turbines have been installed in shallow water where technology of onshore wind turbines with upgraded electrical systems and corrosion systems can be used.

Monopile, gravity base and suction bucket are economically suitable as offshore wind turbine foundations for shallow water, Figure 3 presents these foundations.

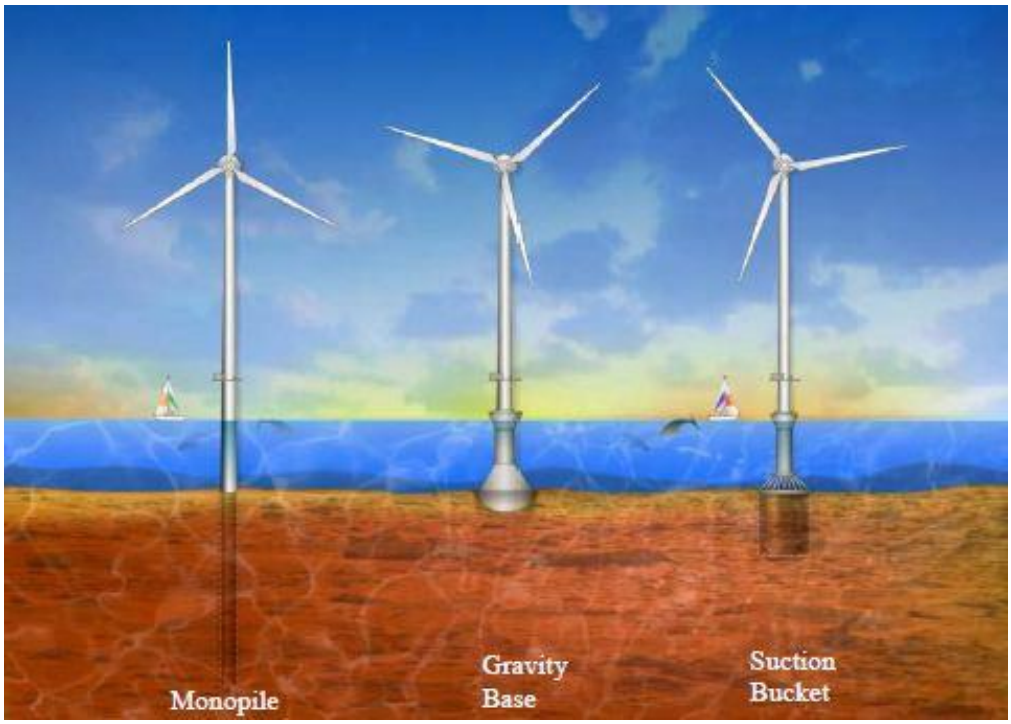

Figure 3. Offshore wind turbine foundations for shallow water. [3]

Simplicity, minimum design developments of existing onshore monopiles and minimum footprint on the seabed are the main reasons that monopiles are the most deployed foundations in shallow waters including the 160 MW Horns Rev 1 offshore wind farm located in the North Sea, 14-20 km off the Danish west coast [6]. However, application of monopiles are limited in deeper waters due to their flexibility, i.e. the natural frequency of the structure is lowered into a range of the excitation sources' frequencies. Furthermore, higher mass and more specialized installation equipment, and therefore higher cost are required to accommodate monopiles in deeper waters. [3]

Gravity base foundation doesn't have the flexibility issues of monopiles but require significant preparation of seabed and extensive soil analysis. Gravity base foundations have been installed in the 165.6 MW Nysted offshore wind farm located in the Baltic Sea, 10 km off the coast of Denmark [7]. Suction bucket foundations [8] also show some advantages for some shallow waters, e.g. avoiding the limitation of large pile drivers presented by monopile foundations. However, both gravity base and suction bucket foundations will grow rapidly in cost with deeper waters [3].

Tripod tower, guyed monopole, full-height jacket (truss) and submerged jacket with transition to tube tower are some examples of economically accepted foundations for transitional waters. As an example, submerged jacket with transition tube tower is the selected foundation for the 588 MW Beatrice offshore wind farm located 13.5 km off the Caithness coast of UK. Beatrice offshore wind farm will be fully operational in 2019 [9].

To compare with foundations used in shallow waters, foundations used in transitional have wider base with multiple anchor points. Figure 5 illustrates some foundations for transitional waters [3].

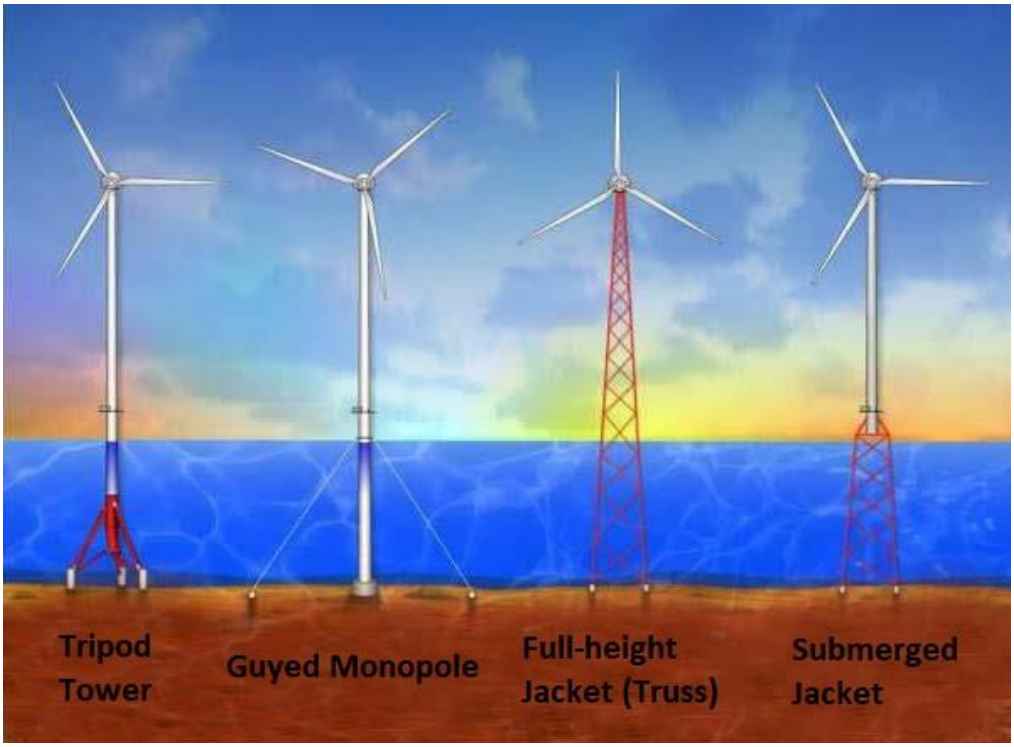

Figure 4. Some foundations for transitional waters. [3]

A floating substructure is the best economical option for deep waters. Providing enough buoyancy to support the weight of the wind turbine and withstanding environmental loads, i.e. wind, wave and current loads, are two vital characteristics of a floating substructure. Numerous substructure configurations are possible for deep water. Figure 5 shows three floating substructure concepts which use various methods to achieve static stability. In the spar-buoy concept, structure can be moored by catenary or taut lines, and stability achieves by using ballast to lower the center of mass below the center of buoyancy. In the tension leg platform

(TLP) concept, stability achieves by using mooring line tension provided by surplus buoyancy in the tank. In the barge concept, catenary lines are generally used as mooring system and stability achieves through its waterplane area. [4]

Spar-buoy concept has successfully deployed at the 30 MW Hywind Scotland Pilot Park located 30 km off the east coast of Scotland. [10]

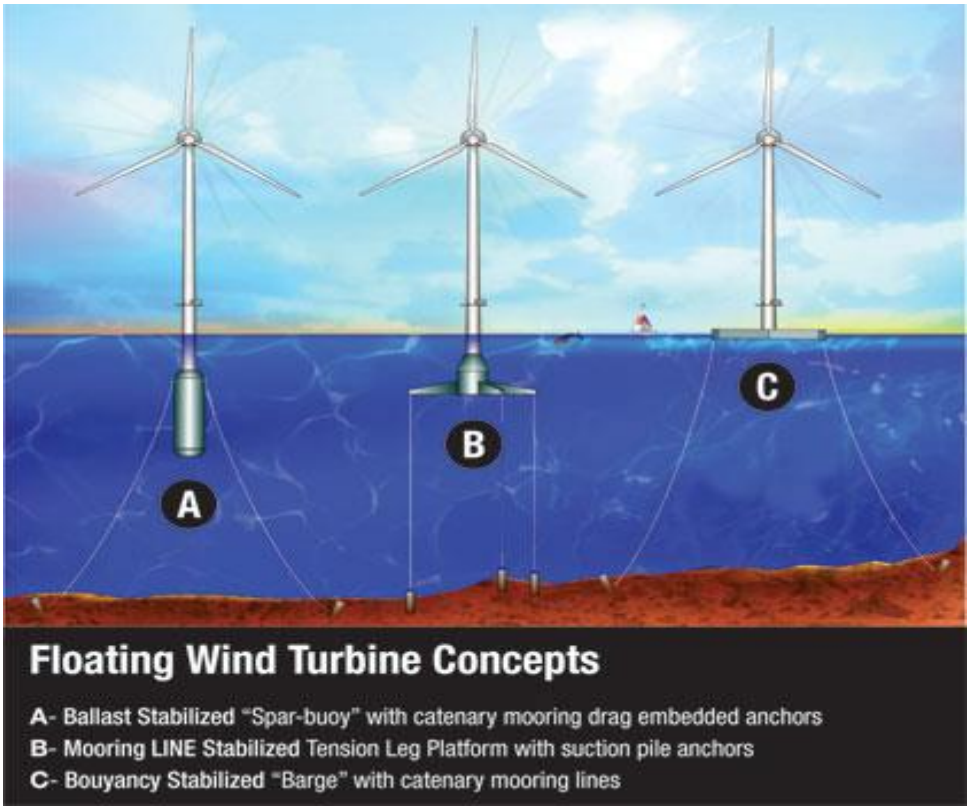

Figure 5. Floating substructure concepts for deep waters. [4]

Numerous floater concepts with variety of mooring systems, tanks and ballast options have been presented for offshore wind turbines. GICON-TLP [11], WindFloat [12], Dutch Tri-floater [13], Concrete Star [14], Ideol [15] and PelaStar tension leg platform [16] are some of these concepts illustrated in Figure 6.

Figure 6. Various floater concepts. [17]

The experiences from the offshore oil and gas industries proves the technical feasibility of offshore floating wind turbines. Despite many similarities, a direct transfer without adaption from offshore oil and gas technology to offshore wind industry would not be technically and economically feasible. For instance, while large wind driven overturning moments dominate the design of a floating wind turbine, payload and wave driven forces dominate the design of a floating oil and gas platform. [3]

The loads on the offshore floating wind turbines are dominated by aerodynamic and hydrodynamic effects, as shown in Figure 7. Additional offshore loads such as impact of floating debris and sea ice, effect of varying sea level and effect of marine growth build-up on the substructure must also be considered in a design process.

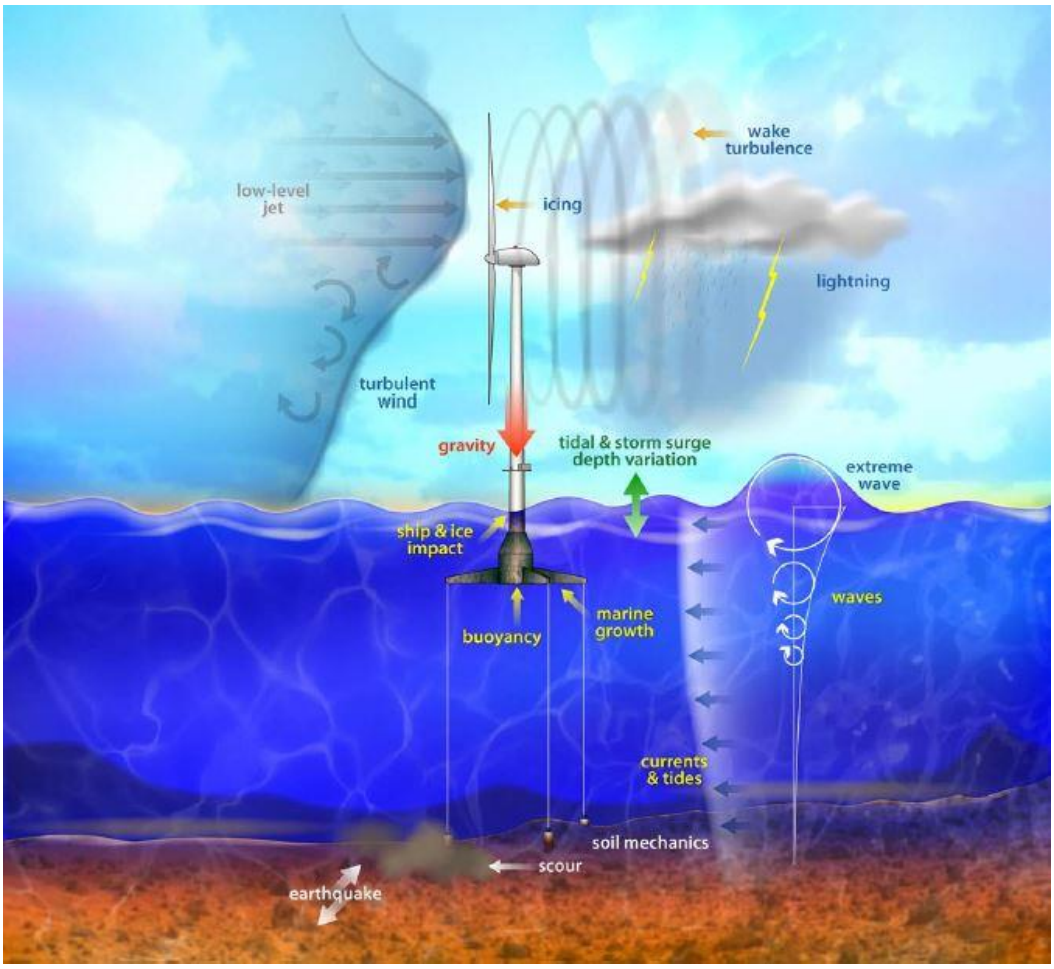

Figure 7. Loads on an offshore wind turbine. [18]

The interaction between the wind and the airfoils of each rotor blade is the starting point of the power production of a wind turbine. By air blowing over airfoil of the blades, aerodynamic lift and drag forces are generated. The resulting aerodynamic loads on the structure can be divided into three categories:

- Steady aerodynamic forces,
- Periodic aerodynamic forces,
- Randomly fluctuating aerodynamic forces.

The main different between these three aerodynamic forces are their causations. Mean wind speed generates the steady aerodynamic forces, while periodic aerodynamic forces generated by wind shear, off-axis winds, rotation of rotor and tower shadow, and randomly fluctuating aerodynamic forces generated by turbulence, gust and dynamic effect. [18]

Loads on fixed bottom wind turbines are mainly dominated by aerodynamic forces, while for offshore floating wind turbines, hydrodynamic loads become more important. The significance of hydrodynamic forces depends on the floating wind turbine concept and the severity of wave and wind conditions.

The linear hydrodynamic loads consist of three separate components, i.e. hydrostatic, diffraction and radiation forces and moments. To calculate the total non-steady-state, transient linear hydrodynamic loads acting on a floating substructure with a mooring system in irregular incident waves, the true linear hydrodynamic model, described in detail in Matha [18], can be utilized.

The long-term statistical correlation of wind speed, wave height and wave period, which are expressed in the long-term joint probability density distribution, show that aerodynamic and hydrodynamic loads are related, i.e. the waves are generated by the winds in the long term. In other words, load cases with higher wind speeds are usually accompanied by higher wave heights resulting in higher aerodynamic and hydrodynamic loads on the structure. [18]

2.2 Hywind Demo

Hywind, shown in Figure 8, is a spar-buoy floating wind turbine concept presented by Statoil. The demonstration of this concept, Hywind Demo, has been installed at 10 km west coast of Karmøy, Norway, in June 2009. Hywind Demo is equipped with a Siemens wind turbine with rated electric power of 2.3 MW and was one of the first full scale offshore floating wind turbine in the world. The well-proven offshore oil and gas concepts and components has been used in the Hywind Demo. [19]

Figure 8. The Hywind concept. [19]

Hywind Demo can be divided into three main parts, i.e. substructure (hull), tower and the Siemens wind turbine.

The hull is the structure on which the tower is supported. The hull is a 100 m deep cylinder with a maximum diameter of 8.3 m. The hull has permanent ballast comprising gravel and water to lower the center of gravity of the structure. Therefore, center of gravity is located below the center of buoyancy which is why a spar buoy has exceptional stability properties. Moreover, the tower with a height of about 50 m is mounted on top of the hull. Furthermore, the Siemens wind turbine with 65 m hub height above the sea surface and 82.4 m rotor diameter is located on the tower. Hywind Demo schematic is presented in Figure 9.

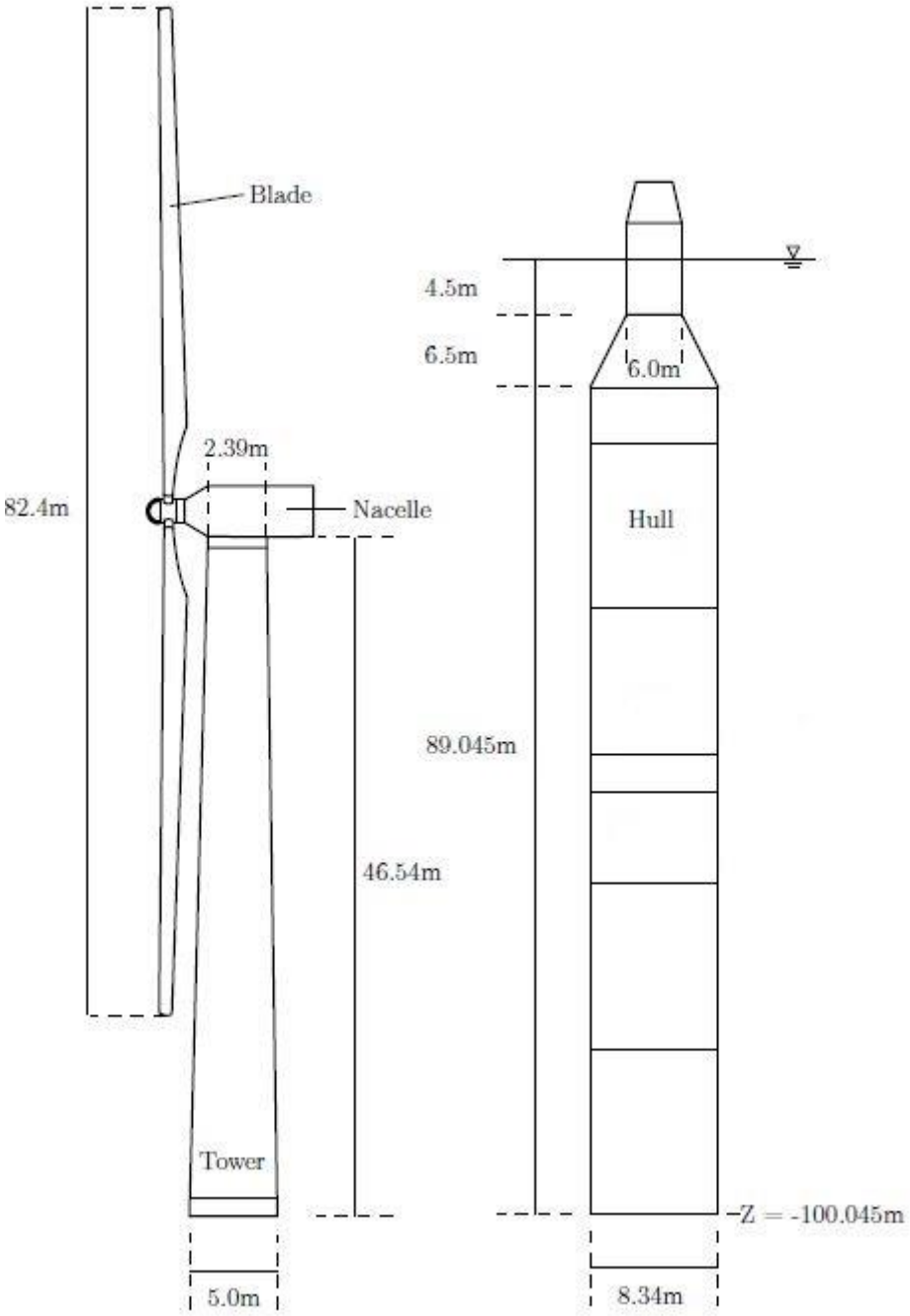

Figure 9. Hywind Demo schematic. [20]

Hywind Demo is moored to the seabed with catenary mooring system consists of three mooring lines and six delta lines connected to fairleads at approximately half the draft of the hull. Every two delta lines connect to a delta-plate and one mooring line, presented in Figure 10. Steel chains and ropes as well as clump weights are used to obtain sufficient force-displacement characteristics in the mooring lines. A 45 tons clump weight is connected to the mooring line

approximately 150 m from the hull, illustrated in Figure 11. To prevent the structure from drifting from its location and to provide adequate stiffness in yaw motion of the structure are the main responsibilities of the mooring system. [20]

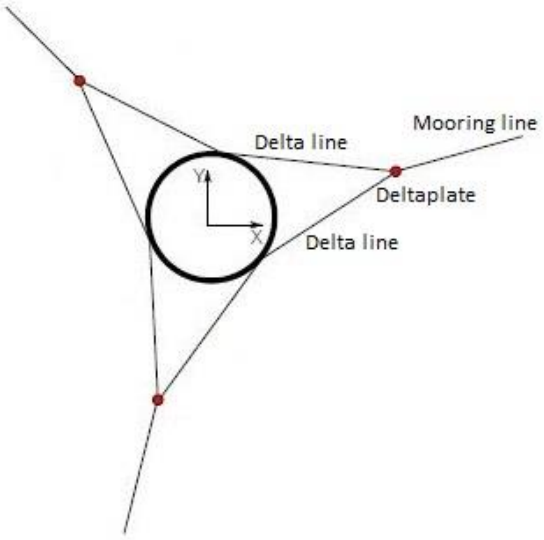

Figure 10. Overhead view of the hull and the mooring system. [20]

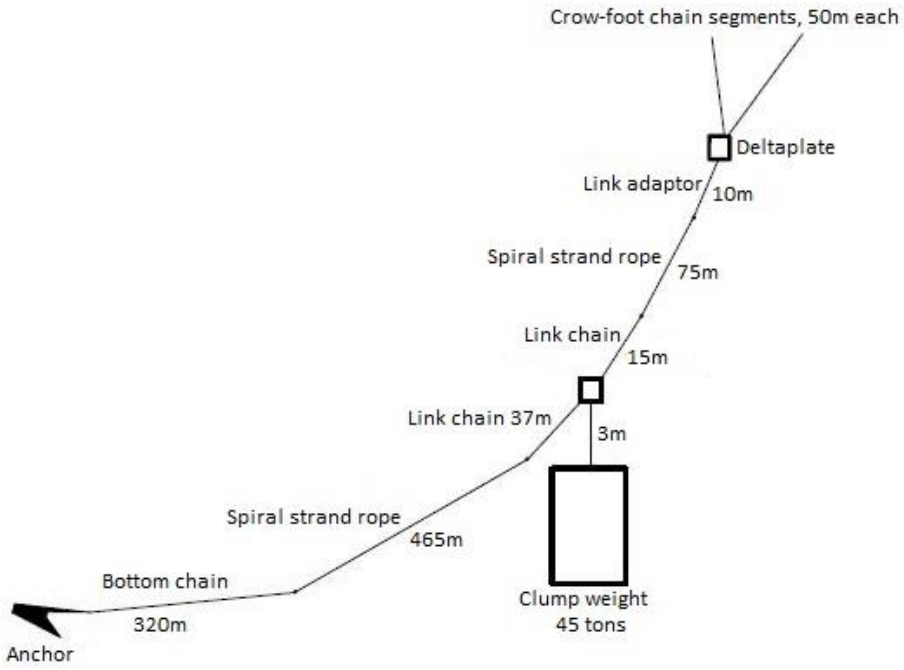

Figure 11. One mooring line schematic of Hywind Demo. [20]

Main characteristics of Hywind Demo structure and the Siemens wind turbine employed in Hywind Demo are listed in Table 1 and Table 2 respectively.

Table 1. Main specification of Hywind Demo structure. [19]

Draft hull [m]	100
Water depth [m]	210
Displacement [tons]	5388
Diameter at sea level [m]	6
Diameter at keel [m]	8.3
Tower including transition piece [tons]	399
Substructure [tons]	1305
Ballast [tons]	3516

Table 2. Characteristic data for the Siemens wind turbine. [19]

Rated electric power [MW]	2.3
Rotor diameter [m]	82.4
Rotor speed [rpm]	6-18
Rotor weight [tons]	54
Nacelle weight (excluding rotor) [tons]	82
Hub height above sea surface [m]	65
Cut-in wind speed [m/s]	3-5
Rated wind speed [m/s]	13
Cut-out wind speed [m/s]	25

Statoil provided the complete model of Hywind Demo, simulated by the computational tool SIMA (Simulation of Marine Operations) [21], for the present thesis.

2.3 OC3-Hywind

Wind turbines are designed and analyzed using simulation tools, i.e. design codes. The complexity of design codes to analyze offshore wind turbines, and the limited data available to validate them, emphasize the need to verify their accuracy. The Offshore Code Comparison Collaboration (OC3) was established to meet this need. [22]

The specifications of the wind turbine were the fundamental set of inputs to the codes controlled within OC3. The OC3 used the publicly available specifications of NREL 5 MW baseline wind turbine [23].

The rated mechanical power of the NREL wind turbine is 5.3 MW, with rated electric power of 5 MW and a generator efficiency of 94.4%. The rotor radius is 63 m, and rotor mass and nacelle mass are 110000 kg and 240000 kg respectively. The hub height for the turbine is 90 m above still water level (SWL). Cut-in, rated and cut-out wind speed for the turbine are 3 m/s, 13 m/s and 25 m/s respectively.

Some of the main specifications of NREL 5 MW baseline wind turbine are tabulated in Table 3. [23]

Table 3. Main specifications of NREL 5 MW baseline wind turbine. [23]

Rated electric power [MW]	5
Rated mechanical power [MW]	5.296610
Rotor orientation, configuration	Upwind, three blades
Control	Variable speed, collective pitch
Rotor diameter [m]	126
Cut-in, Rated rotor speed [rpm]	6.9, 12.1
Rotor mass [kg]	110000
Nacelle mass [kg]	240000
Hub height above SWL [m]	90
Cut-in wind speed [m/s]	3
Rated wind speed [m/s]	11.4
Cut-out wind speed [m/s]	25

Four different support structures investigated in separate phases of the OC3 project to cover the variety of support structures required for cost effectiveness at varying offshore sites [22]:

- In Phase I, support structure was a monopile with a rigid foundation in 20 m water depth.
- In Phase II, the foundation of the monopile from Phase I made flexible to represent the soil-pile interactions by applying different models.
- In Phase III, support structure was a tripod in intermediate water (45 m).
- In Phase IV, support structure was a floating spar-buoy in deep water (320 m).

The same NREL 5 MW baseline wind turbine was installed in all phases.

All the phases I, II, III, IV are described in detail in Jonkman [22].

The rotor-nacelle assembly of the NREL 5 MW baseline wind turbine including aerodynamic and structural properties remains unchanged in phase IV, however the support structure (tower and substructure) and control system properties are changed. [24]

The spar-buoy concept of Hywind, developed by Statoil, was chosen for the modelling of Phase IV of OC3 project. Simplicity in design and suitability to modelling and commercialization are the reasons that this concept selected for Phase IV. Statoil supplied detailed platform and mooring system data. The data provided was for the conceptual version of the Hywind platform developed to support a 5 MW wind turbine. Aspects of the original data adapted by Jason Jonkman so that the platform design is appropriate for supporting the NREL 5 MW baseline wind turbine. The new system referred to as the OC3-Hywind system.

The top of the OC3-Hywind spar-buoy platform is at 10 m above SWL and the draft of the platform is 120 m. The platform consists of two cylindrical regions connected by a linearly tapered conical region. To reduce the hydrodynamic loads near the free surface, the cylinder diameter of 9.4 m below the taper reduces to 6.5 m above the taper. The mass of the floating platform, including ballast is 7466330 kg. This mass includes weight of the rotor-nacelle assembly, tower, platform and the weight of mooring system in water, balances with the buoyancy of the undisplaced platform in still water. The mooring system of the structure consists of three mooring lines, with 120° angle between adjacent line. Some of structural properties of the platform are mentioned in Table 4. [24]

Table 4. Floating platform structural properties. [24]

Draft hull [m]	120
Elevation to platform top (tower base) above SWL	10
Water depth [m]	320
Diameter at sea level [m]	6.5
Diameter at keel [m]	9.4
Platform mass, including ballast [kg]	7466330

OC3-Hywind is simulated by the computational tool SIMA and is available as an example of coupled RIFLEX-SIMO model in SIMA.

Figure 12 presents schematics of both Hywind Demo and OC3-Hywind concept with their main dimensions.

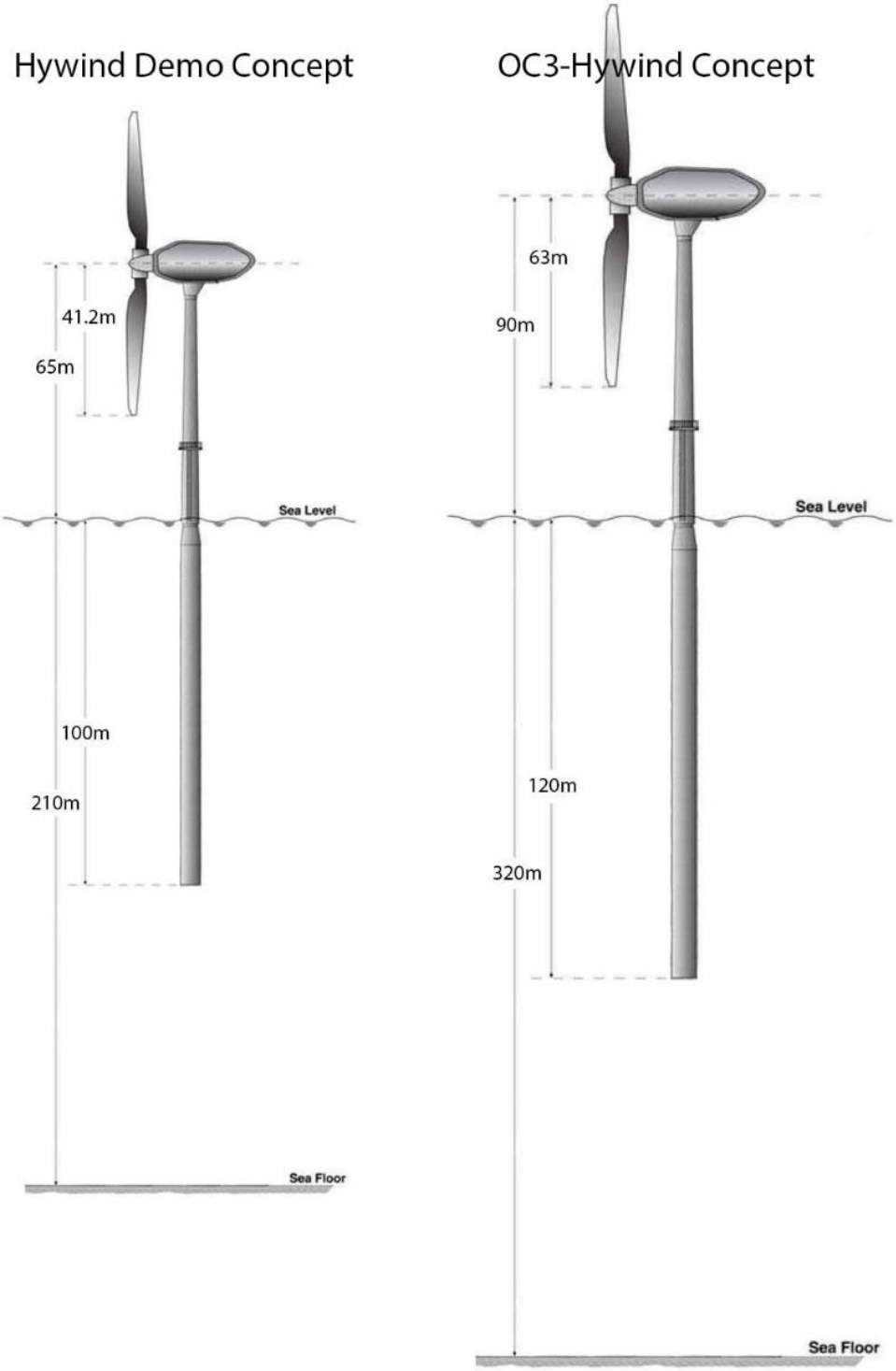

Figure 12. Dimensional comparison between Hywind Demo concept and OC3-Hywind concept. The illustration is taken from Malhotra [25].

2.4 Coherence of the numerical wind field

Wind simulation is an important part of a wind turbine structural analysis. As the relationship between atmospheric turbulence and aerodynamic loads on wind turbine blades is highly nonlinear, there continues to be interest in numerically simulating the winds and then calculating time series of blade loads. [26]

A good description of the wind field including turbulence intensity and spatial characteristics of turbulence is important for a good estimate of dynamic loads on some spatially extended structures, such as towers, large bridges wind turbines. For many of these structures the cross-spectra of wind fluctuations at different points on the structures are so vital in the estimation of dynamic wind loads. The spectrum of the modal forces on the structure can be written as weighted integrals of the cross-spectra under some simplifications. For more complicated structures such as wind turbines which have moving parts and nonlinear structural responses, there is not a simple relation between characteristics of the flow and the forces. However, for these structures also cross-spectra are important for the description of dynamic loads. [27]

The magnitude of cross-power spectral density between points x and y can be defined in terms of the power spectral densities and the coherence function by Eq. (1):

$$\left|\boldsymbol{S_{xy}(f)}\right| = \boldsymbol{Coh_{xy}}\left(\boldsymbol{f}, \Delta \boldsymbol{r_{xy}}, \boldsymbol{U_{xy}}\right)\sqrt{\boldsymbol{S_x(f).S_y(f)}} \quad (1)$$

Where the coherence is a function of frequency (f), distance between points x and y $\left(\Delta r_{xy}\right)$ and mean wind speed at points x and y (U_{xy}). The imaginary parts of the cross-spectra are zero by assuming that there is an average phase of zero between any two points. Therefore, the entire spectral matrix is defined by the power spectral densities and the coherence. [26]

Hence, the coherence which is a measurement of correlation of spectra measured at two arbitrarily chosen points, x and y, is defined in Eq. (2):

$$\boldsymbol{Coh_{xy}(f)} = \frac{\boldsymbol{S_{xy}(f)}}{\sqrt{\boldsymbol{S_x(f).S_y(f)}}} \quad (2)$$

Where S_x and S_y are the one-sided power spectral density functions for the random processes x and y and S_{xy} is the cross-power spectral density function.

To estimate wind loads on structures for both lateral and vertical separations, the root-coherence, defined in Eq. (3), could be used. The root-coherence is expressed as the normalized cross-spectral density of the wind fluctuations at two arbitrarily chosen points, x and y. [28]

$$\boldsymbol{Root\_coh_{xy}(f)} = \sqrt{\boldsymbol{Co_{coh_{xy}}^{2}(f)} + \boldsymbol{Quad_{coh_{xy}}^{2}(f)}} \tag{3}$$

Where Cc_coh_{xy} and $Quad\_coh_{xy}$ are the co-coherence and quad-coherence of the velocity fluctuations respectively. Co-coherence and quad-coherence are defined in Eq. (4) and Eq. (5) respectively.

$$\boldsymbol{Co\_coh_{xy}(f)} = \boldsymbol{Re}\left(\frac{\boldsymbol{S_{xy}(f)}}{\sqrt{\boldsymbol{S_x(f).S_y(f)}}}\right) \tag{4}$$

$$\boldsymbol{Quad\_coh_{xy}(f)} = \boldsymbol{Im}\left(\frac{\boldsymbol{S_{xy}(f)}}{\sqrt{\boldsymbol{S_x(f).S_y(f)}}}\right) \tag{5}$$

Where S_{xy} is the cross-spectral density of the velocity fluctuations at two arbitrarily chosen points, x and y. The co-coherence is used to quantify only the in-phase correlation of the wind velocity fluctuations and is therefore a governing parameter to estimate wind loads on structures [28]. In the present thesis, only the co-coherence is considered.

To simulate the turbulent wind field, the design standard for wind turbines, IEC 61400-1 [29], recommends both the Kaimal spectral [30] combined with exponential coherence model (Kaimal model) and the Mann uniform shear turbulence model (Mann model) [27]. The turbulent wind spectrum at the hub height is similar for both turbulence models, although there are significant differences in the spatial distribution [31]. The Kaimal model uses a one-point spectrum and an exponential coherence function between points (u′) in the longitudinal direction and no coherence in other wind components. The Mann turbulence model generates turbulence using a spectral velocity tensor and therefore there is coherence in all three wind directions [32]. The Mann turbulence model includes a more natural and direct representation of the three dimensional turbulent flow, although both models contain the same amount of information. [31]

The numerical wind fields which used in analysis of the structures was generated by DTU turbulence generator which is based on Mann model. [33]

CHAPTER 3 Methods

To better understand the sensitivity of the responses to various environmental parameters, a sensitivity study was performed. In this study, the sensitivity of various motion parameters was investigated as function of the wave conditions, wind speed, turbulence intensity, wind shear as well as the spatial resolution of the numerical wind field. Moreover, the responses of OC3-Hywind were studied to understand the effect of bigger wind turbine structure.

Both Hywind Demo and OC3-Hywind were modelled by computational tool SIMA. The total length of simulations were 2000 seconds while first 200 seconds of simulations were eliminated due to transition part, therefore 30 minutes of simulations were investigated.

The numerical model of Hywind Demo has previously been compared to full scale measurements by Skaare et al. [19]. The environmental conditions studied by Skaare et al. [19] are considered as the base cases which are shown in Table 5 and Table 6 for the below- and above-rated wind speed respectively.

Table 5. Environmental conditions for below-rated wind speed base case. [19]

Mean estimated wind speed [m/s]	Turbulence intensity [%]	Wind direction (towards) [°]	H_s [m]	T_p [s]	Wave direction (towards) [°]	Mean current speed [m/s]	Current direction (towards) [°]
10.8	10	195	1.4	8.6	146	0.32	316

Table 6. Environmental conditions for above-rated wind speed base case. [19]

Mean estimated wind speed [m/s]	Turbulence intensity [%]	Wind direction (towards) [°]	H_s [m]	T_p [s]	Wave direction (towards) [°]	Mean current speed [m/s]	Current direction (towards) [°]
18.7	11	327	4.0	10.0	355	0.43	337

Firstly, results were checked to be consistent with the results produced by Skaare et al [19]. Thereafter, the environmental characteristics were varied around the values corresponding to the base cases.

Environmental parameters such as wave characteristics, turbulence intensity of wind field, the exponent (α) in wind shear profile power law and the spatial resolution of the numerical wind field were changed. Keep in mind that to perform sensitivity study of a parameter, only that parameter was changed while other environmental parameters remained unchanged.

3.1 Environmental parameters variation

The same following environmental parameters variation were applied to both Hywind Demo and OC3-Hywind SIMA model.

3.1.1 Wave characteristics variation

Nine cases of significant wave heights, H_s, and wave peak periods, T_p, for each below- and above-rated wind speed were studied. The cases with highest probability of occurrence form scatter diagram based upon approximately 18 years of measurement data from the North Sea, presented in APPENDIX 1, were selected. Wave characteristics cases are presented in Table 7 and Table 8 for the below- and above-rated wind speed respectively. Case2 in Table 7 is the base case for the below-rated wind speed, while Case3 in Table 8 is the base case in the above-rated wind speed.

Table 7. Wave characteristics cases in the below-rated wind speed (Case2 is the base case).

	Case1	Case2	Case3	Case4	Case5	Case6	Case7	Case8	Case9
H_s [m]	0.75	1.4	2.25	4.25	5.75	7.25	8.75	10.25	12.25
T_p [s]	6.5	8.6	8.5	9.5	10.5	11.5	12.5	13.5	15.5

Table 8. Wave characteristics cases in the above-rated wind speed (Case3 is the base case).

	Case1	Case2	Case3	Case4	Case5	Case6	Case7	Case8	Case9
H_s [m]	0.75	2.25	4	4.25	5.75	7.25	8.75	10.25	12.25
T_p [s]	6.5	8.5	10	9.5	10.5	11.5	12.5	13.5	15.5

3.1.2 Turbulence intensity variation

The turbulence intensity is defined as the ratio of the root-mean-square of the wind velocity fluctuations, u', to the mean wind velocity, u_{mean}. The defined coordinate system and wind components are presented in Figure 13. Three cases of turbulence intensity of wind field were investigated for both below and above-rated wind speed. The cases are presented in Table 9. Case_TI2 in Table 9 is the base case for both below- and above-rated wind speed.

Table 9. Turbulence intensity (TI) cases (Case_TI2 is the base case).

	Case_TI1	Case_TI2	Case_TI3
TI in below-rated wind speed	5%	10%	15%
TI in above-rated wind speed	5%	11%	15%

3.1.3 Alpha variation

The formula of wind shear profile power law, which is a frequently used engineering approximation, is presented in Eq. (6):

$$\frac{\boldsymbol{u}}{\boldsymbol{u_{ref}}} = \left(\frac{\boldsymbol{z}}{\boldsymbol{z_{ref}}}\right)^{\boldsymbol{\alpha}} \tag{6}$$

Where u is the mean wind speed at height z, u_{ref} is the known mean wind speed at a reference height z_{ref} and α is the power law exponent.

Therefore, the mean wind velocity at a certain height, z, could be found by Eq. (7):

$$\boldsymbol{u} = \boldsymbol{u_{ref}}\left(\frac{\boldsymbol{z}}{\boldsymbol{z_{ref}}}\right)^{\boldsymbol{\alpha}} \tag{7}$$

In the present thesis, $z_{ref} = 65\ m$ is the hub height for Hywind Demo, $z_{ref} = 90\ m$ is the hub height for OC3-Hywind, $u_{ref} = 10.8\frac{m}{s}$ for the below-rated wind speed, $u_{ref} = 18.7\frac{m}{s}$ for the above-rated wind speed and $\alpha = 0.12$ for the base cases.

The exponent (α) in wind shear profile power law were increased, shown in Table 10, to find out the effect of this parameter on the responses of the structures. Case_alpha4 in Table 10 is the base case for both below- and above-rated wind speed.

Table 10. Alpha (α) cases (Case_alpha4 is the base case).

	Case_alpha1	Case_alpha2	Case_alpha3	Case_alpha4	Case_alpha5
α	0	0.05	0.1	0.12	0.14

3.1.4 Spatial resolution variation

Figure 13 illustrates the spatial resolution of the numerical wind field. For the below-rated wind speed base case, the spatial resolution in x-direction set to be 1.318 m and in y- and z-direction set to be 2 m. However, the spatial resolution for the above-rated wind speed base case in x-direction set to be 2.283 m and in y- and z-direction set to be 2 m.

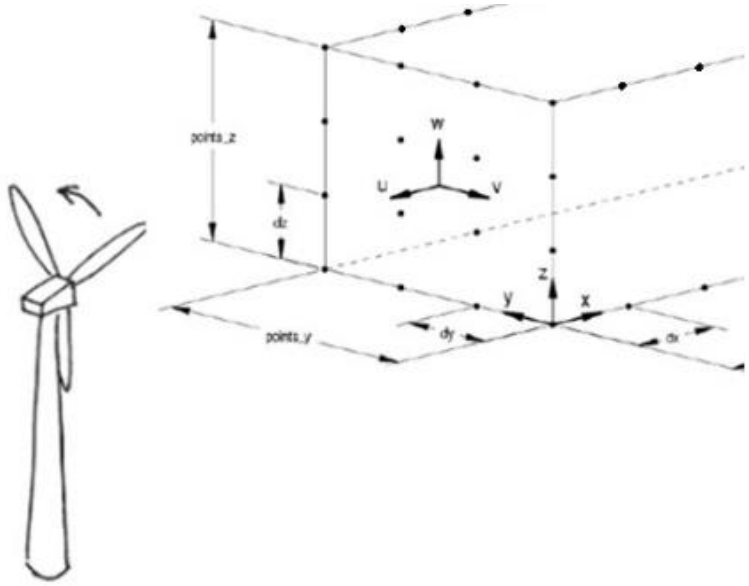

Figure 13. The spatial resolution of the numerical wind field.

Four cases were considered to investigate the effect of spatial resolution of the numerical wind field. While Case_Sp1 is the base case, resolution of Case_Sp2, Case_Sp3 and Case_Sp4 are 2, 4 and 8 times of the resolution of the base case respectively, shown in Table 11.

Table 11. Spatial resolution of the numerical wind field cases where Case_Sp1 is the base case.

	Case_Sp1	Case_Sp2	Case_Sp3	Case_Sp4
times	1	2	4	8

3.2 Evaluated structural responses

In order to understand sensitivity of structural responses to mentioned environmental parameters in previous section, mean and standard deviation of structural responses such as electrical generator output, platform pitch and tip out-of-plane deflection for one blade were investigated.

3.2.1 Electrical power

The ultimate goal of a wind turbine is to convert the kinetic energy of wind to generate electricity. The energy in the wind turns blades around a rotor which is connected to the main shaft. The main shaft spins a generator to create electricity. The power is an integrated effect of the wind over the rotor disk. As electrical power output is the most important structural responses, the sensitivity of this response to environmental parameters is investigated.

3.2.2 Platform pitch

Due to existence of wind shear, gust, turbulence and yaw motion of nacelle, the flow field around a rotating blade is complex. For a floating offshore wind turbine, the flow field becomes more complex due to motion of floating platform. The motion of floating platform includes three translational components, i.e. heave in the vertical, sway in the lateral and surge in the axial, and three rotational components, i.e. yaw about the vertical axis, pitch about the lateral axis and roll about axial axis, illustrated in Figure 14. Therefore, the additional effect of the wind contribution which is basically transmitted to the rotor due to the motion of floating platform needs to be considered. In the six degrees of freedom of the floating offshore wind turbine, platform pitch and yaw motion significantly lead to the unsteady aerodynamic effects on the rotating blades. [5]

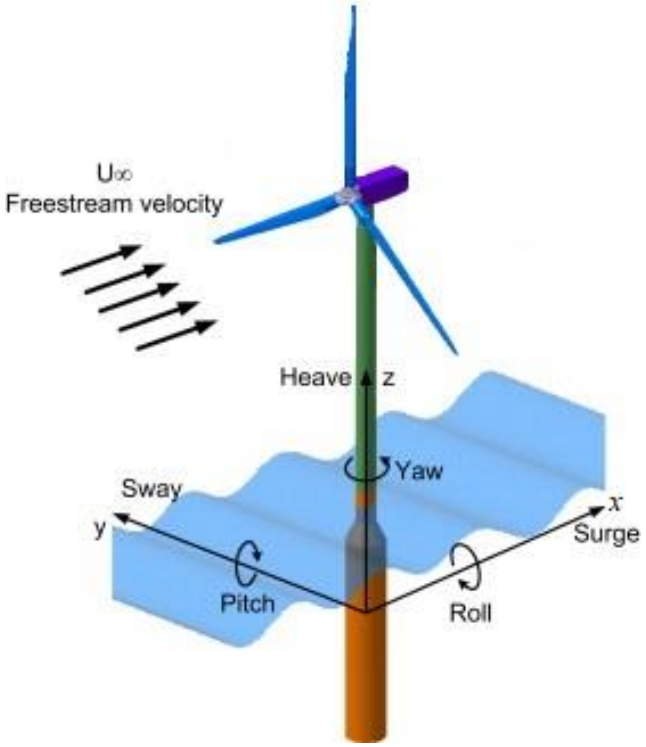

Figure 14. Degrees of freedom of a floating offshore wind turbine. [5]

Platform pitch is also an integrated effect, with some smoothing also over time due to the low eigenfrequency. Therefore, the sensitivity of platform pitch to environmental parameters was studied in the present thesis due to the mentioned importance of this structural response.

3.2.3 Tip out-of-plane deflection for one blade

One of the main criteria for the design of a blade is to ensure that blade tip out-of-plane deflections do not violate the minimum distance between the blade tip and turbine tower to avoid collision between the blade and turbine tower. Moreover, as the alpha variation in wind shear profile is expected to affect a local structural response, sensitivity of tip out-of-plane deflection of one blade to environmental parameters was also evaluated. Tip out-of-plane deflection of one blade is much more local effect, picking up turbulence as well as shear profile.

Figure 15 shows an illustration in order to better understand tip out-of-plane deflection of one blade relative to the undeflected blade.

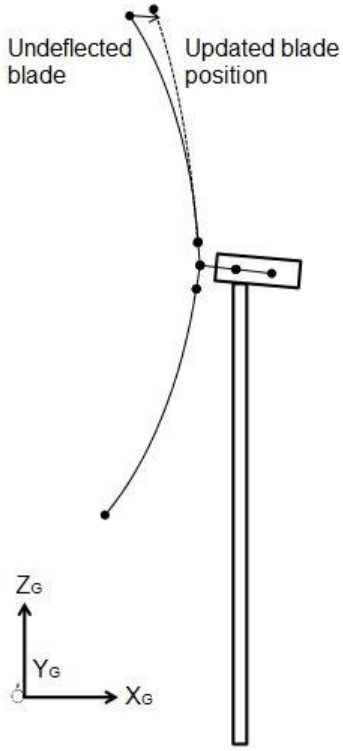

Figure 15. illustration of tip out-of-plane deflection of one blade. The illustration is taken from MARINTEK [21].

The responses of blade1 was selected to present tip out-of-plane deflection of one blade. It should be noted that the results for blade2 and blade3 are slightly different than blade1, however only the results for blade1 are presented in the present master thesis.

CHAPTER 4 Environment Components Modeling

Comprehensive simulation tools called design codes, which are capable of predicting the coupled dynamic loads and response of the system, are used to design and analyze wind turbines. For onshore wind turbine analysis, these design codes are known as “aero-servo-elastic” tools. These tools are compound of aerodynamic (aero) models, control system (servo) models and structural-dynamic (elastic) models in a coupled simulation environment. While in the offshore environment, additional dynamics pertinent to offshore structures, such as incident wave, sea current, hydrodynamics and foundation dynamics of the support structure, must also be considered. Moreover, the dynamic coupling between the motions of the substructure and the wind turbine, as well as the dynamic characteristics of the mooring system must also be accounted. Therefore, design codes known as “aero-hydro-servo-elastic” tools are used for offshore wind turbine analysis. [4]

The design tool SIMA (coupled RIFLEX-SIMO) which is an aero-hydro-servo-elastic simulation tool was used for analysis of the model of Hywind Demo and OC3-Hywind wind turbines.

Extensive SIMA model of Hywind Demo was provided by STATOIL and the SIMA model of OC3-Hywind is available as an example of coupled RIFLEX-SIMO model in SIMA software. The changes which applied to the models were limited to environmental conditions. The same environmental conditions, presented in Table 5 and Table 6, were applied to both Hywind Demo and OC3-Hywind. In the following sections, all three environment components which were applied to the structures in the above-rated wind speed base case will be presented.

4.1 Environment components

4.1.1 Wind

The wind profile used for the wind spectrum is described by Eq. (8):

$$\bar{u}(z) = \bar{u}_r \left(\frac{z}{z_r}\right)^{\alpha} \tag{8}$$

Where z is height above water plane, z_r is reference height which is hub height, $\bar{u}_r$ is average velocity at the reference height above water plane, α is height coefficient and $\bar{u}$ is average velocity at height z.

"Fluctuating three components" spectrum was used as the wind spectrum. The wind spectrum was compound of mean wind velocity and wind velocity fluctuations. The wind spectrum used wind shear profile power law with a reference point at hub height and added wind velocity fluctuations to the wind profile. Longitudinal, lateral and vertical wind velocity fluctuations were generated by DTU turbulence generator [33]. All three wind velocity fluctuation components were generated for all nodes of the numerical wind field. The numerical wind field is illustrated in Figure 16.

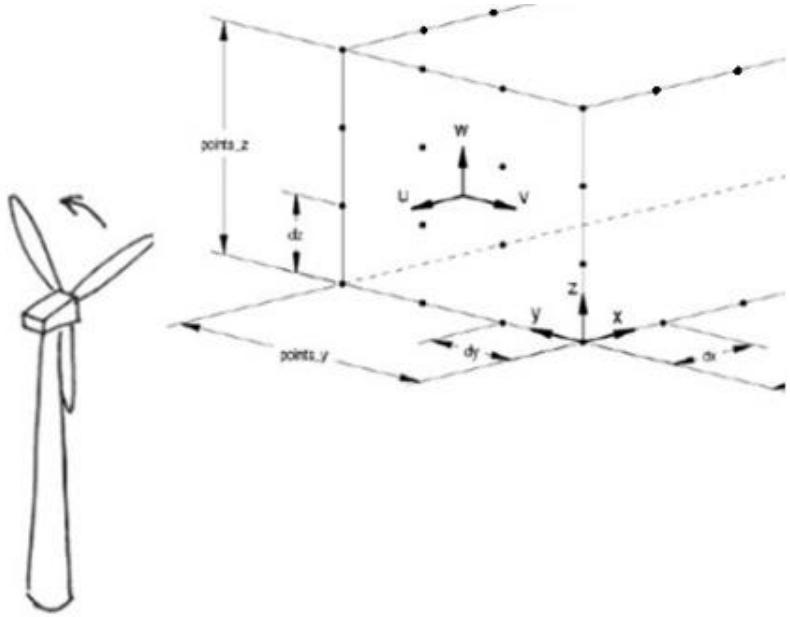

Figure 16. The illustration of the numerical wind field.

It is important to be noted that the length of numerical wind field in y- and z-direction are 128 m and in x-direction for the above-rated wind speed base case is 35600 m (multiplication of mean wind speed, 18.7 m/s, and simulation time, 2000 s).

Figure 17 shows the average longitudinal wind velocity fluctuation (u´) for the above-rated wind speed base case in y-z plane. The average longitudinal wind velocity fluctuation (u´) in y-z plane should be zero when there are many realizations. However, the average u´ has small variation and also there is dominant positive average u´ in the left side of y-z plane because there is only one realization in Figure 17.

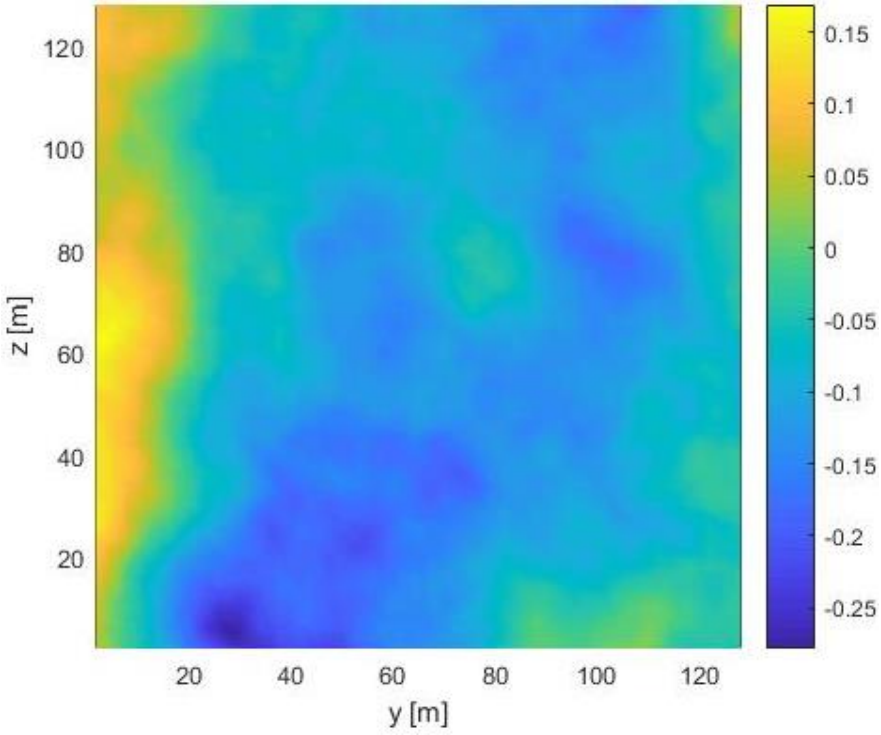

Figure 17. Average longitudinal wind velocity fluctuation (u´) for the above-rated wind speed base case in y-z plane.

Figure 18 illustrates the standard deviation of longitudinal wind velocity fluctuation (u´) for the above rated wind speed base case along z-axis. Based on the design standard for wind turbines, IEC 61400-1 [29], the average standard deviation of u´ shall be assumed to be invariant with height when there are many realizations. However, the average standard deviation has small variation as there is only one realization in Figure 18.

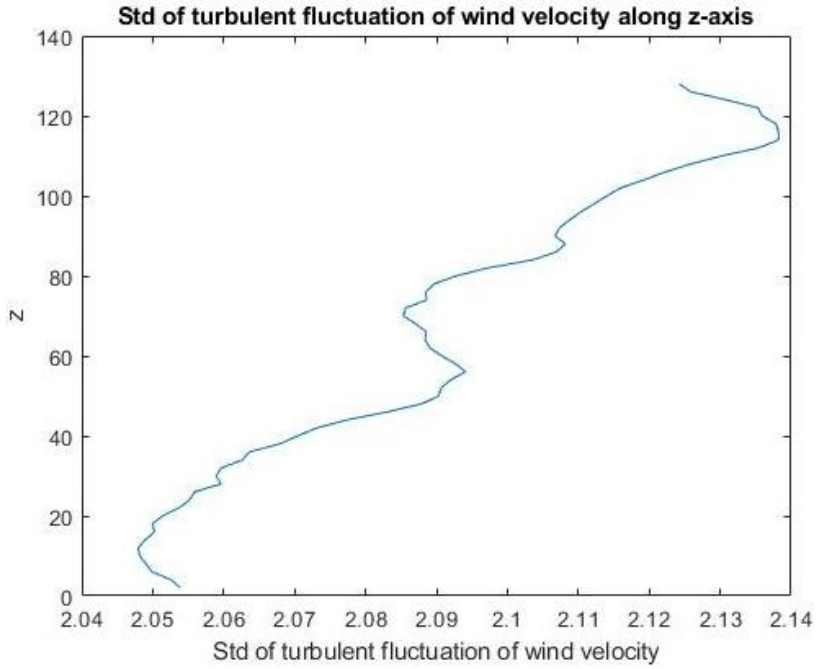

Figure 18. Std of longitudinal wind velocity fluctuation (u´) for the above-rated wind speed base case along z-axis.

The stated wind direction towards the wind turbine is 195 degrees for the below-rated wind speed base case in Table 5 and 327 degrees for the above-rated wind speed base case in Table 6. It is important to be noted that the wind turbine was turned towards wind direction, i.e. the wind direction in the SIMA model was 0 degree. Moreover, the wave and current directions were adjusted relative to the wind direction.

4.1.2 Wave

A three parameter JONSWAP spectrum was used as the wave spectrum applied to the structure. Figure 19 shows Jonswap wave spectrum used in the above-rated wind speed base case with $H_s = 4$ m and $T_p = 10$ s.

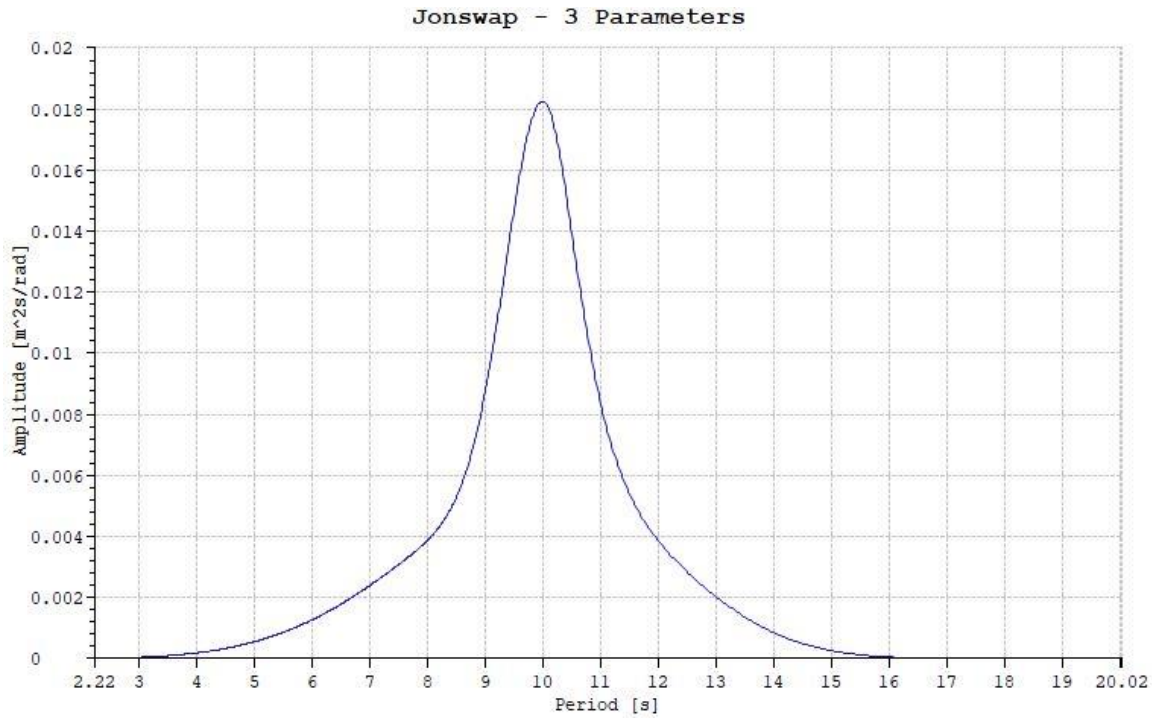

Figure 19. Jonswap wave spectrum used in the above-rated wind speed base case.

The stated wave direction towards the wind turbine is 146 degrees for the below-rated wind speed base case in Table 5 and 355 degrees for the above-rated wind speed base case in Table 6. As the wind turbine was turned toward the wind direction, the relative angle of wave direction to the wind turbine is -49 degrees for the below-rated wind speed base case and 28 degrees for the above-rated wind speed base case in SIMA model.

4.1.3 Current

The constant current profile was used in SIMA model. The constant current value is 0.32 m/s for the below-rated wind speed base case and 0.43 m/s for the above-rated wind speed base case. The relative angle of current profile to the wind turbine is 121 degrees for the below-rated wind speed base case and 10 degrees for the above-rated wind speed base case.

CHAPTER 5 Results

Hywind Demo and OC3-Hywind concepts were employed for investigation and analysis. Wave characteristics (H_s and T_p), turbulence intensity (TI), alpha (α) in wind shear power law and spatial resolution of the numerical wind field were varied and their effects were investigated on the structures' responses. For each sensitivity study, mean and standard deviation of structures' responses such as electrical generator output, platform pitch and tip out-of-plane deflection for one blade were investigated to understand the importance of each studied parameter on the responses. The results for both below- and above-rated wind speed are presented. It is important to be noted that only some of the results without any interpretation are presented in following sections while the full results are presented in APPENDIX 2.

5.1 Hywind Demo results

5.1.1 Below-rated wind speed

5.1.1.1 Variation of wave characteristics

Higher wave characteristics (H_s and T_p) generated higher standard deviations while the mean values remained almost constant in evaluated responses.

As an example, Figure 20 shows a dramatic growth in standard deviation of platform pitch from 0.2202 degree for case1 compare to 1.489 degrees for case9. Moreover, mean platform pitch remains fairly static, changes from 1.564 degrees for case1 to 1.524 degrees for case9. Mean and standard deviation of platform pitch for all cases are presented in Table 12.

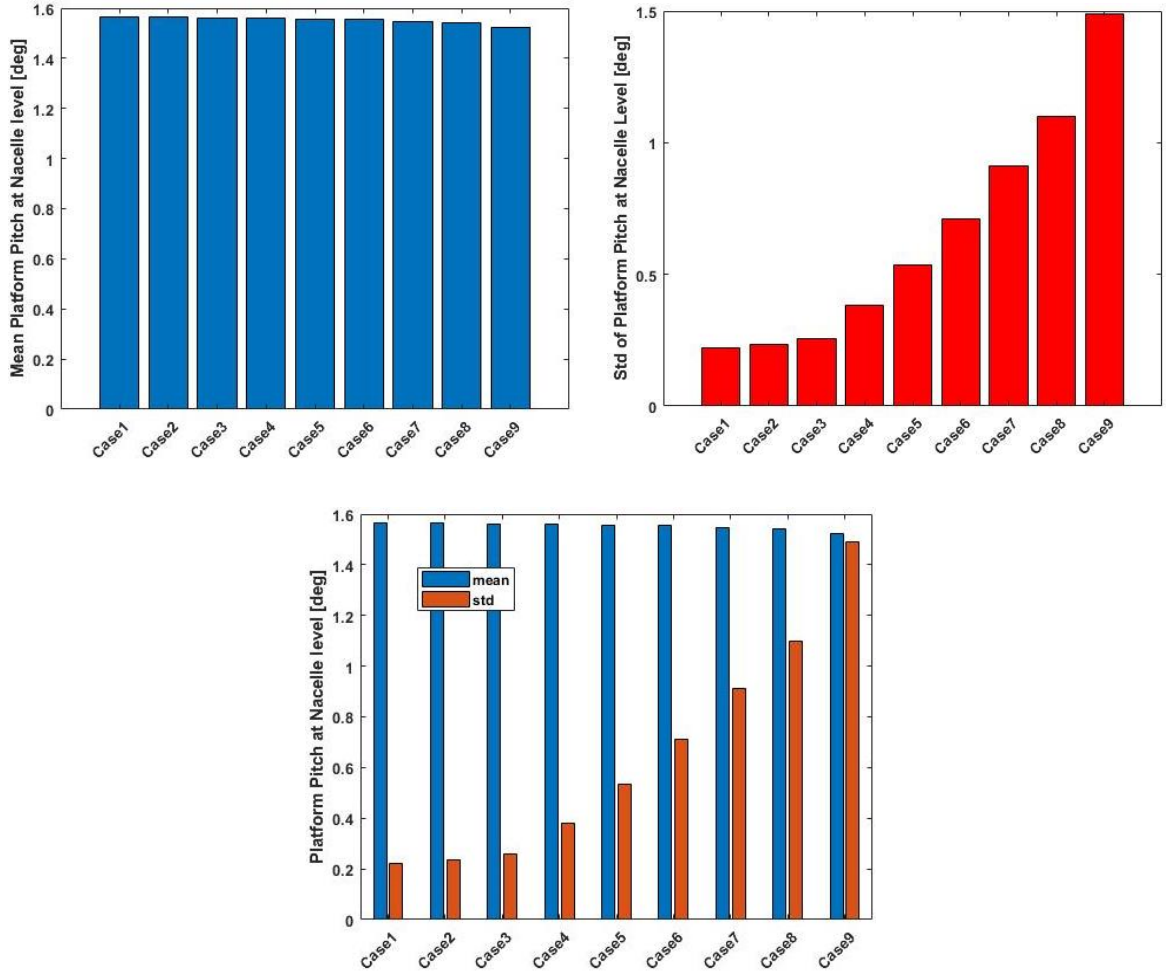

Figure 20. Mean and standard deviation of platform pitch for different wave characteristics in the below-rated wind speed.

Table 12. Mean and standard deviation of platform pitch.

	Case1	Case2	Case3	Case4
	H_s=0.75 [m] T_p=6.5 [sec]	H_s=1.4 [m] T_p=8.6 [sec]	H_s=2.25 [m] T_p=8.5 [sec]	H_s=4.25 [m] T_p=9.5 [sec]
Mean platform pitch [deg]	1.564	1.563	1.562	1.561
Std of platform pitch [deg]	0.2202	0.2345	0.2574	0.3825

	Case5	Case6	Case7	Case8	Case9
	H_s=5.75 [m] T_p=10.5 [sec]	H_s=7.25 [m] T_p=11.5 [sec]	H_s=8.75 [m] T_p=12.5 [sec]	H_s=10.25 [m] T_p=13.5 [sec]	H_s=12.25 [m] T_p=15.5 [sec]
Mean platform pitch [deg]	1.558	1.555	1.548	1.541	1.524
Std of platform pitch [deg]	0.5337	0.7096	0.9098	1.0990	1.4890

5.1.1.2 Variation of turbulence intensity

Higher turbulence intensity produced significantly higher standard deviations while mean values decreased gently in evaluated responses.

For instance, Figure 21 illustrates that by increasing the turbulence intensity from 5% to 15%, the standard deviation of electrical generation output increases from 127.5 to 341 kW, while the mean electrical generation output slightly decreases from 1.339 MW to 1.291 MW. Mean and standard deviation of electrical generator output for different turbulence intensities are presented in Table 12.

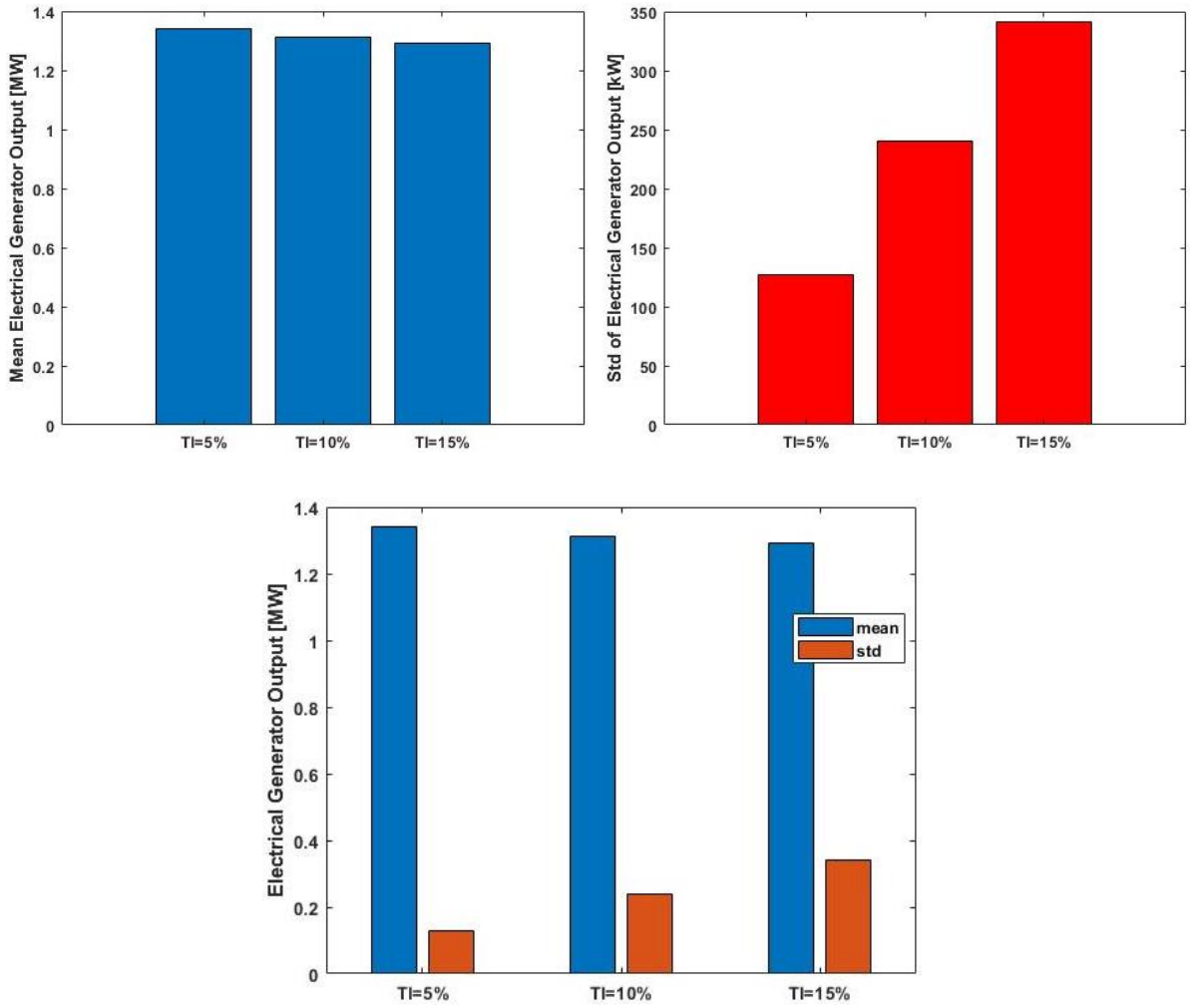

Figure 21. Mean and standard deviation of electrical generator output for different turbulence intensities in the below-rated wind speed.

Table 13. Mean and standard deviation of electrical generator output.

	TI=5%	TI=10%	TI=15%
Mean electrical generator output [MW]	1.339	1.313	1.291
Std of electrical generator output [kW]	127.5	240.8	341

5.1.1.3 Variation of alpha in wind shear profile power law

Varying α in wind shear profile power law showed no significant effect on both mean and standard deviation of the investigated responses.

To present an example, Figure 22 depicts that mean tip out-of-plane of one blade reduces gradually from 1.742 m to 1.725 m when alpha increases from 0 to 0.14. However, standard deviation of the response gradually increases from 17.21 cm to 18.3 cm. Mean and standard deviation of tip out-of-plane deflection of one blade for different alphas are tabulated in Table 14.

Table 14. Mean and standard deviation of tip out-of-plane deflection of one blade.

	α=0	α=0.05	α=0.10	α=0.12	α=0.14
Mean tip out-of-plane deflection of one blade [m]	1.742	1.736	1.730	1.727	1.725
Std of tip out-of-plane deflection of one blade [cm]	17.21	17.35	17.73	18.00	18.30

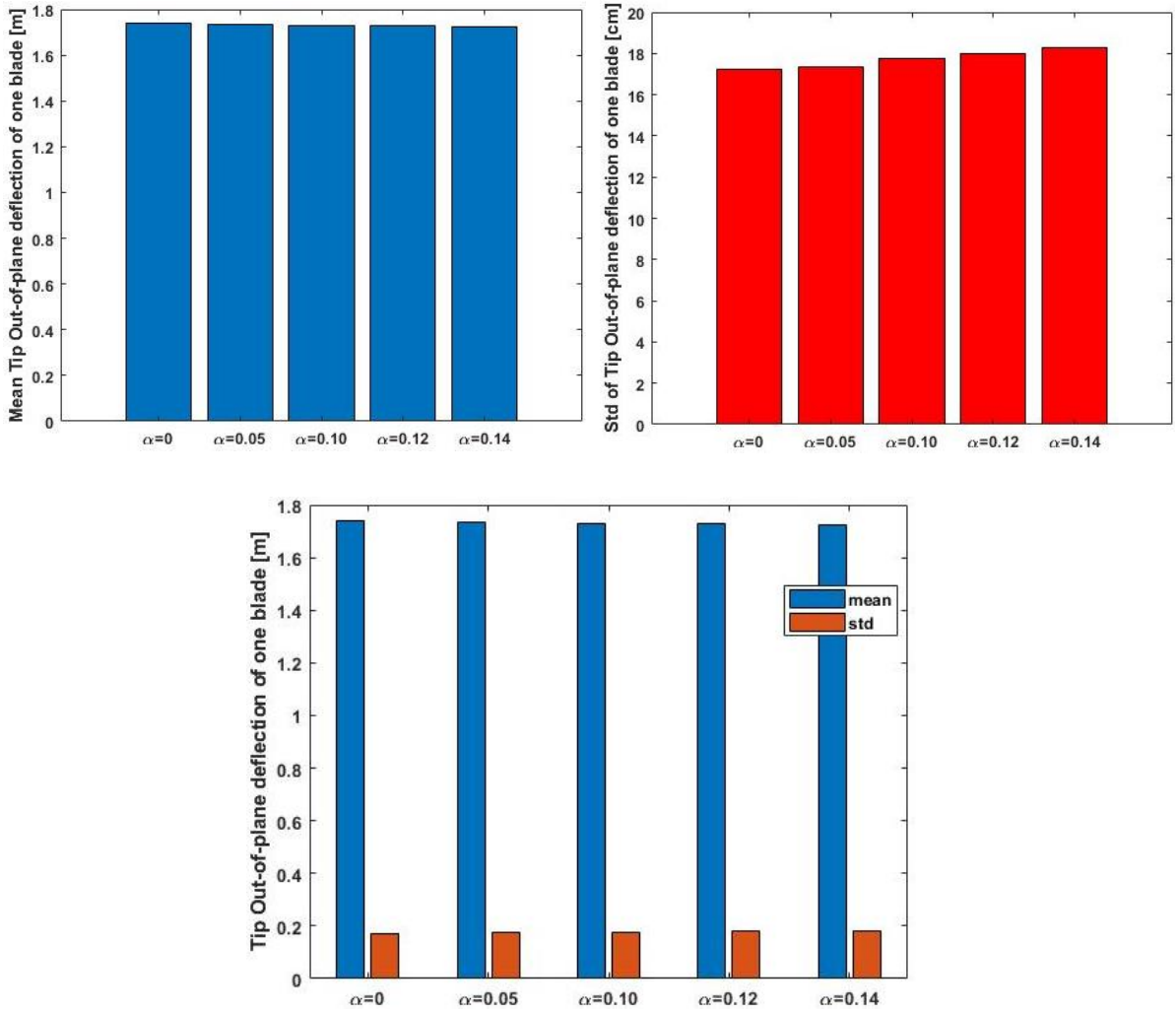

Figure 22. Mean and standard deviation of tip out-of-plane deflection of one blade for different alphas in wind shear power law in the below-rated wind speed.

5.1.1.4 Variation of the spatial resolution of the numerical wind field

Both mean and standard variation values of the studied responses fluctuated by changing the spatial resolution of the numerical wind field.

For example, the results, shown in Figure 23, indicate that the mean electrical generator output fluctuates from 1.313 MW for case1 to 1.384 MW for case 2, 1.391 MW for case3 and 1.374 MW for case4. Moreover, the standard deviation of the response also shows the pattern of fluctuation with lowest value of 208 kW for case2 and highest value of 250 kW for case3. Table 15 presents mean and standard deviation of electrical generator output for all cases.

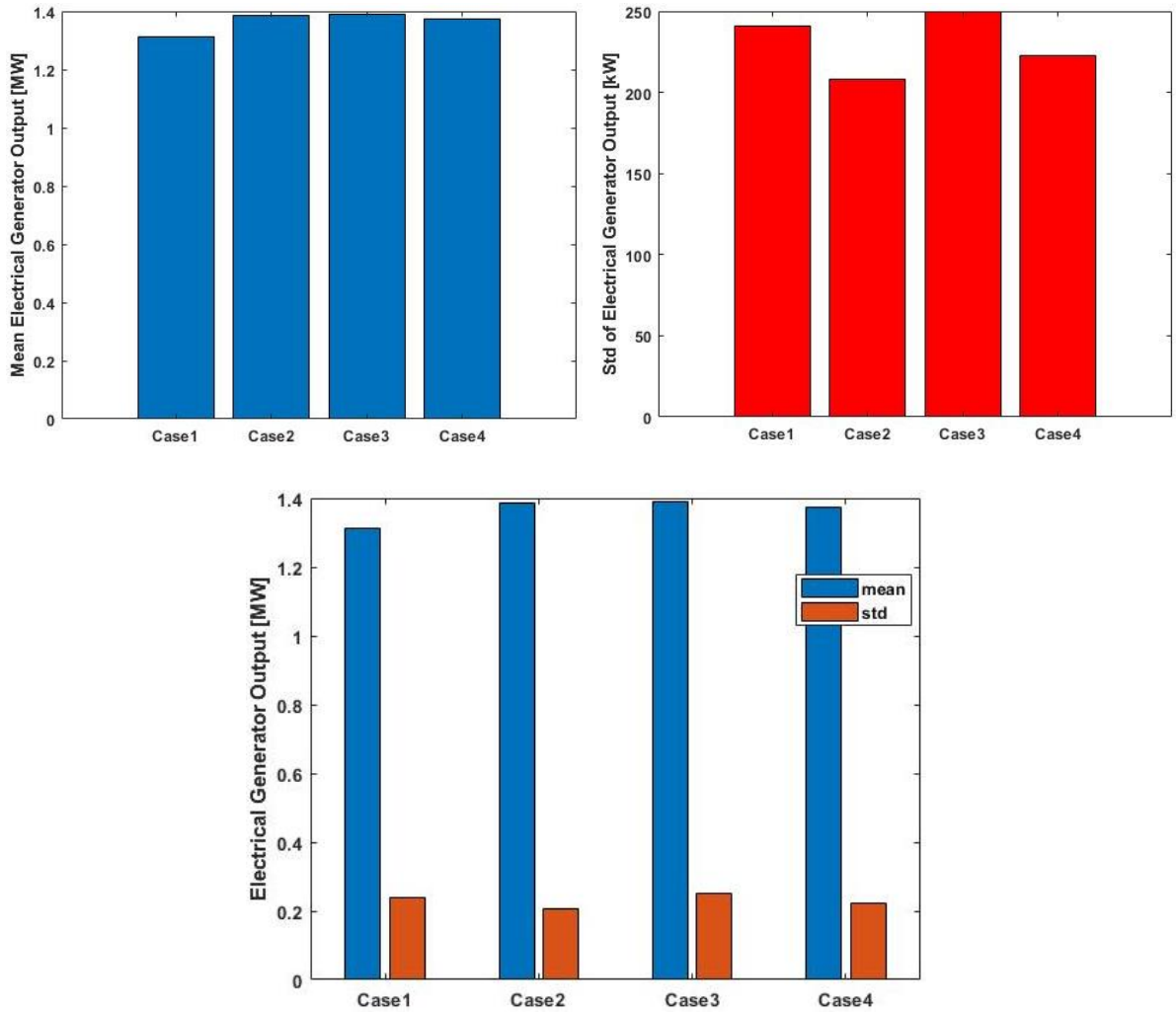

Figure 23. Mean and standard deviation of electrical generator output for different spatial resolutions in the below-rated wind speed.

Table 15. Mean and standard deviation of electrical generator output.

	Case1	Case2	Case3	Case4
	dx=1.318 [m] dy=2 [m] dz=2 [m]	dx=2.636 [m] dy=4 [m] dz=4 [m]	dx=5.272 [m] dy=8 [m] dz=8 [m]	dx=10.544 [m] dy=16 [m] dz=16 [m]
Mean electrical generator output [MW]	1.313	1.384	1.391	1.374
Std of electrical generator output [kW]	240.8	208	250	222.8

5.1.2 Above-rated wind speed

5.1.2.1 Variation of wave characteristics

While mean values of the evaluated responses remained almost constant, standard deviation of the responses rapidly increased as significant wave height and wave peak period increased.

As an example, Figure 24 illustrates that standard deviation of tip out-of-plane deflection of one blade rises from 37.93 cm for case1 to 54.4 cm for case9 while the mean tip out-of-plane deflection of one blade is almost stable and changes barely between 1.039 m and 1.049 m. Mean and standard deviation of tip out-of-plane deflection of one blade for different wave characteristics are presented in Table 16.

Table 16. Mean and standard deviation of tip out-of-plane deflection of one blade.

	Case1	Case2	Case3	Case4
	H_s=0.75 [m] T_p=6.5 [sec]	H_s=2.25 [m] T_p=8.5 [sec]	H_s=4 [m] T_p=10 [sec]	H_s=4.25 [m] T_p=9.5 [sec]
Mean tip out-of-plane deflection of one blade [m]	1.039	1.039	1.042	1.041
Std of tip out-of-plane deflection of one blade [cm]	37.93	38.80	41.62	41.54

	Case5	Case6	Case7	Case8	Case9
	H_s=5.75 [m] T_p=10.5 [sec]	H_s=7.25 [m] T_p=11.5 [sec]	H_s=8.75 [m] T_p=12.5 [sec]	H_s=10.25 [m] T_p=13.5 [sec]	H_s=12.25 [m] T_p=15.5 [sec]
Mean tip out-of-plane deflection of one blade [m]	1.043	1.049	1.045	1.048	1.043
Std of tip out-of-plane deflection of one blade [cm]	44.66	47.86	50.29	52.51	54.40

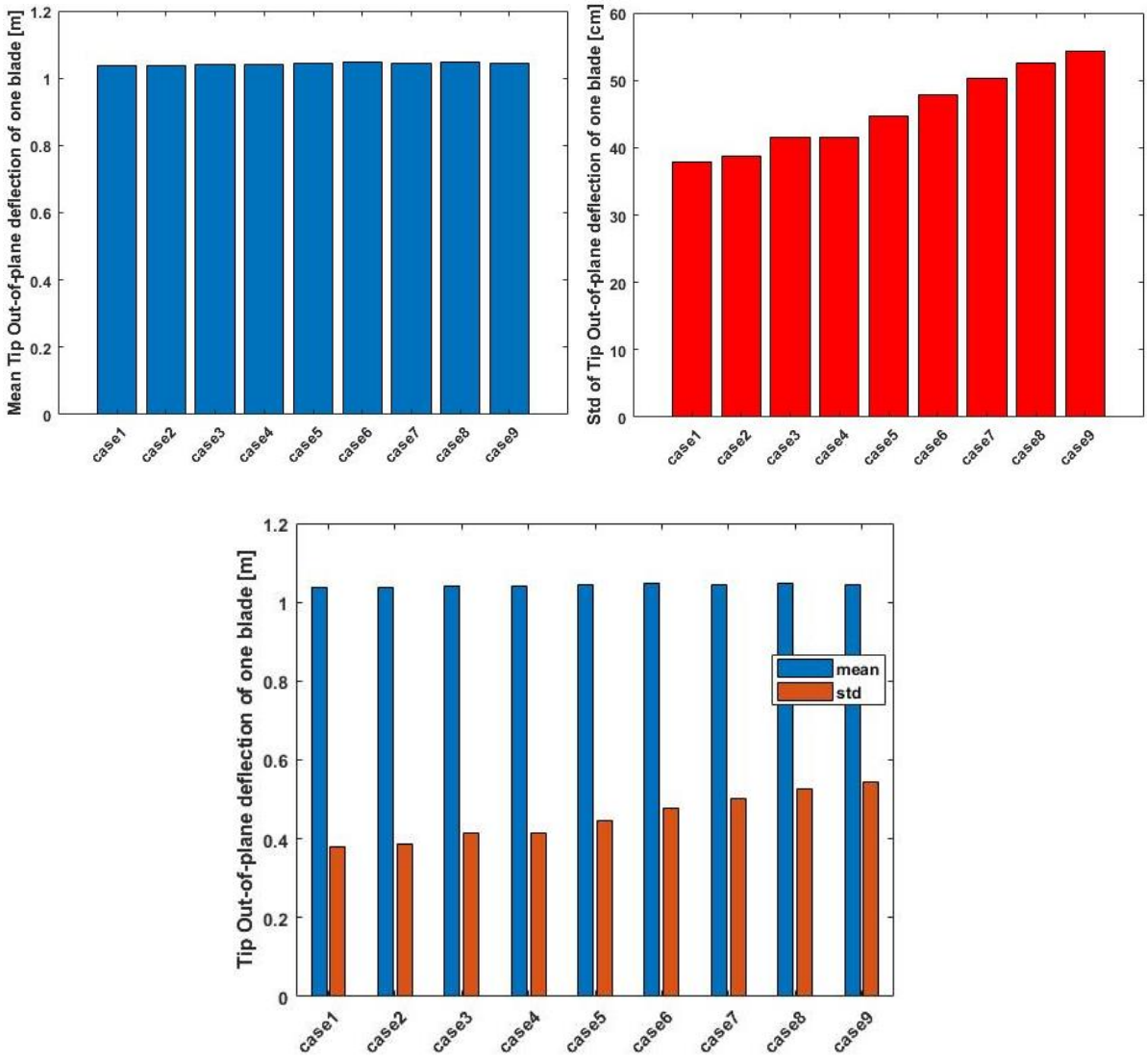

Figure 24. Mean and standard deviation of tip out-of-plane deflection of one blade for different wave characteristics in the above-rated wind speed.

5.1.2.2 Variation of turbulence intensity

By increasing turbulence intensity, the standard deviation of the responses grew significantly, and mean value of the studied responses changed gently.

To present an example, it can be seen from Figure 25 that standard deviation of platform pitch goes up from 0.3696 degree to 0.5502 degree for turbulence intensity of 5% and 15% respectively. Moreover, the mean value of platform pitch increases slowly from 1.295 degrees

for TI=5% to 1.325 degrees for TI=15%. Mean and standard deviation of platform pitch for different turbulence intensities are presented in Table 17.

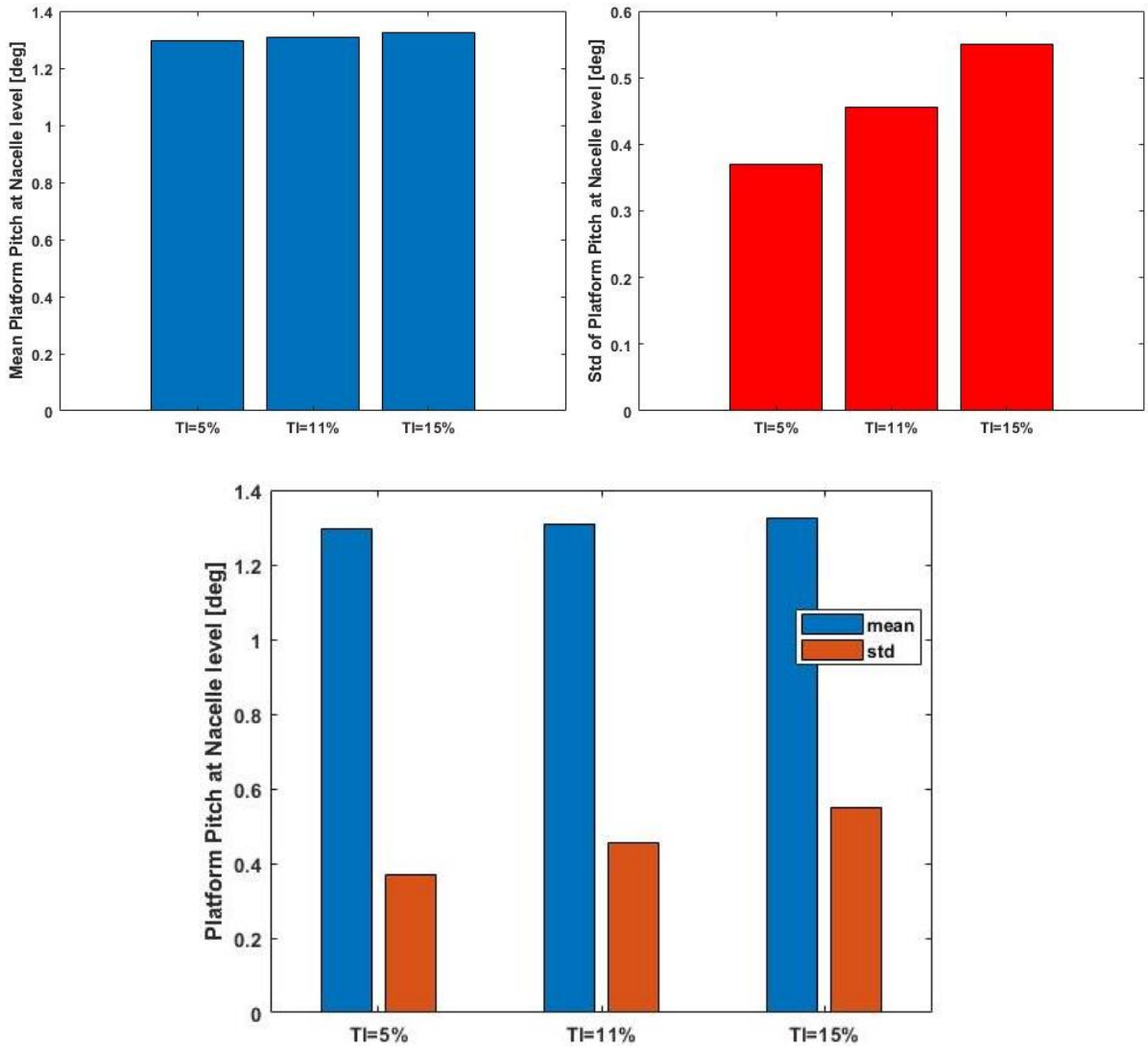

Figure 25. Mean and standard deviation of platform pitch for three turbulence intensities in above-rated wind speed.

Table 17. Mean and standard deviation of platform pitch.

	TI=5%	TI=11%	TI=15%
Mean platform pitch [deg]	1.295	1.310	1.325
Std of platform pitch [deg]	0.3696	0.4556	0.5502

5.1.2.3 Variation of alpha in wind shear profile power law

The results showed that the effect of alpha variation in wind shear profile is negligible in both mean and standard deviation of the investigated responses.

For example, Figure 26 proves that the standard deviation of tip out-of-plane deflection of one blade increases gently from 38.85 cm to 42.56 cm by increasing of alpha from 0 to 0.14 while the mean value remains constant at approximately 1.04 m, with minimum value of 1.037 m and maximum value of 1.042 m. Mean and standard deviation of tip out-of-plane deflection of one blade for different alphas are tabulated in Table 18.

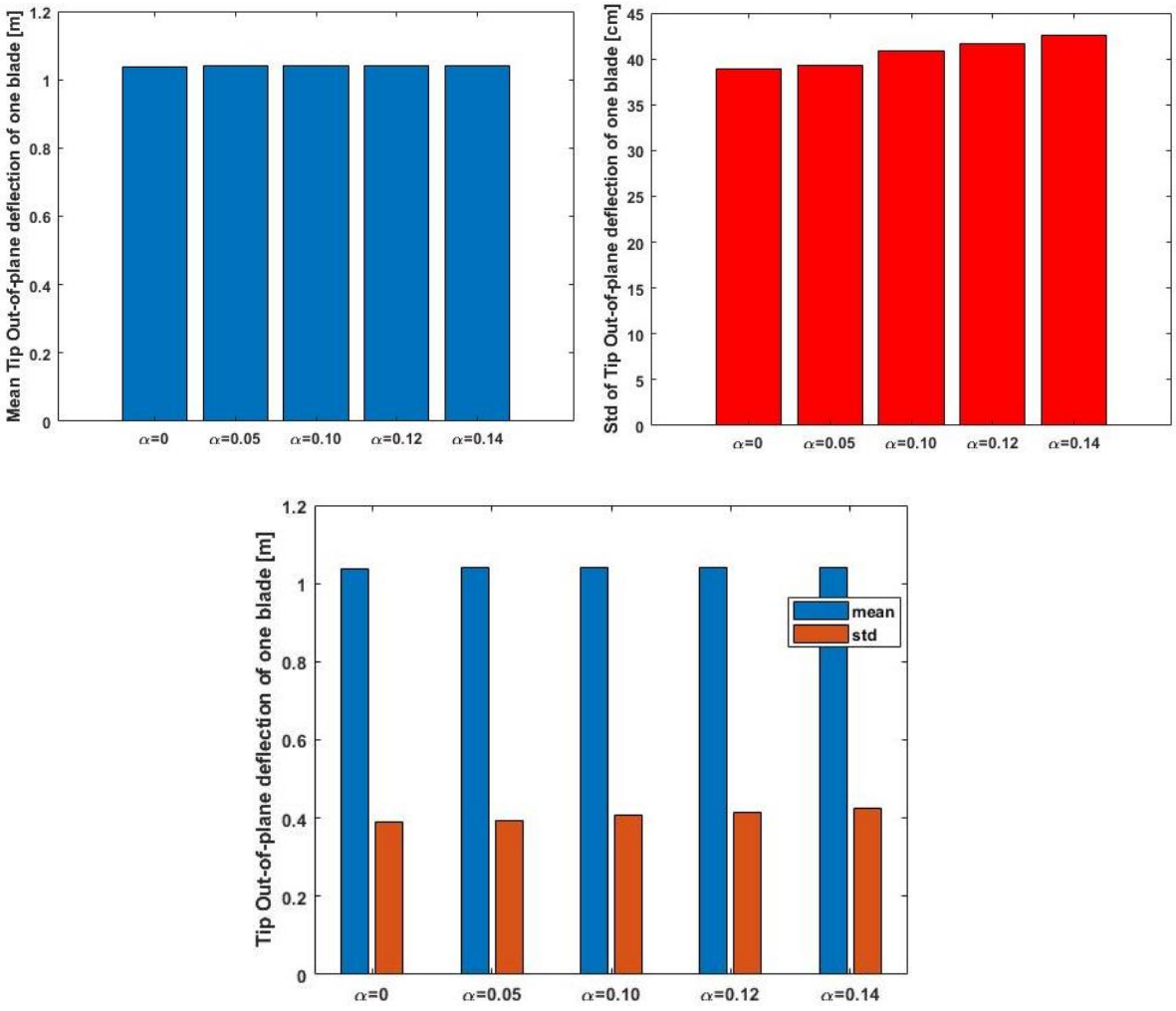

Figure 26. Mean and standard deviation of tip out-of-plane deflection of one blade for different alphas in wind shear power law in the above-rated wind speed.

Table 18. Mean and standard deviation of tip out-of-plane deflection of one blade.

	α=0	α=0.05	α=0.10	α=0.12	α=0.14
Mean tip out-of-plane deflection of one blade [m]	1.037	1.041	1.042	1.042	1.041
Std of tip out-of-plane deflection of one blade [cm]	38.85	39.35	40.81	41.62	42.56

5.1.2.4 Variation of the spatial resolution of the numerical wind field

The results showed minor effect of the spatial resolution variation on the studied responses.

For instance, Figure 27 illustrates a fluctuation in the standard deviation of electrical generator output between 20.26 kW for case3 and 30.02 kW for case1, while mean value changes slightly between 2.297 MW for case1 and 2.299 MW for case2 and case3. Mean and standard deviation of electrical generator output for different spatial resolutions are presented in Table 19.

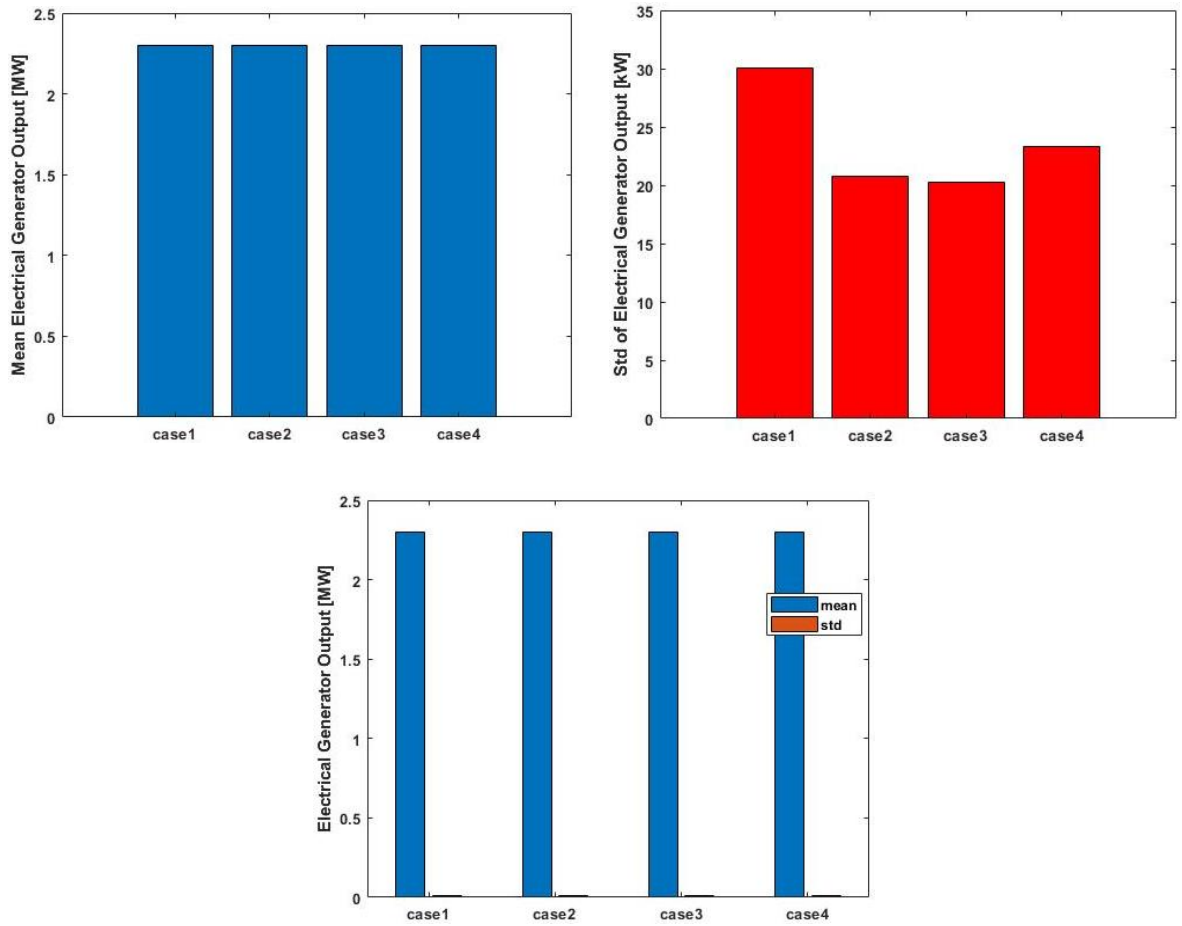

Figure 27. Mean and standard deviation of electrical generator output for different spatial resolutions in the above-rated wind speed.

Table 19. Mean and standard deviation of electrical generator output.

	Case1	Case2	Case3	Case4
	dx=2.283 [m] dy=2 [m] dz=2 [m]	dx=4.566 [m] dy=4 [m] dz=4 [m]	dx=9.132 [m] dy=8 [m] dz=8 [m]	dx=18.264 [m] dy=16 [m] dz=16 [m]
Mean electrical generator output [MW]	2.297	2.299	2.299	2.298
Std of electrical generator output [kW]	30.02	20.74	20.26	23.32

5.2 OC3-Hywind results

5.2.1 Below-rated wind speed

5.2.1.1 Variation of wave characteristics

The results showed the standard deviation of the studied responses rose by higher wave characteristics while the mean value of the responses remained almost unchanged.

To present an example, Figure 28 illustrates that standard deviation of platform pitch rises about 100% when wave characteristics increase from case1 to case9. The standard deviation is 0.5157 degree for case1 and grows to 1.023 degrees for case9. The mean platform pitch changes only 0.282 degree, from 4.968 degrees for case1 to 4.686 degrees for case9. Mean and standard deviation of platform pitch for different wave characteristics are presented in Table 20.

Table 20. Mean and standard deviation of platform pitch.

	Case1	Case2	Case3	Case4
	H_s=0.75 [m] T_p=6.5 [sec]	H_s=1.4 [m] T_p=8.6 [sec]	H_s=2.25 [m] T_p=8.5 [sec]	H_s=4.25 [m] T_p=9.5 [sec]
Mean platform pitch [deg]	4.968	4.967	4.966	4.957
Std of platform pitch [deg]	0.5157	0.5195	0.5229	0.5466

	Case5	Case6	Case7	Case8	Case9
	H_s=5.75 [m] T_p=10.5 [sec]	H_s=7.25 [m] T_p=11.5 [sec]	H_s=8.75 [m] T_p=12.5 [sec]	H_s=10.25 [m] T_p=13.5 [sec]	H_s=12.25 [m] T_p=15.5 [sec]
Mean platform pitch [deg]	4.937	4.907	4.864	4.791	4.686
Std of platform pitch [deg]	0.6011	0.6666	0.7614	0.8673	1.0230

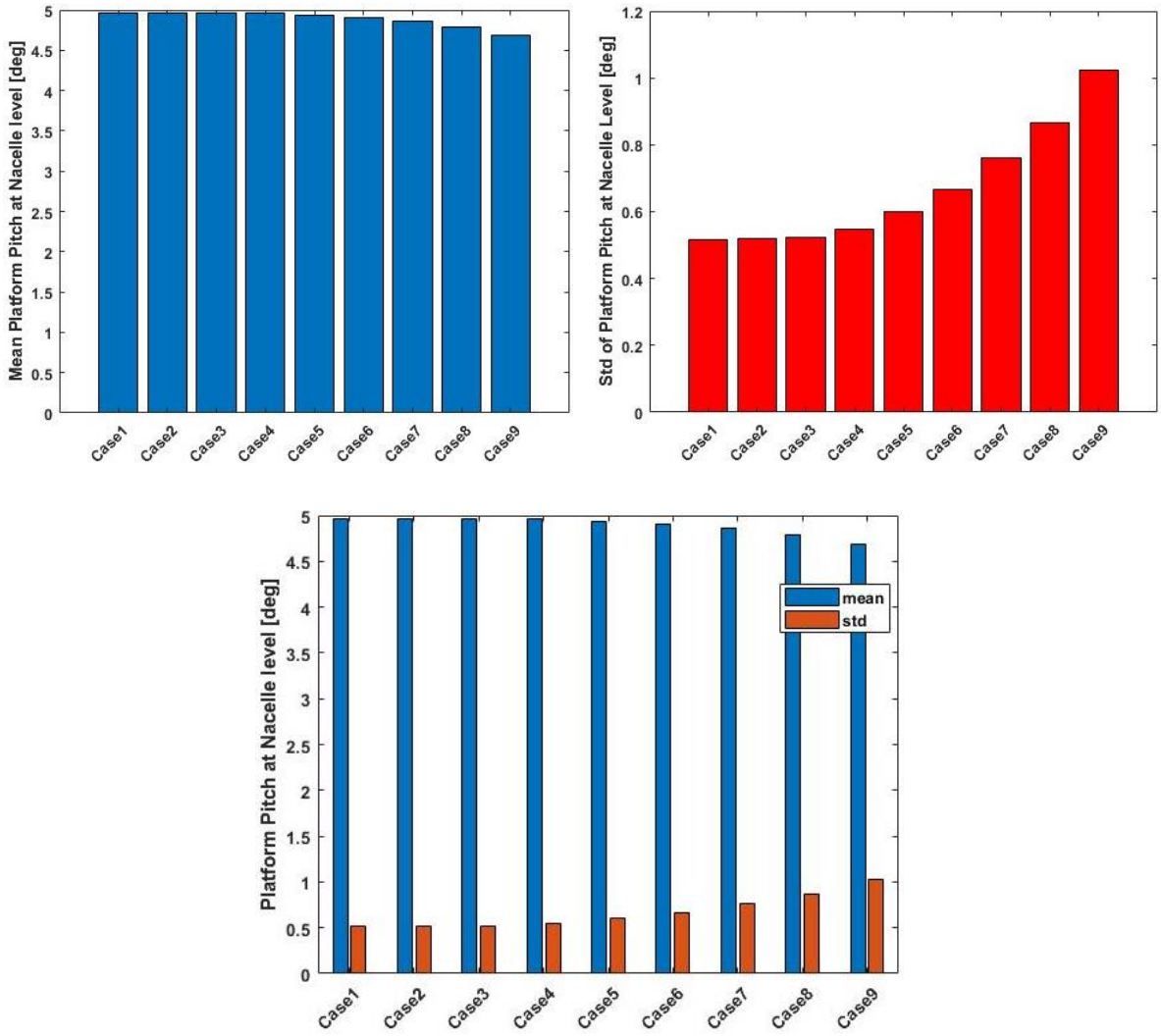

Figure 28. Mean and standard deviation of platform pitch for different wave characteristics in the below-rated wind speed.

5.2.1.2 Variation of turbulence intensity

While the mean value of the investigated responses dropped gradually, the standard deviation of the responses rose significantly when the turbulence intensity increased from 5% to 15%.

For example, from Figure 29 the decline of mean mechanical power from 4.544 MW when TI=5% to 4.252 MW when TI=15% can be clearly observed. The standard deviation grows though by increasing turbulence intensity. The standard deviation is 401.7 kW and 859.8 kW

when turbulence intensity equals to 5% and 15% respectively. Mean and standard deviation of mechanical power for different turbulence intensities are tabulated in Table 21.

Table 21. Mean and standard deviation of mechanical power.

	TI=5%	TI=10%	TI=15%
Mean mechanical power [MW]	4.544	4.411	4.252
Std of mechanical power [kW]	401.7	663.9	859.8

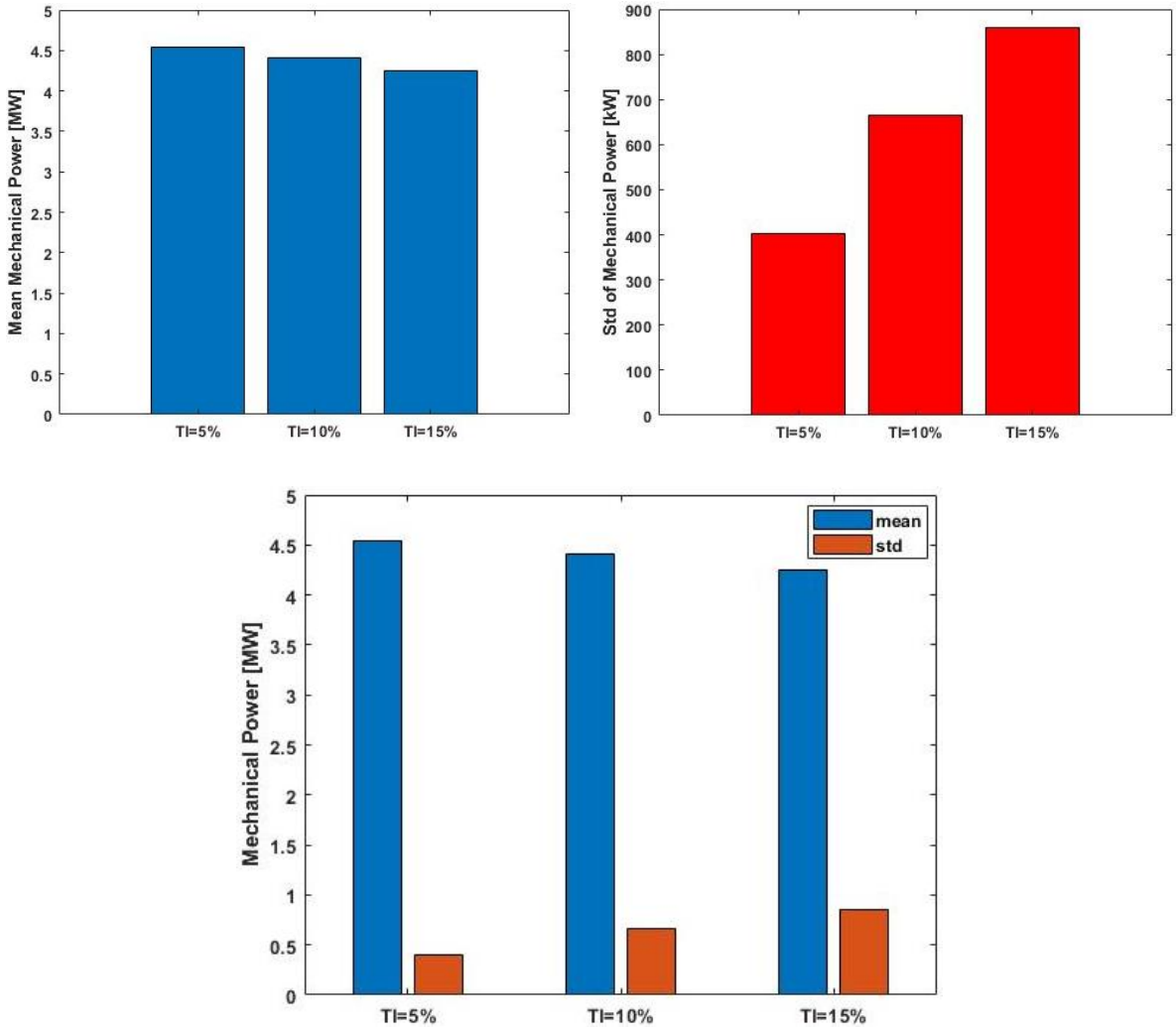

Figure 29. Mean and standard deviation of mechanical power for different turbulence intensities in the below-rated wind speed.

5.2.1.3 Variation of alpha in wind shear profile power law

The variation of alpha in wind shear profile power law has a slight effect on both mean and standard deviation of the evaluated responses.

For instance, the mean tip out-of-plane deflection of one blade changes from 5.197 m for α=0.14 to 5.217 m for α=0.05, presented in Figure 30. It can be seen from the data that the minimum standard deviation, 55.32 cm, occur when α=0.05. Moreover, the standard deviation is in its maximum, 59.23 cm, for α=0.14. Mean and standard deviation of tip out-of-plane deflection of one blade for different alphas are tabulated in Table 22.

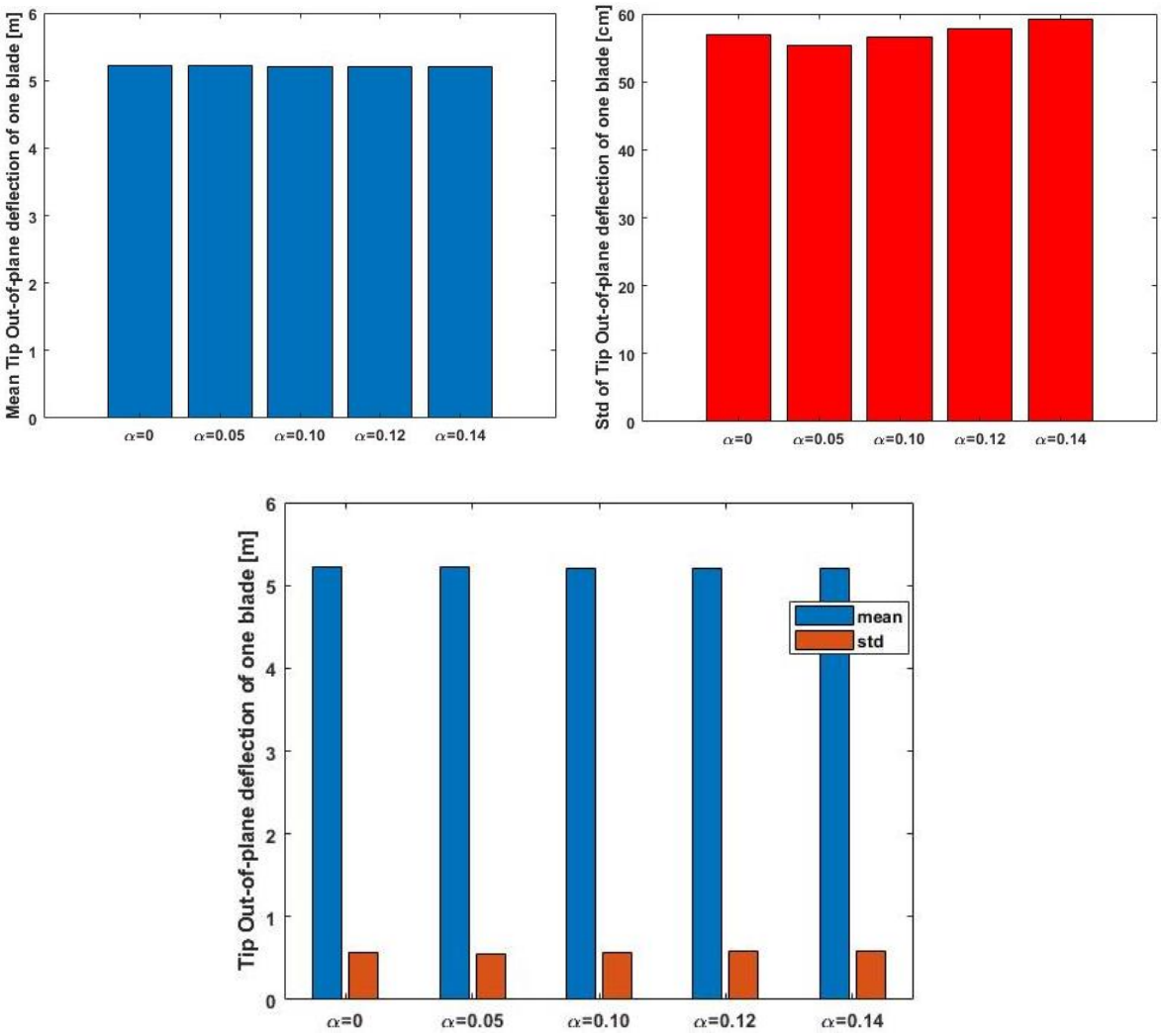

Figure 30. Mean and standard deviation of tip out-of-plane deflection of one blade for different alphas in wind shear power law in the below-rated wind speed.

Table 22. Mean and standard deviation of tip out-of-plane deflection of one blade.

	α=0	α=0.05	α=0.10	α=0.12	α=0.14
Mean tip out-of-plane deflection of one blade [m]	5.216	5.217	5.208	5.202	5.197
Std of tip out-of-plane deflection of one blade [cm]	56.92	55.32	56.67	57.73	59.23

5.2.1.4 Variation of the spatial resolution of the numerical wind field

The results indicated fluctuation in the studied responses of the structures with respect to the variation of spatial resolution of the numerical wind field.

As an example, Figure 31 illustrates that mean mechanical power is in its maximum, 4.661 MW, for case2 while the minimum mean value is 4.411 MW for case1. The data also show that the standard deviation fluctuates more widely. The standard deviation is 663.9 kW and 563.3 kW for case1 and case2 respectively. Mean and standard deviation of mechanical power for different spatial resolutions are presented in Table 23.

Table 23. Mean and standard deviation of mechanical power.

	Case1	Case2	Case3	Case4
	dx=1.318 [m] dy=2 [m] dz=2 [m]	dx=2.636 [m] dy=4 [m] dz=4 [m]	dx=5.272 [m] dy=8 [m] dz=8 [m]	dx=10.544 [m] dy=16 [m] dz=16 [m]
Mean mechanical power [MW]	4.411	4.661	4.573	4.602
Std of mechanical power [kW]	663.9	563.3	664	614.6

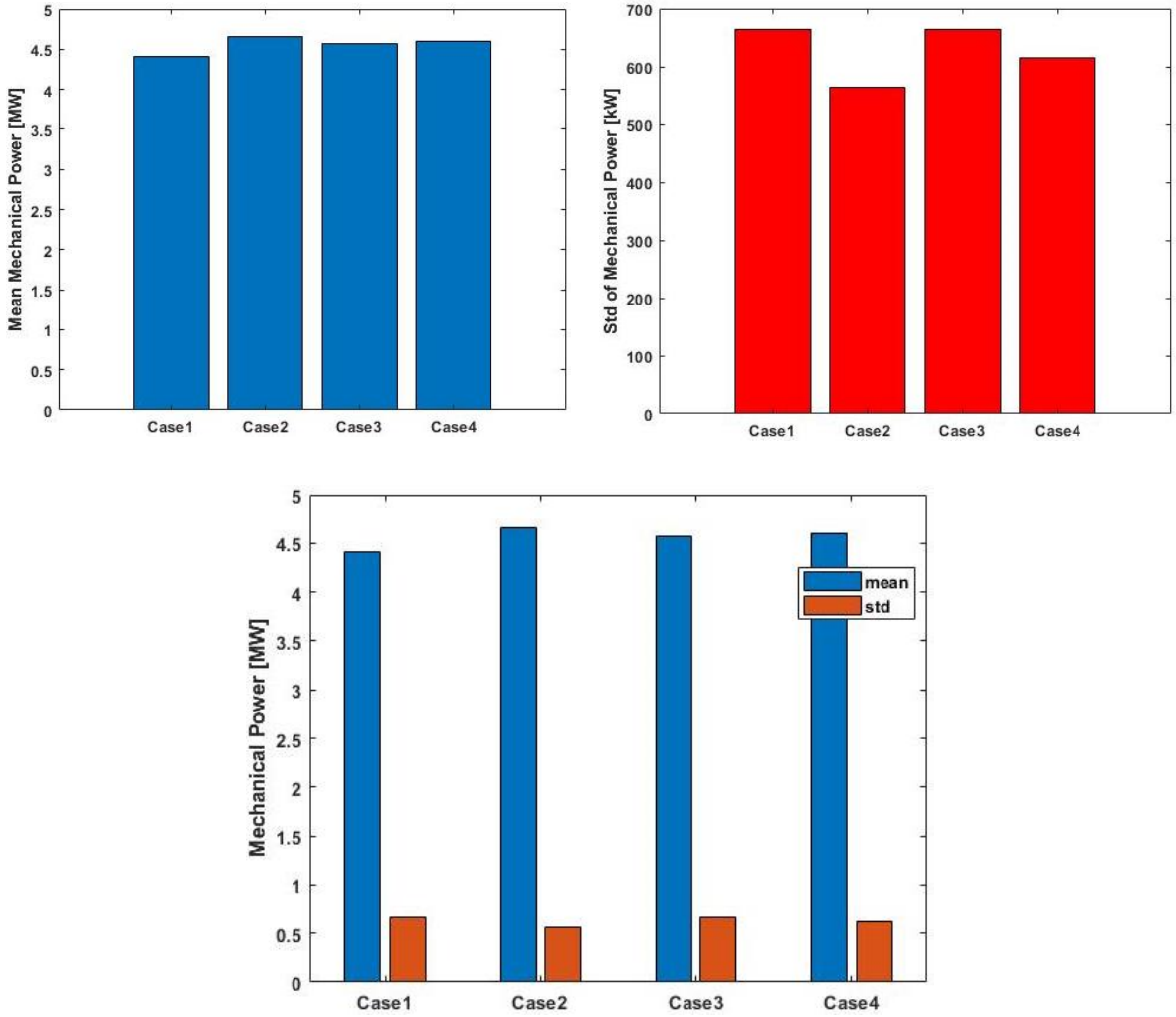

Figure 31. Mean and standard deviation of mechanical power for different spatial resolutions in the below-rated wind speed.

5.2.2 Above-rated wind speed

5.2.2.1 Variation of wave characteristics

The analyses showed that by increasing significant wave heights and wave peak periods, standard deviation of the investigated responses increased while the mean values remained almost steady.

To present an example, Figure 32 indicates that the standard deviation of tip out-of-plane deflection of one blade is 107.3 cm for case1 and rises constantly to 136.4 cm for case9.

Moreover, the mean value goes up and down slightly. The mean value fluctuates between 1.403 m for case1 and 1.339 m for case9. It also can be seen from Figure 32 that the standard deviation is higher than the mean value in case9, 1.364 m and 1.339 m respectively. Mean and standard deviation of tip out-of-plane deflection of one blade for different wave characteristics are presented in Table 24.

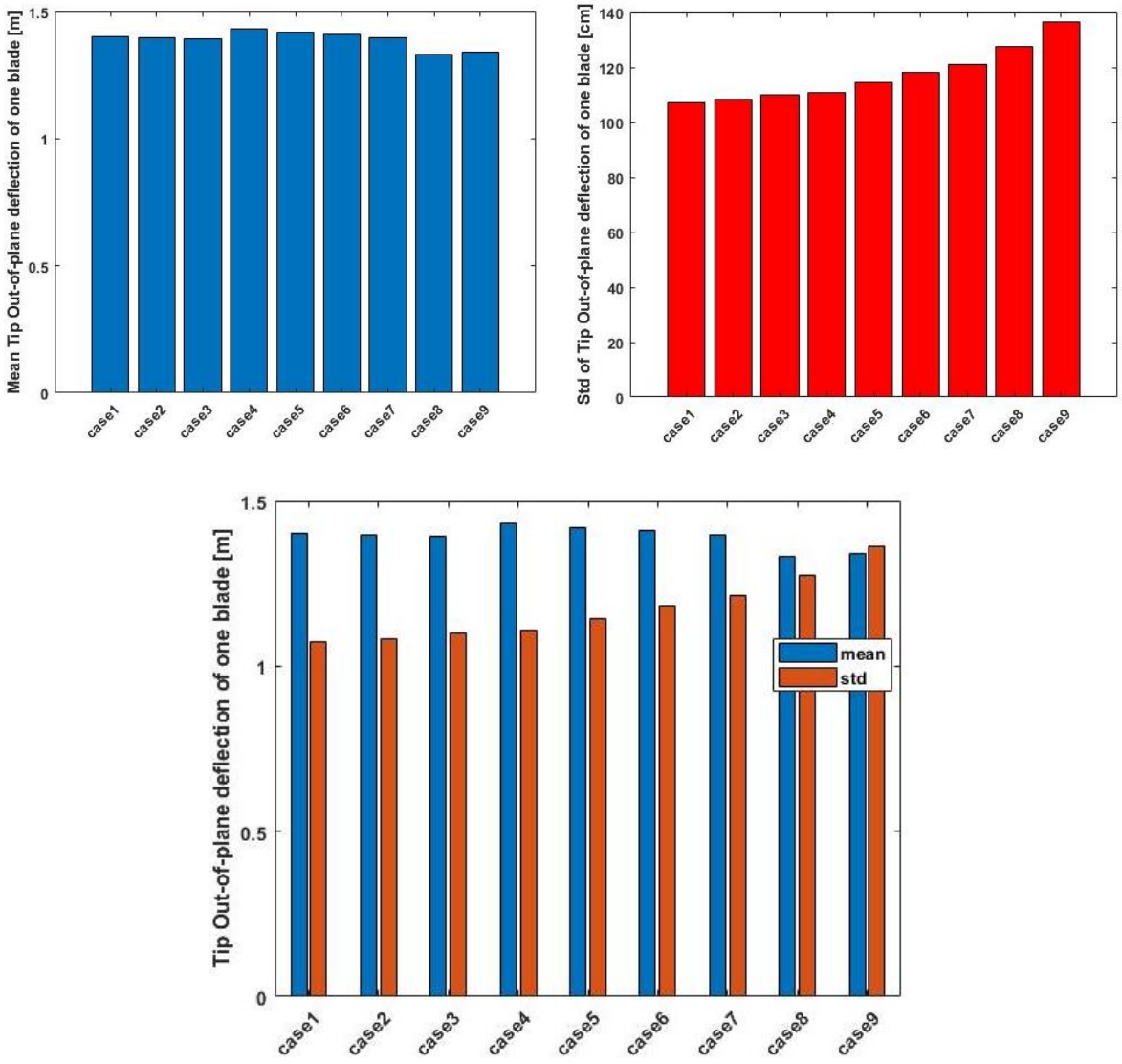

Figure 32. Mean and standard deviation of tip out-of-plane deflection of one blade for different wave characteristics in the above-rated wind speed.

Table 24. Mean and standard deviation of tip out-of-plane deflection of one blade.

	Case1	Case2	Case3	Case4
	H_s=0.75 [m] T_p=6.5 [sec]	H_s=2.25 [m] T_p=8.5 [sec]	H_s=4 [m] T_p=10 [sec]	H_s=4.25 [m] T_p=9.5 [sec]
Mean tip out-of-plane deflection of one blade [m]	1.403	1.397	1.391	1.431
Std of tip out-of-plane deflection of one blade [cm]	107.3	108.2	110.2	110.9

	Case5	Case6	Case7	Case8	Case9
	H_s=5.75 [m] T_p=10.5 [sec]	H_s=7.25 [m] T_p=11.5 [sec]	H_s=8.75 [m] T_p=12.5 [sec]	H_s=10.25 [m] T_p=13.5 [sec]	H_s=12.25 [m] T_p=15.5 [sec]
Mean tip out-of-plane deflection of one blade [m]	1.419	1.411	1.399	1.331	1.339
Std of tip out-of-plane deflection of one blade [cm]	114.3	118.3	121.2	127.4	136.4

5.2.2.2 Variation of turbulence intensity

The standard deviation of studied responses grew rapidly when turbulence intensity increases from 5% to 15%. However, the mean value slightly dropped by increasing turbulence intensity.

For example, Figure 33 illustrates that the standard deviation of platform pitch changes widely from 0.3396 degree for TI=5% to 0.8310 degree for TI=15%. The mean value drops about 0.1 degree when turbulence intensity grows 10%. The mean value is 2.810 degree for TI=5% and 2.706 degrees for TI=15%. Mean and standard deviation of platform pitch for different turbulence intensities are tabulated in Table 25.

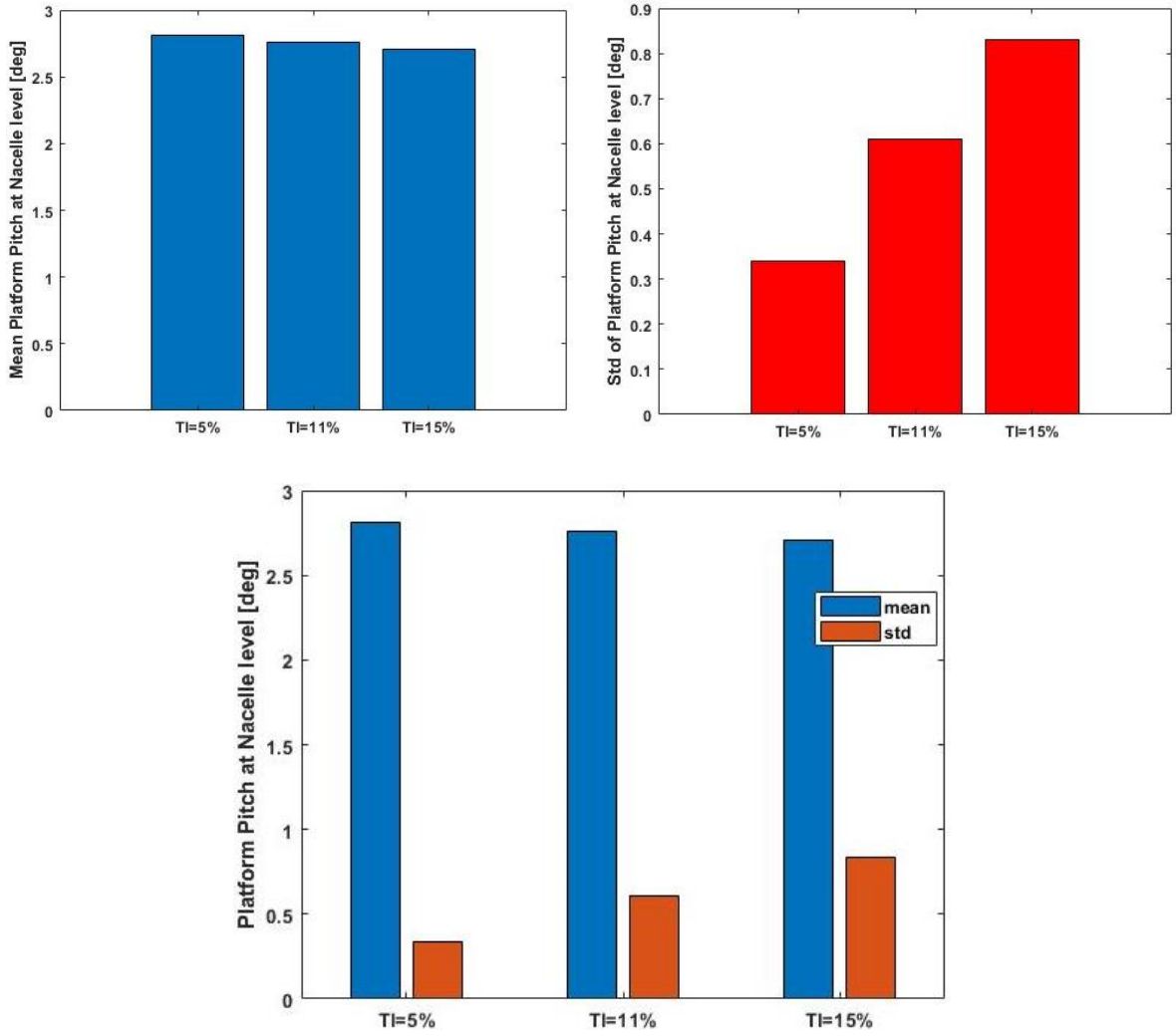

Figure 33. Mean and standard deviation of platform pitch for different turbulence intensities in the above-rated wind speed.

Table 25. Mean and standard deviation of platform pitch.

	TI=5%	TI=11%	TI=15%
Mean platform pitch [deg]	2.810	2.759	2.706
Std of platform pitch [deg]	0.3396	0.6109	0.8310

5.2.2.3 Variation of alpha in wind shear profile power law

Influence of alpha variation on standard deviation of tip out-of-plane deflection of one blade was noticeable. However, the effect of alpha variation was barely observed on other mean and standard deviation of the evaluated responses.

For instance, by variation of alpha, the difference between maximum and minimum of the mean tip out-of-plane deflection of one blade is 2.1 cm while the difference between maximum and minimum of the standard deviation is 21 cm, illustrated in Figure 34. The mean value falls from 1.405 m when α=0 to 1.384 m when α=0.14. However, the standard deviation grows from 94.7 cm when α=0 to 115.7 cm when α=0.14. Mean and standard deviation of tip out-of-plane deflection of one blade for different alphas are presented in Table 26.

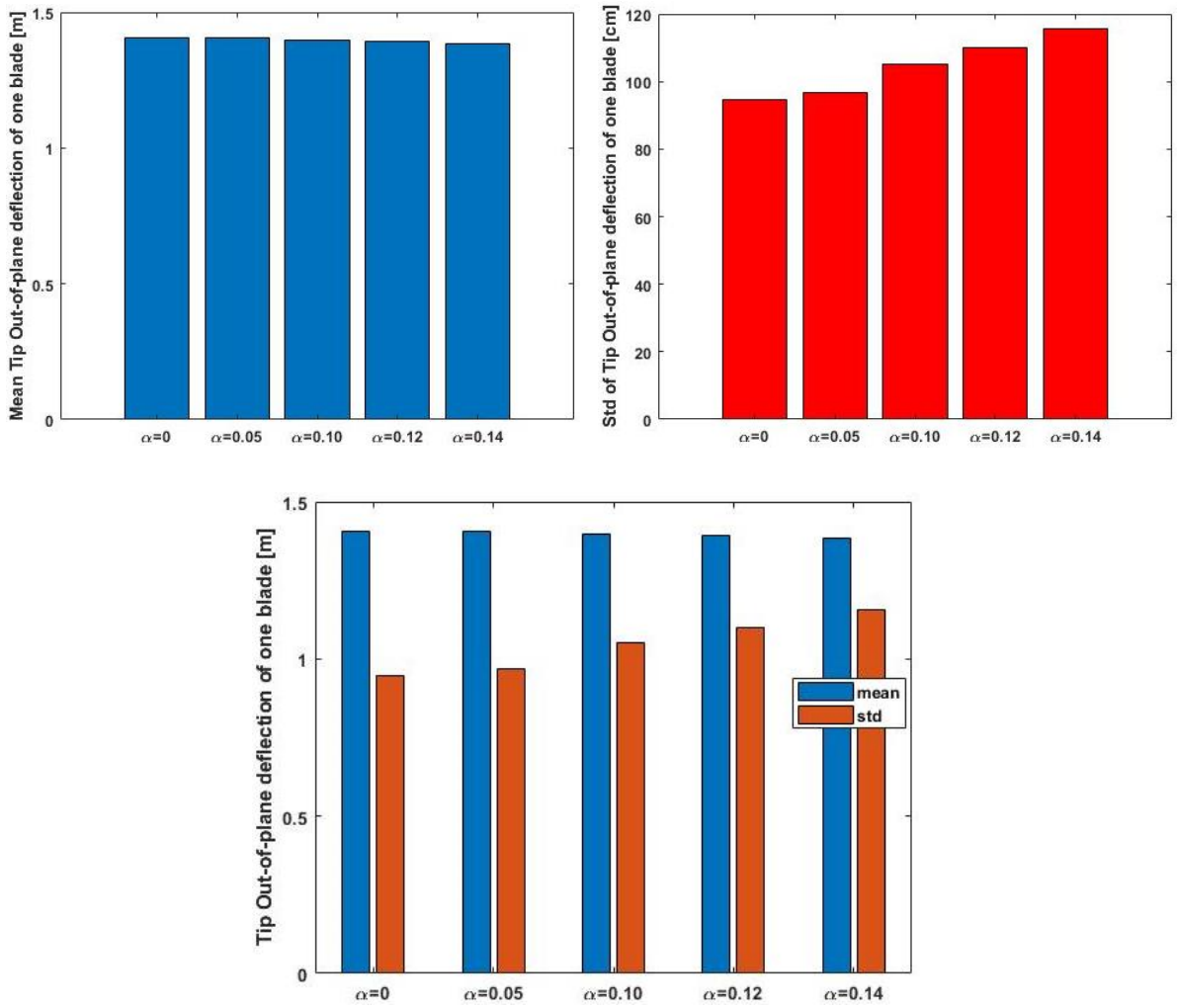

Figure 34. Mean and standard deviation of tip out-of-plane deflection of one blade for different alphas in wind shear power law in the above-rated wind speed.

Table 26. Mean and standard deviation of tip out-of-plane deflection of one blade.

	α=0	α=0.05	α=0.10	α=0.12	α=0.14
Mean tip out-of-plane deflection of one blade [m]	1.405	1.404	1.397	1.391	1.384
Std of tip out-of-plane deflection of one blade [cm]	94.7	96.7	105.3	110.2	115.7

5.2.2.4 Variation of the spatial resolution of the numerical wind field

By variation of spatial resolution of the numerical wind field, the standard deviation of the studied responses showed fluctuations, although the mean values remained almost stable.

As an example, Figure 35 indicates that mean mechanical power is almost constant for different cases. However, the standard deviation shows more variation over different cases, increase from 144.4 kW for case1 to 162.4 kW for case2 and decreases to 143.8 kW for case4. Mean and standard deviation of mechanical power for different spatial resolutions are tabulated in Table 27.

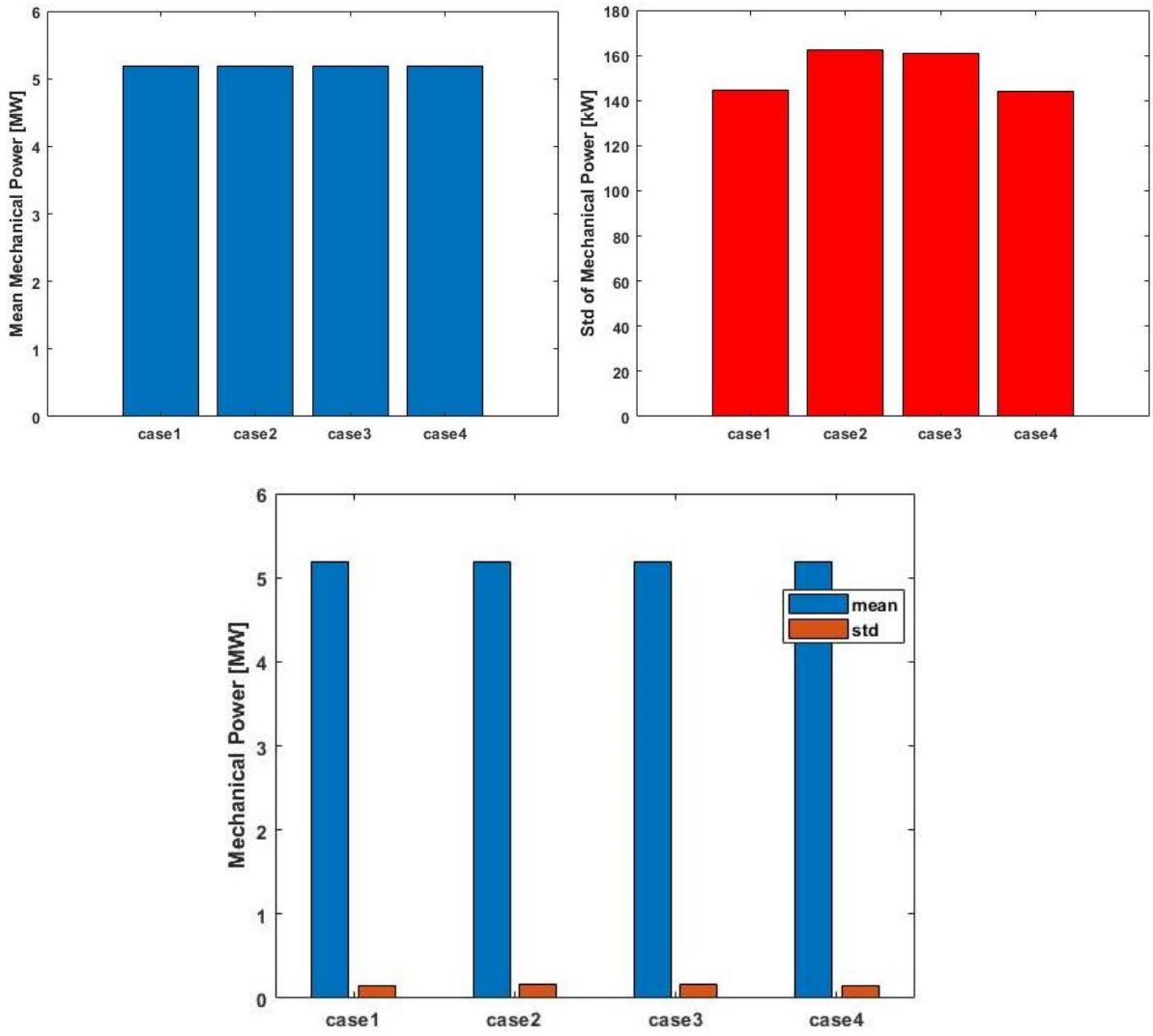

Figure 35. Mean and standard deviation of mechanical power for different spatial resolutions in the above-rated wind speed.

Table 27. Mean and standard deviation of mechanical power.

	Case1	Case2	Case3	Case4
	dx=2.283 [m] dy=2 [m] dz=2 [m]	dx=4.566 [m] dy=4 [m] dz=4 [m]	dx=9.132 [m] dy=8 [m] dz=8 [m]	dx=18.264 [m] dy=16 [m] dz=16 [m]
Mean mechanical power [MW]	5.190	5.188	5.187	5.190
Std of mechanical power [kW]	144.4	162.4	160.7	143.8

5.3 Coherence of the numerical wind field

Mann turbulence generator was used to generate a numerical wind field for both the below- and above-rated wind speed. By generating the numerical wind field, longitudinal (u´), lateral (v´) and vertical (w´) velocity fluctuations were available for each node.

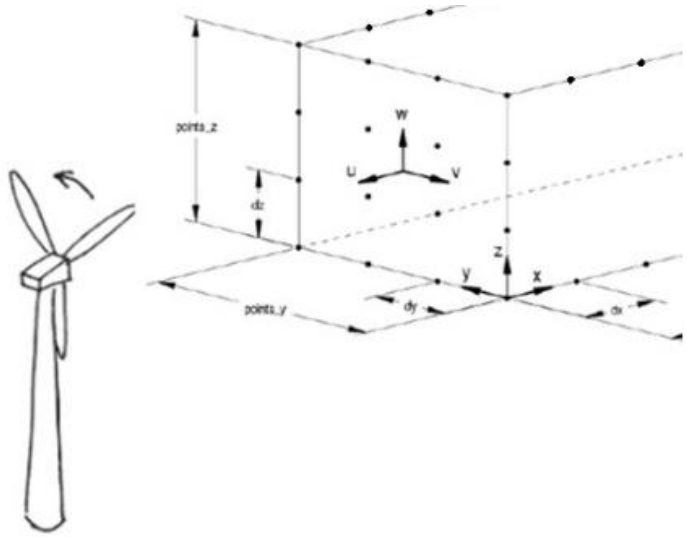

Figure 36. Numerical wind field.

longitudinal velocity fluctuation spectra for all nodes in y-z plane were calculated. Moreover, cross-spectral of longitudinal velocity fluctuation between each node and mid-node in y-z plane were calculated. Co-coherence, presented in Eq. (4), of longitudinal velocity fluctuation between each node and mid-node in y-z plane for frequency of 0.2 Hz and for the above-rated wind speed, 18.7 m/s, with 11% turbulence intensity is illustrated in Figure 37.

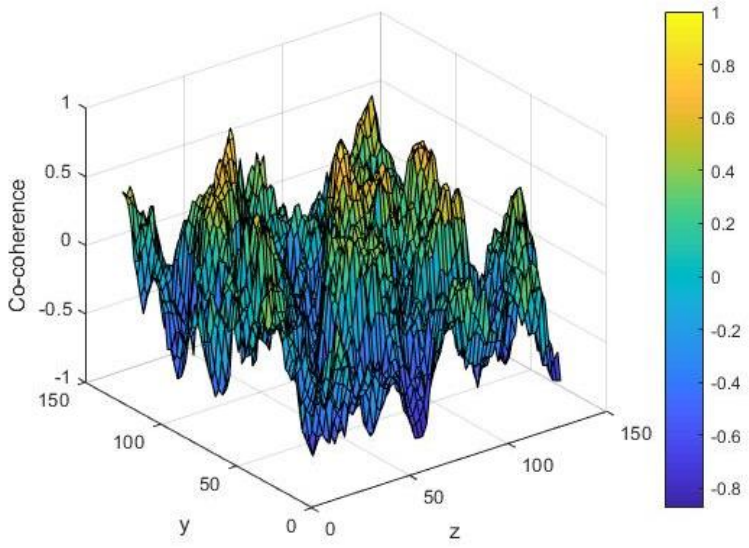

Figure 37. Co-coherence of longitudinal wind velocity fluctuation (u´) between each point and mid-point for frequency of 0.2 Hz.

Figure 38 shows the average co-coherence of longitudinal wind velocity fluctuation (u´) in various radius around mid-node in y-z plane for frequency of 0.2 Hz.

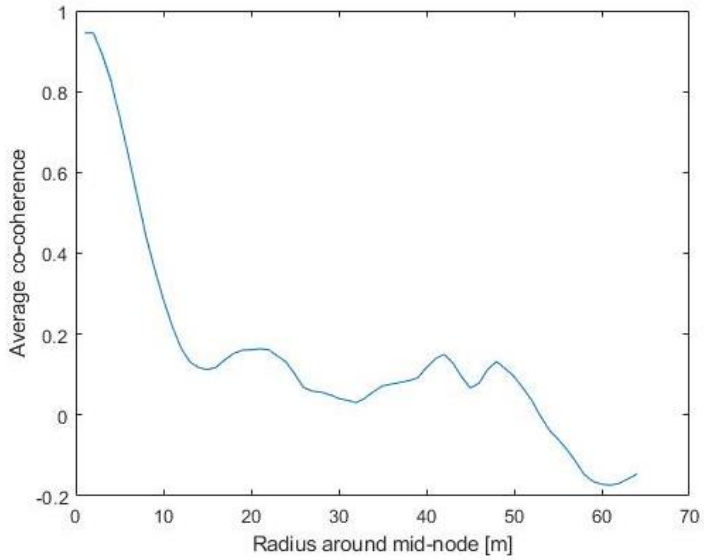

Figure 38. Average co-coherence of longitudinal wind velocity fluctuation (u´) in a radius around mid-node for frequency of 0.2 Hz.

Figure 39 presents co-coherence of longitudinal velocity fluctuation between each node and mid-node in y-z plane for frequency of 0.04 Hz and for the above-rated wind speed, 18.7 m/s, with 11% turbulence intensity.

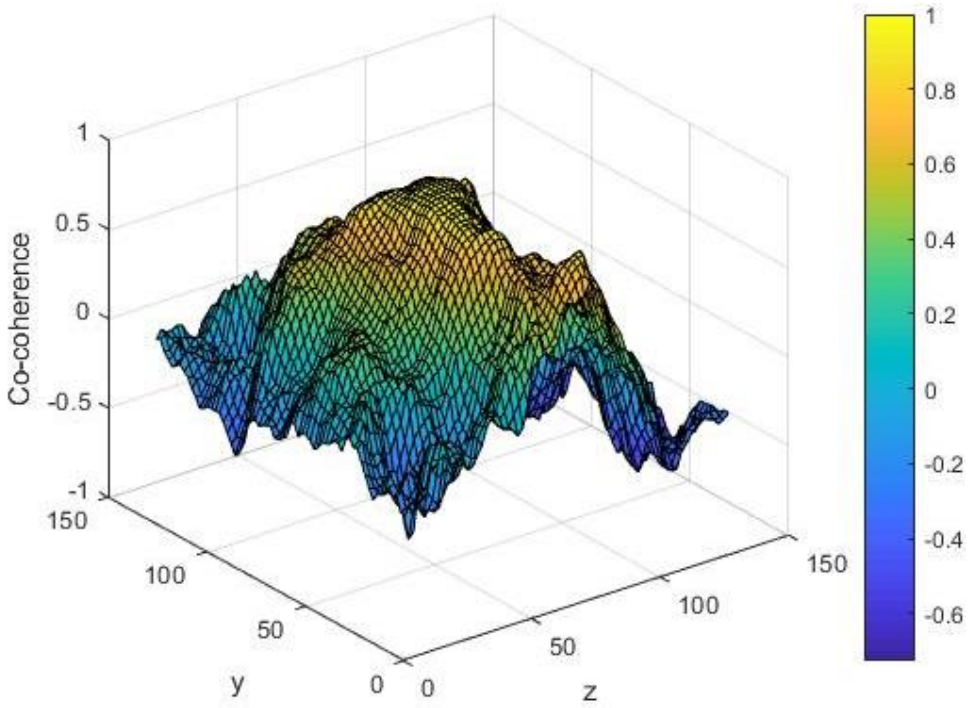

Figure 39. Co-coherence of longitudinal wind velocity fluctuation (u´) between each point and mid-point for frequency of 0.04 Hz.

Figure 40 presents the average co-coherence of longitudinal wind velocity fluctuation (u´) in various radius around mid-node in y-z plane for frequency of 0.04 Hz.

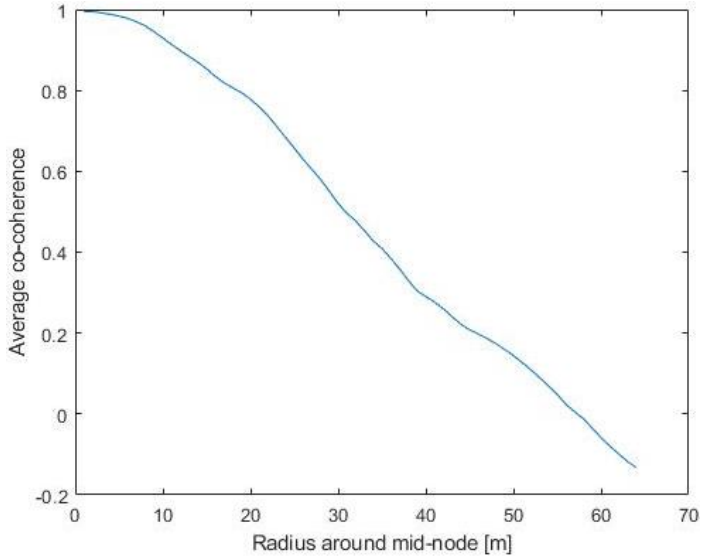

Figure 40. Average co-coherence of longitudinal wind velocity fluctuation (u´) in a radius around mid-node for frequency of 0.04 Hz.

CHAPTER 6 Discussion

In this chapter the results of dynamic analysis of both Hywind Demo and OC3-Hywind structures presented in previous chapter will be discussed. Moreover, the result of coherence will be discussed.

6.1 The dynamic responses of the structures

Various environmental parameters, i.e., wave characteristics, turbulence intensity, alpha in wind shear profile power law and spatial resolution of the numerical wind field, were varied to understand the effect of these parameters on structures' responses, i.e., electrical generator output, platform pitch and tip out-of-plane deflection of one blade. The effect of the parameters on the responses of Hywind Demo and OC3-Hywind presented in CHAPTER 5 will be discussed in following sections.

6.1.1 Wave characteristics

As presented in CHAPTER 5, standard deviation of responses rose significantly by increasing significant wave height (H_S) and wave peak period (T_P) for both studied structures and for both the below- and above-rated wind speed. Higher significant wave height and wave peak period cause higher excitation force on the structure which result in higher standard deviation of the responses.

Table 28 an Table 29 present that for both Hywind Demo and OC3-Hywind, mean power output increases, while standard deviation of power output decreases for the above-rated wind speed compared to the below-rated wind speed. It is important to be noted that all the minimum

and maximum values of structural responses in this chapter are presented to only have a quick overview over the variation of the responses. The exact numbers could be changed if the seed number changes.

Table 28. The maximum and minimum values of the Hywind Demo responses when wave characteristics were varied.

		Min.	Max.
below-rated wind speed (10.8 m/s)	Mean power output [MW]	1.313	1.316
	Std of power output [kW]	239.40	411.60
	Mean platform pitch [deg]	1.524	1.564
	Std of platform pitch [deg]	0.2202	1.4890
	Mean tip out-of-plane deflection of one blade [m]	1.697	1.727
	Std of tip out-of-plane deflection of one blade [cm]	17.91	27.73
above-rated wind speed (18.7 m/s)	Mean power output [MW]	2.281	2.300
	Std of power output [kW]	11.07	112.30
	Mean platform pitch [deg]	1.294	1.360
	Std of platform pitch [deg]	0.2819	1.6770
	Mean tip out-of-plane deflection of one blade [m]	1.039	1.049
	Std of tip out-of-plane deflection of one blade [cm]	37.93	54.40

Table 29. The maximum and minimum values of the OC3-Hywind responses when wave characteristics were varied.

		Min.	Max.
below-rated wind speed (10.8 m/s)	Mean power output [MW]	4.410	4.433
	Std of power output [kW]	659.20	890.60
	Mean platform pitch [deg]	4.686	4.968
	Std of platform pitch [deg]	0.5157	1.0230
	Mean tip out-of-plane deflection of one blade [m]	4.905	5.202
	Std of tip out-of-plane deflection of one blade [cm]	57.19	109.20
above-rated wind speed (18.7 m/s)	Mean power output [MW]	5.140	5.195
	Std of power output [kW]	140.00	213.80
	Mean platform pitch [deg]	2.736	2.765
	Std of platform pitch [deg]	0.5735	1.1070
	Mean tip out-of-plane deflection of one blade [m]	1.331	1.431
	Std of tip out-of-plane deflection of one blade [cm]	107.30	136.40

The growth in the mean power output for the above-rated wind speed compared to below-rated wind speed can be explained by Eq. (9):

$$\boldsymbol{P_{out} = \frac{1}{2} C_P A \rho u^3} \quad (9)$$

Where P_{out} is the output power, C_P is the power extraction coefficient, A is swept area of blades, $\boldsymbol{\rho}$ is air density and u is the wind velocity.

As it can be seen from the Eq. (9), the wind speed is extremely important for the amount of energy a wind turbine can convert to electricity, i.e. the power output will increase cubically with wind speed. Therefore, as the wind velocity is higher for the above-rated wind speed compared to the below-rated wind speed, mean power output is higher.

In order to understand why the standard deviation of output power decreased for the above-rated wind speed compared to the below-rated wind speed, the power curve for a wind turbine, presented in Figure 41, has to be investigated. It is obvious from Eq. (9) that power is proportional to the cube of wind speed and the figure shows this proportional for a below-rated wind speed. Therefore, small wind speed changes in a below-rated wind speed cause large power output differences. However, wind speed changes in an above-rated wind speed cause so small power output differences due to blade pitch control mechanism.

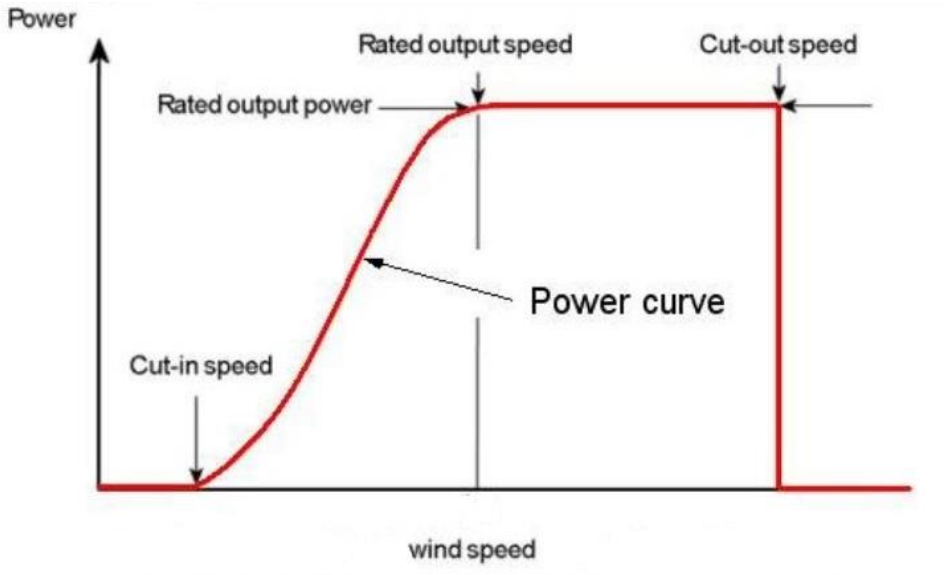

Figure 41. Typical wind turbine power output curve.

The results presented in Table 28 and Table 29 also show that for both structures, mean platform pitch declines, while standard deviation of platform pitch increases for the above-rated wind speed compared to the below-rated wind speed.

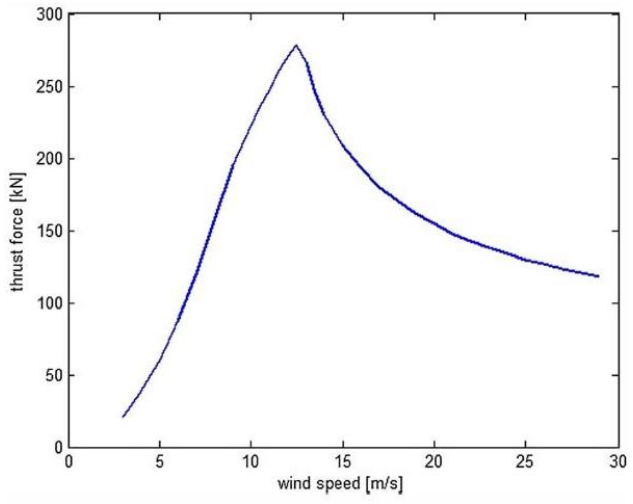

Figure 42. Thrust force on the Hywind Demo wind turbine. [19]

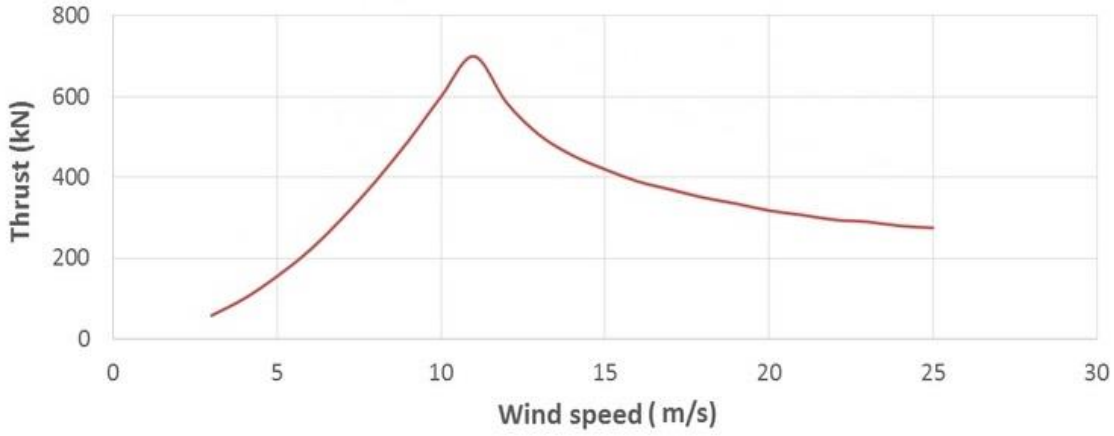

Figure 43. Thrust force on the 5 MW NREL baseline wind turbine. [34]

The decline in mean platform pitch for the above-rated wind speed compared to the below-rated wind speed can be explained by thrust force on the Hywind Demo and OC3-Hywind illustrated in Figure 42 and Figure 43 respectively. As it is clear from the figures, thrust force is higher for the below-rated wind speed, 10.8 m/s, compared to thrust force for the above-rated wind speed, 18.7 m/s. As thrust force is higher for the below-rated wind speed, therefore the mean platform pitch is bigger for the below-rated compared to above-rated wind speed.

The standard deviation of platform pitch increased for the above-rated wind speed compared to the below-rated wind speed. There could be two reasons for higher standard deviation of platform pitch for the above-rated wind speed,

- It could be related to less resonant response in power spectrum of the response. There is auto damping in the below-rated wind speed while the damping in the above-rated wind speed depends on turbine controller,
- As there are almost the same turbulence intensity for both below- and above-rated wind speed base case, therefore there is higher wind velocity fluctuations for the above-rated wind speed, and higher wind velocity fluctuations introduce higher standard deviation.

The numbers in Table 28 and Table 29 also indicate that for both Hywind Demo and OC3-Hywind, mean tip out-of-plane deflection of one blade decreases, while standard deviation of tip out-of-plane deflection of one blade increases for the above-rated wind speed compared to the below-rated wind speed.

The decrease in mean tip out-of-plane deflection of one blade for the above-rated compared to the below-rated wind speed can also be explained by the thrust force. As the thrust force is lower for the above-rated wind speed, 18.7 m/s, compared to the below-rated wind speed, 10.8 m/s, therefore tip out-of-plane deflection of one plane is smaller for the above-rated wind speed.

The rise in standard deviation of tip out-of-plane deflection of one blade for the above-rated wind speed compared to the below-rated wind speed could also be explained with the same reasons that stated for the standard deviation of platform pitch.

By comparing the results for Hywind Demo and OC3-Hywind in Table 28 and Table 29, it can be found that the standard deviation for all three studied responses are higher for OC3-Hywind than Hywind Demo, except maximum standard deviation of platform pitch at nacelle level.

6.1.2 Turbulence intensity

The results presented in CHAPTER 5 indicated that the standard deviation of investigated responses rose significantly when turbulence intensity increased for both studied structures and for both the below- and above-rated wind speed.

The turbulence intensity is defined as the ration of the root-mean-square of the wind velocity fluctuations, u', to the mean wind velocity, u_{mean}. Therefore, by increasing turbulence intensity, there are higher wind velocity fluctuations which cause higher standard deviation of the responses. Furthermore, the effect of turbulence on the global structural responses, e.g. the platform pitch, can be explained by large-scale turbulence, while the effect of turbulence on the local structural responses, e.g. the tip blade deflections, can be explained by small-scale turbulence.

The effect of turbulence intensity variation on the evaluated responses of structures are presented in Table 30 and Table 31. By comparing the results can be realized:

- For both Hywind Demo and OC3-Hywind, mean power output goes up, while standard deviation of power output declines for the above-rated wind speed compare to the below-rated wind speed.
- For both structures, mean platform pitch drops, while standard deviation of platform pitch increases for the above-rated wind speed compared to the below-rated wind speed.

Table 30. The maximum and minimum values of the Hywind Demo responses when turbulence intensity was varied.

		Min.	Max.
below-rated wind speed (10.8 m/s)	Mean power output [MW]	1.291	1.339
	Std of power output [kW]	127.50	341.00
	Mean platform pitch [deg]	1.529	1.595
	Std of platform pitch [deg]	0.1406	0.3394
	Mean tip out-of-plane deflection of one blade [m]	1.699	1.751
	Std of tip out-of-plane deflection of one blade [cm]	11.63	24.24
above-rated wind speed (18.7 m/s)	Mean power output [MW]	2.290	2.300
	Std of power output [kW]	11.25	68.51
	Mean platform pitch [deg]	1.295	1.325
	Std of platform pitch [deg]	0.3696	0.5502
	Mean tip out-of-plane deflection of one blade [m]	1.015	1.069
	Std of tip out-of-plane deflection of one blade [cm]	26.51	53.18

- For both structures, mean tip out-of-plane deflection of one blade declines, while standard deviation of tip out-of-plane deflection of one blade rises for the above-rated wind speed compare to the below-rated wind speed.
- By comparing the results of Hywind Demo and OC3-Hywind, it can be found that the standard deviation for all three studied responses are higher for OC3-Hywind than Hywind Demo, except minimum standard deviation of platform pitch at nacelle level.

Table 31. The maximum and minimum values of the OC3-Hywind responses when turbulence intensity was varied.

		Min.	Max.
below-rated wind speed (10.8 m/s)	Mean power output [MW]	4.252	4.544
	Std of power output [kW]	401.70	859.80
	Mean platform pitch [deg]	4.673	5.203
	Std of platform pitch [deg]	0.2820	0.7967
	Mean tip out-of-plane deflection of one blade [m]	4.895	5.437
	Std of tip out-of-plane deflection of one blade [cm]	32.06	84.30
above-rated wind speed (18.7 m/s)	Mean power output [MW]	5.154	5.241
	Std of power output [kW]	74.63	195.80
	Mean platform pitch [deg]	2.706	2.810
	Std of platform pitch [deg]	0.3396	0.8310
	Mean tip out-of-plane deflection of one blade [m]	1.361	1.452
	Std of tip out-of-plane deflection of one blade [cm]	77.02	137.90

6.1.3 Alpha in wind shear profile power law

The results for both studied structures and for both the below- and above-rated wind speed presented in CHAPTER 5 revealed insignificant effect of alpha variation on the standard deviation of the responses. However, the alpha variation has greater effect on local structural response, i.e. tip out-of-plane deflections for one blade, than global structural responses.

The maximum and minimum values of the responses are presented in Table 32 and Table 33.

Table 32. The maximum and minimum values of the Hywind Demo responses when alpha was varied.

		Min.	Max.
below-rated wind speed (10.8 m/s)	Mean power output [MW]	1.310	1.334
	Std of power output [kW]	240.10	243.00
	Mean platform pitch [deg]	1.563	1.563
	Std of platform pitch [deg]	0.2344	0.2352
	Mean tip out-of-plane deflection of one blade [m]	1.725	1.742
	Std of tip out-of-plane deflection of one blade [cm]	17.21	18.30
above-rated wind speed (18.7 m/s)	Mean power output [MW]	2.297	2.298
	Std of power output [kW]	28.52	30.80
	Mean platform pitch [deg]	1.267	1.315
	Std of platform pitch [deg]	0.4541	0.4557
	Mean tip out-of-plane deflection of one blade [m]	1.037	1.042
	Std of tip out-of-plane deflection of one blade [cm]	38.85	42.56

Table 33. The maximum and minimum values of the OC3-Hywind responses when alpha was varied.

		Min.	Max.
below-rated wind speed (10.8 m/s)	Mean power output [MW]	4.400	4.491
	Std of power output [kW]	643.60	665.40
	Mean platform pitch [deg]	4.918	4.972
	Std of platform pitch [deg]	0.5176	0.5241
	Mean tip out-of-plane deflection of one blade [m]	5.197	5.217
	Std of tip out-of-plane deflection of one blade [cm]	55.32	59.23
above-rated wind speed (18.7 m/s)	Mean power output [MW]	5.190	5.191
	Std of power output [kW]	142.90	144.60
	Mean platform pitch [deg]	2.633	2.774
	Std of platform pitch [deg]	0.6036	0.6117
	Mean tip out-of-plane deflection of one blade [m]	1.384	1.405
	Std of tip out-of-plane deflection of one blade [cm]	94.70	115.70

When the standard deviation of tip out-of-plane deflections for one blade presented in the tables are considered, it could be found that for the both studied structures, the variation of alpha has greater effect in the above-rated wind speed compared to the below-rated wind speed due to higher wind speed variations within swept area of blades. Furthermore, the variation of alpha has more greater effect on OC3-Hywind compared to Hywind Demo due to higher wind speed

variations for OC3-Hywind than Hywind Demo. Mean below- and above-rated wind speed with different alpha within swept area of blades of Hywind Demo and OC3-Hywind are illustrated in Figure 44 and Figure 45 respectively. Crossing point of all wind speed profiles in Figure 44 and Figure 45 is in hub height, i.e. 65 m for Hywind Demo and 90 m for OC3-Hywind.

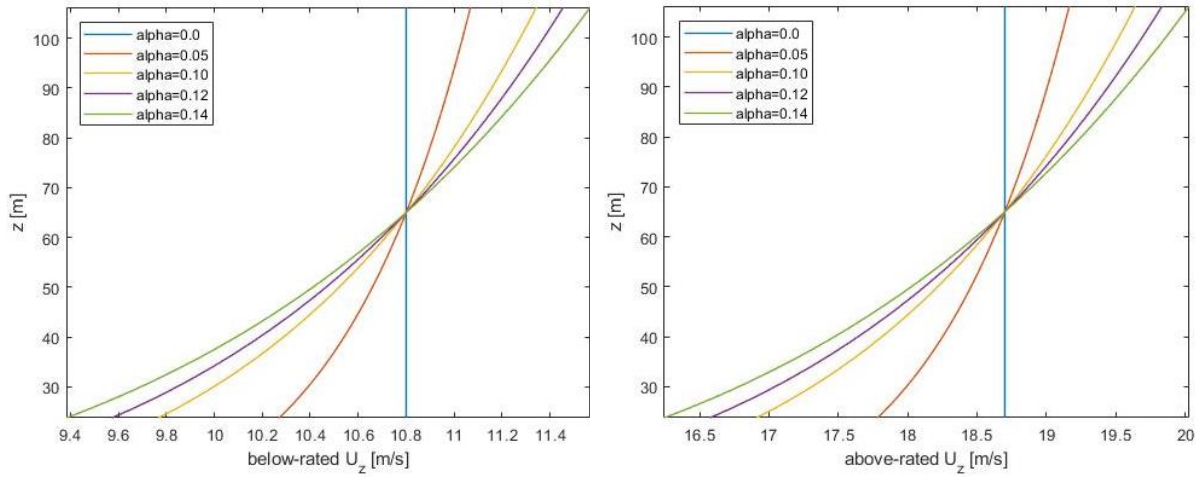

Figure 44. Mean below- and above-rated wind speed profiles with different alpha within swept area of blades of Hywind Demo.

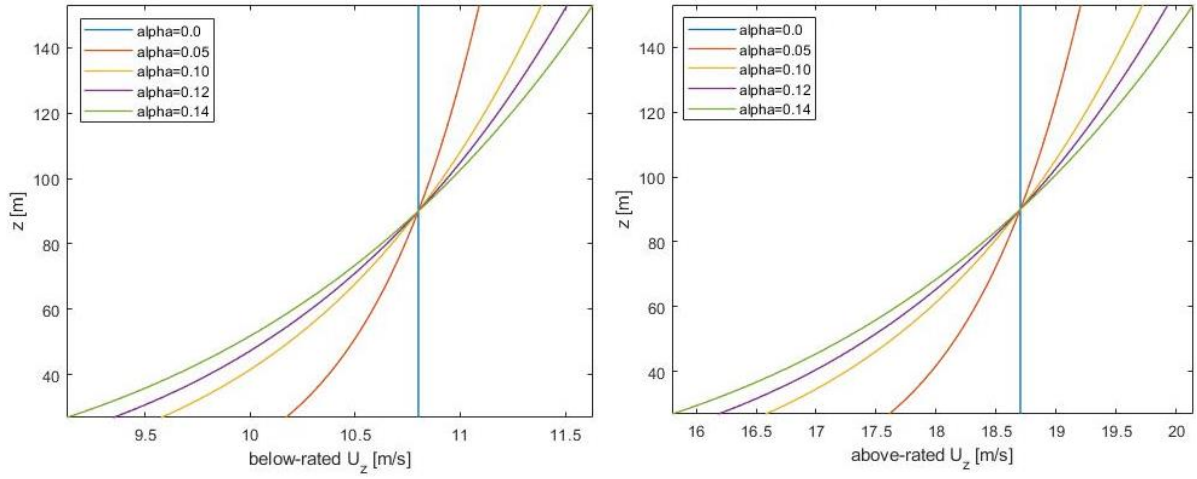

Figure 45. Mean below- and above-rated wind speed profiles with different alpha within swept area of blades of OC3-Hywind.

High turbulence intensity of wind could also be an important player that variation of alpha has insignificant effect on the responses. For instance, Figure 46 and Figure 47 show that when turbulence intensity reduced from 11% to 1% for the above-rated wind speed base case for

Hywind Demo, the variation of standard deviation of tip out-of-plane deflection of one blade increases significantly.

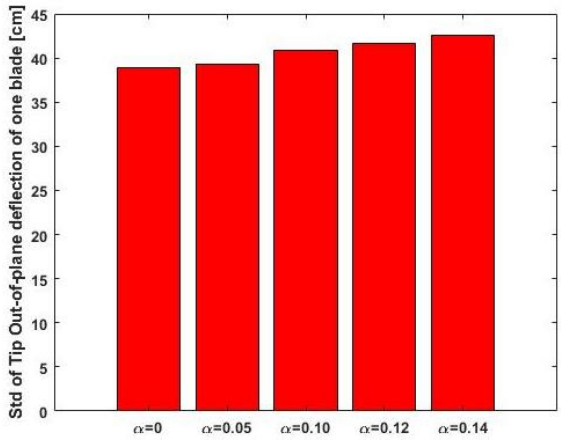

Figure 46. Standard deviation of tip out-of-plane deflection of one blade for various alphas for the above-rated wind speed base case for Hywind Demo with turbulence intensity of 11%.

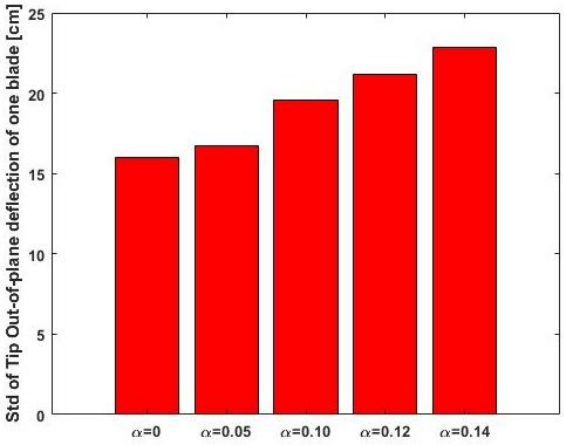

Figure 47. Standard deviation of tip out-of-plane deflection of one blade for various alphas for the above-rated wind speed base case for Hywind Demo with turbulence intensity of 1%.

Although the effect of alpha variation on the results of the investigated responses is small, the results presented in Table 32 and Table 33 reveals:

- For both structures, mean power output grows, while standard deviation of power output goes down for the above-rated wind speed compared to the below-rated wind speed.

- For both structures, mean platform pitch falls, while standard deviation of platform pitch rises for the above-rated wind speed compared to the below-rated wind speed.
- For both structures, mean tip out-of-plane deflection of one blade decreases, while standard deviation of tip out-of-plane deflection of one blade goes up for the above-rated wind speed compared to the below-rated wind speed.
- By comparing the results of Hywind Demo and OC3-Hywind, it can be realized that the standard deviation for all studied responses are higher for OC3-Hywind than Hywind Demo.

6.1.4 Spatial resolution of the numerical wind field

The results in CHAPTER 5 disclosed that the standard deviation of studied responses fluctuated by variation of spatial resolution of the numerical wind field. The reason of these fluctuations is variation of wind speed due to spatial resolution variation. As the grid size of the numerical wind field changes, the average wind speed applied on the structure will change and therefore the structural responses will change. Table 34 and Table 35 present the minimum and maximum values of structural responses of Hywind Demo and OC3-Hywind respectively.

Table 34. The maximum and minimum values of the Hywind Demo responses when spatial resolutions were varied.

		Min.	Max.
below-rated wind speed (10.8 m/s)	Mean power output [MW]	1.313	1.391
	Std of power output [kW]	208.00	250.00
	Mean platform pitch [deg]	1.563	1.619
	Std of platform pitch [deg]	0.2234	0.2370
	Mean tip out-of-plane deflection of one blade [m]	1.727	1.769
	Std of tip out-of-plane deflection of one blade [cm]	16.54	18.19
above-rated wind speed (18.7 m/s)	Mean power output [MW]	2.297	2.299
	Std of power output [kW]	20.26	30.02
	Mean platform pitch [deg]	1.275	1.310
	Std of platform pitch [deg]	0.4360	0.4677
	Mean tip out-of-plane deflection of one blade [m]	0.9912	1.0420
	Std of tip out-of-plane deflection of one blade [cm]	38.35	41.62

Table 35. The maximum and minimum values of the OC3-Hywind responses for when spatial resolutions were varied.

		Min.	Max.
below-rated wind speed (10.8 m/s)	Mean power output [MW]	4.411	4.661
	Std of power output [kW]	563.30	664.00
	Mean platform pitch [deg]	4.967	5.118
	Std of platform pitch [deg]	0.5195	0.6419
	Mean tip out-of-plane deflection of one blade [m]	5.141	5.316
	Std of tip out-of-plane deflection of one blade [cm]	56.73	63.41
above-rated wind speed (18.7 m/s)	Mean power output [MW]	5.187	5.190
	Std of power output [kW]	143.80	162.40
	Mean platform pitch [deg]	2.712	2.759
	Std of platform pitch [deg]	0.5673	0.6248
	Mean tip out-of-plane deflection of one blade [m]	1.293	1.391
	Std of tip out-of-plane deflection of one blade [cm]	107.50	111.00

By considering the maximum and minimum results of the responses for both structures, presented in Table 34 and Table 35, it could be realized that:

- For both Hywind Demo and OC3-Hywind:
  - The standard deviation of power output drops while the mean power output increases for above-rated wind speed compared to below-rated wind speed.
  - While the standard deviation of platform pitch grows, mean platform pitch falls for above-rated wind speed compared to below-rated wind speed.
  - The standard deviation of tip out-of-plane deflection of one blade shoots up while mean tip out-of-plane deflection of one blade declines for above-rated wind speed compared to below-rated wind speed.
- The standard deviation of OC3-Hywind responses are higher compared to the standard deviation of Hywind Demo responses.

6.2 Coherence of the numerical wind field

Co-coherence of longitudinal wind velocity fluctuation (u´) for frequencies of 0.04 Hz and 0.2 Hz were presented in CHAPTER 5. As it was clear from the results, the co-coherence of u´ for the higher frequency had not a sensible pattern. Figure 48 also shows the co-coherence for higher frequency in flatten view. As it is clear from the figure, the middle nodes have the highest co-coherence as expected.

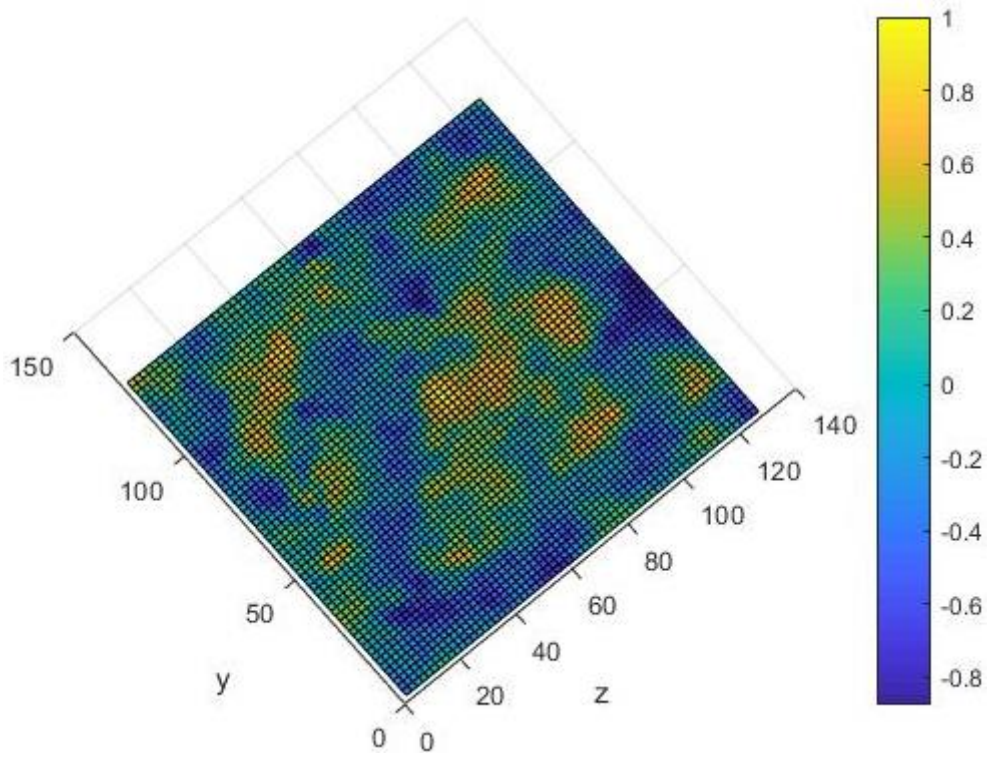

Figure 48. flatten view of co-coherence of longitudinal wind velocity fluctuation (u´) between each point and mid-point for frequency of 0.2 Hz.

However, the average co-coherence of longitudinal wind velocity fluctuation (u´) in radius around mid-node decreased sharply from small radius around mid-node until the radius of 14 m around mid-node, presented in Figure 38. For greater radius around mid-node, the average co-coherence was almost flattened.

For frequency of 0.04 Hz, the result showed a clear pattern, more correlation of spectra around the mid-node and less correlation of spectra away from mid-node. Figure 49 also clearly shows the pattern of correlations.

It was also obvious from averaging of co-coherence of longitudinal wind velocity fluctuation (u´) in various radius that the correlation of spectra faded away when the radius around the mid-node increased.

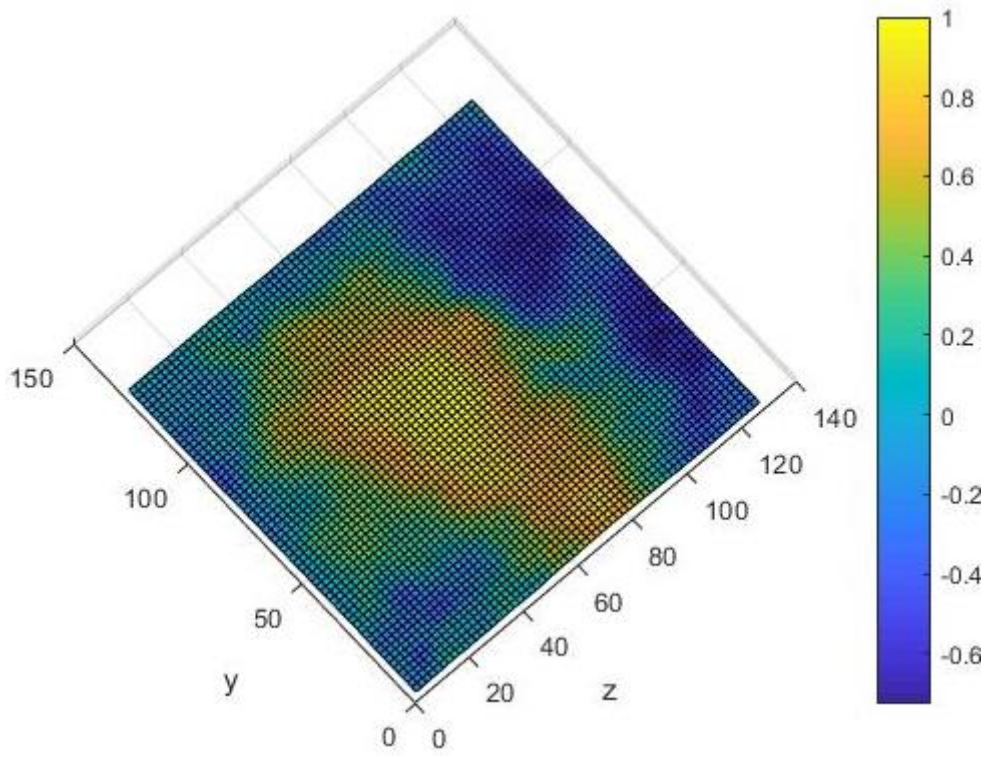

Figure 49. flatten view of co-coherence of longitudinal wind velocity fluctuation (u´) between each point and mid-point for frequency of 0.04 Hz.

More correlation of spectra between two nodes is more favorable for structure. Higher wind loads will be applied on structure when there is small correlation of spectra between two arbitrary points in rotor plane.

Conclusion

The aim of this study was to conduct a sensitivity study to understand the sensitivity of various structural responses as function of the various environmental parameters using the computational tool SIMA. Also, coherence of the numerical wind field was investigated.

Based on the below- and the above-rated wind speed base case, environmental components in both Hywind Demo and OC3-Hywind SIMA models were modified. Then, in each simulation, one environmental parameter was changed while other parameters remained unchanged. Thereafter, the sensitivity of the responses to the parameter variation were evaluated.

The wave characteristics variation and turbulence intensity variation had significant effect on the dynamic behaviour of both Hywind Demo and OC3-Hywind. The standard deviation of the investigated responses showed clear agreement with variation of the wave characteristics and turbulence intensity, i.e. the standard deviations rose by increasing significant wave height and wave peak period or turbulence intensity.

The wind shear exponent (α) variation had insignificant impact on the evaluated global structural responses, i.e. power output and platform pitch. However, the studied local structural response, i.e. tip out-of-plane deflection of one blade, had greater sensitivity to alpha variation. Moreover, the tip out-of-plane deflection of one blade for the above-rated wind speed had greater standard deviation compared to the below-rated wind speed due to higher wind velocity variation within rotor area. Also, the tip out-of-plane deflection of one blade for OC3-Hywind had greater standard deviation compared to Hywind Demo due to bigger rotor diameter and therefore greater wind velocity variation. It is also important to be noted that by reducing

turbulence intensity, tip out-of-plane deflection of one blade had greater sensitivity to alpha variation.

The evaluated structural responses fluctuated by changing the spatial resolution of the numerical wind field. As the grid size of the numerical wind field changed, the average wind speed applied on the structure changed and therefore the structural responses changed.

When the responses of two structures compare to each other, the responses of OC3-Hywind were greater than the responses of Hywind Demo. The reason was due to larger rotor size of OC3-Hywind compared to rotor size of Hywind Demo. The larger the rotor size, the greater the thrust loads on the structure. The greater thrust loads on the structure caused greater platform pitch and tip out-of-plane deflection of one blade. It is also obvious that larger rotor swept area produces higher power output.

Co-coherence of longitudinal wind velocity fluctuation (u´) showed higher correlation between nodes for lower frequency than higher frequency for one realization.

Recommendations for Further Work

The most important further works are conducting more simulations to converge the structural responses.

In addition, the sensitivity study with respect to other important environmental parameters must be performed to better understand the structural responses. It also would be useful if the sensitivities of different parameters could be rank based on Robertson [35].

For coherence of numerical wind field evaluation, more realizations need to have more reliable results.

Moreover, it is recommended to perform the sensitivity of even larger wind turbine, e.g. 10 MW wind turbine, to environmental parameters.

Bibliography

1. Ehrlich, R., *RENEWABLE ENERGY - A First Course*. 2013: CRC Press.
2. Roddier, D. and J. Weinstein, *Floating Wind Turbines.* Mechanical Engineering, 2010. **132**(4): p. 28-32.
3. Musial, W., S. Butterfield, and B. Ram, *Energy From Offshore Wind*, in *Offshore Technology Conference*. 2006: Houston.
4. Jonkman, J., *Dynamics Modeling and Loads Analysis of an Offshore Floating Wind Turbine*. November 2007, National Renewable Energy Laboratory (NREL).
5. Tran, T.-T. and D.-H. Kim, *The platform pitching motion of floating offshore wind turbine: A preliminary unsteady aerodynamic analysis.* Journal of Wind Engineering and Industrial Aerodynamics, 2015. **142**: p. 65-81.
6. VATTENFALL. *Horns Rev 1*. January 15th, 2018]; Available from: https://powerplants.vattenfall.com/horns-rev.
7. Ørsted. *Nysted*. January 15th, 2018]; Available from: https://orsted.com/en/Our-business/Wind-Power/Our-wind-farms.
8. Ibsen, L.B., M. Liingaard, and S.A. Nielsen, *Bucket Foundation, a status.* Proceedings of the Copenhagen Offshore Wind, 2005.
9. *Beatrice Offshore Wind Farm*. January 15th, 2018]; Available from: https://www.beatricewind.com/.
10. STATOIL. *World's first floating wind farm has started production*. Januray 15th, 2018]; Available from: https://www.statoil.com/en/news/worlds-first-floating-wind-farm-started-production.html.
11. Adam, F., et al., *GICON-TLP for wind turbines - Validation of calculated results*, in *The Twenty-third International Offshore and Polar Engineering Conference*. 2013: Anchorage, Alaska.
12. Roddier, D., et al., *WindFloat: A floating foundation for offshore wind turbines.* 2010. **2**(3).
13. Bulder, B.H., et al., *Study to feasibility of and boundary conditions for floating offshore wind turbines*. 2002.
14. Landbø, T., *OO-STAR WIND FLOATER, THE FUTURE OF OFFSHORE WIND?*, in *EERA DEEPWIND*. 2018: Trondheim, Norway.
15. IDEOL. *THE FLOATING FOUNDATION*. February 10th, 2018]; Available from: http://ideol-offshore.com/en/floating-foundation.

16. PELASTAR. *PelaStar tension leg platform (TLP) technology*. February 10th, 2018]; Available from: http://pelastar.com/.
17. Nielsen, F.G. *Hywind – From idea to world's first wind farm based upon floaters*. 2017 February 10th, 2018]; Available from: https://www.uib.no/sites/w3.uib.no/files/attachments/hywind_energy_lab.pdf.
18. Matha, D., *Model Development and Loads Analysis of an Offshore Wind Turbine on a Tension Leg Platform, with a Comparison to Other Floating Turbine Concepts*. April 2009, National Renewable Energy Laboratory (NREL).
19. Skaare, B., et al., *Analysis of measurements and simulations from the Hywind Demo floating wind turbine.* Wind Energy, 2015. **18**: p. 1105-22.
20. Neuenkirchen Godø, S., *Dynamic Response of Floating Wind Turbines*. June 2013, NTNU.
21. MARINTEK, *SIMA User Guide*. 2018: Available as an application built into SIMA.
22. Jonkman, J. and W. Musial, *Offshore Code Comparison Collaboration (OC3) for IEA Task 23 Offshore Wind Technology and Deployment*. December 2010, National Renewable Energy Laboratory (NREL).
23. Jonkman, J., et al., *Definition of a 5-MW Reference Wind Turbine for Offshore System Development*. February 2009, National Renewable Energy Laboratory (NREL).
24. Jonkman, J., *Definition of the Floating System for Phase IV of OC3*. May 2010, National Renewable Energy Laboratory (NREL).
25. Malhotra, S., *Selection, Design and Construction of Offshore Wind Turbine Foundations*. 2011: INTECH Open Access Publisher.
26. Veers, P., *Three-Dimensional Wind Simulation*. 1988, Sandia National Laboratories.
27. Mann, J., *The spatial structure of neutral atmospheric surface-layer turbulence.* Journal of Fluid Mechanics, 1994. **273**: p. 141-168.
28. Cheynet, E., et al., *Application of short-range dual-Doppler lidars to evaluate the coherence of turbulence.* Experiments in Fluids, 2016. **57**(12).
29. (IEC), I.E.C., *IEC61400-1 Wind turbines - Part 1: Design requirements*. 3rd Edition, 2005.
30. Kaimal, J.C., et al., *Spectral characteristics of surface-layer turbulence*. Quarterly Journal of the Royal Meteorological Society, 1972. **98**: p. 563–589.
31. Eliassen, L. and C. Obhrai, *Coherence of Turbulent Wind Under Neutral Wind Conditions at FINO1*. Energy Procedia, 2016. **94**: p. 388-398.
32. Eliassen, L. and E.E. Bachynski, *The Effect of Turbulence Model on the Response of a Large Floating Wind Turbine*, in *OMAE2017*. 2017: Trondheim, Norway. p. V010T09A062; 10 pages.
33. DTU Wind Energy. *Pre-processing tools - Mann 64bit turbulence generator*. [cited 2017 November 15th]; Available from: http://www.hawc2.dk/download/pre-processing-tools.
34. Desmond, C., et al., *Description of an 8 MW reference wind turbine.* Journal of Physics Conference Series, 2016. **753**.
35. Robertson, A., et al., *Assessment of Wind Parameter Sensitivity on Extreme and Fatigue Wind Turbine Loads*, in *AIAA Wind Energy Symposium*. 2018.

APPENDIX 1 Scatter diagram

Scatter diagram based upon approximately 18 years of measured data from the North Sea is presented in Figure 50.

	Tp (s)																	
Hs (m)	<4	4-5	5-6	6-7	7-8	8-9	9-10	10-11	11-12	12-13	13-14	14-15	15-16	16-17	17-18	18-19	19-20	>=20
< 0.5	25	14	18	14	24	17	8	9	5	0	2	3	1	1	6	2	0	7
0.5 - 1	79	235	408	539	496	488	426	225	111	46	16	7	6	3	2	0	2	17
1 - 1.5	71	466	896	1223	1227	1219	911	626	470	252	108	70	36	12	13	2	2	49
1.5 - 2	3	134	768	1342	1443	1288	1143	854	618	404	205	129	44	21	10	3	4	21
2 - 2.5	0	22	292	1013	1328	1359	1056	921	669	431	188	186	56	27	17	5	1	16
2.5 - 3	1	2	79	491	1037	1276	1031	795	678	479	208	193	81	35	13	3	2	8
3 - 3.5	0	1	16	189	701	1038	896	729	532	386	235	197	97	40	15	4	1	5
3.5 - 4	0	0	3	57	318	814	767	562	447	371	193	168	89	50	17	3	0	3
4 - 4.5	1	0	1	11	130	568	731	500	341	306	146	142	67	29	25	4	3	2
4.5 - 5	0	0	0	3	44	329	533	444	337	248	122	95	40	31	20	2	4	1
5 - 5.5	0	0	0	1	15	112	339	396	280	195	121	98	31	26	16	5	2	0
5.5 - 6	0	0	0	1	4	46	193	244	224	138	73	70	27	15	15	3	0	1
6 - 6.5	0	0	0	0	0	18	91	177	156	125	65	51	20	15	7	1	2	2
6.5 - 7	0	0	0	0	1	1	34	108	137	106	46	40	14	5	1	2	0	0
7 - 7.5	0	0	0	0	0	1	11	53	93	74	50	30	14	7	8	0	1	0
7.5 - 8	0	0	0	0	0	0	1	29	61	63	27	19	6	3	1	1	0	1
8 - 8.5	0	0	0	0	0	1	0	14	31	43	24	13	6	5	1	0	0	0
8.5 - 9	0	0	0	0	0	0	0	8	19	27	17	8	7	1	0	0	0	0
9 - 9.5	0	0	0	0	0	0	0	2	5	18	13	9	2	1	1	0	0	0
9.5 - 10	0	0	0	0	0	0	0	1	2	7	7	4	3	3	0	0	0	0
10 - 10.5	0	0	0	0	0	0	0	0	3	3	7	4	4	1	0	0	0	0
10.5 - 11	0	0	0	0	0	0	0	0	0	3	1	2	0	0	0	0	0	0
11 - 11.5	0	0	0	0	0	0	0	0	0	4	2	1	0	0	0	0	0	0
11.5 - 12	0	0	0	0	0	0	0	0	0	1	0	0	0	0	0	0	0	0
12 - 12.5	0	0	0	0	0	0	0	0	0	1	0	0	1	0	0	0	0	0
12.5 - 13	0	0	0	0	0	0	0	0	0	0	0	0	0	0	1	0	0	0
13 - 13.5	0	0	0	0	0	0	0	0	0	0	1	0	0	0	0	0	0	0
13.5 - 14	0	0	0	0	0	0	0	0	0	0	0	0	0	0	0	0	0	0
14 - 14.5	0	0	0	0	0	0	0	0	0	0	0	0	0	0	0	0	0	0
14.5 - 15	0	0	0	0	0	0	0	0	0	0	0	0	0	0	0	0	0	0
>=15	0	0	0	0	0	0	0	0	0	0	0	0	0	0	0	0	0	0

Figure 50. Example upon scatter diagram based upon approximately 18 years of measured data from the North Sea.

APPENDIX 2 Complete structural responses

Hywind Demo and OC3-Hywind concepts were employed to investigate and analyse. Wave characteristics (H_s and T_p), turbulence intensity (TI), alpha (α) in wind shear power law and spatial resolution of the numerical wind field varied and investigated their effects on the structures' responses. For each sensitivity study, mean and standard deviation of structures' responses such as electrical generator output, platform pitch and tip out-of-plane deflection for one blade were investigated to understand the importance of each studied parameter on the responses. All the results without any interpretation for both below- and above-rated wind speed are presented.

2.1 Hywind Demo results

2.1.1 Below-rated wind speed

2.1.1.1 Variation of wave characteristics

Higher H_s and T_p generated higher standard deviations while the mean values remained almost constant in evaluated responses.

Figure 51 indicates that the mean electrical generator output remains unchanged in 1.313 MW. However, the standard deviation of electrical generator output rises steadily from 239.4 kW for case 1 to 411.6 kW for case 9.

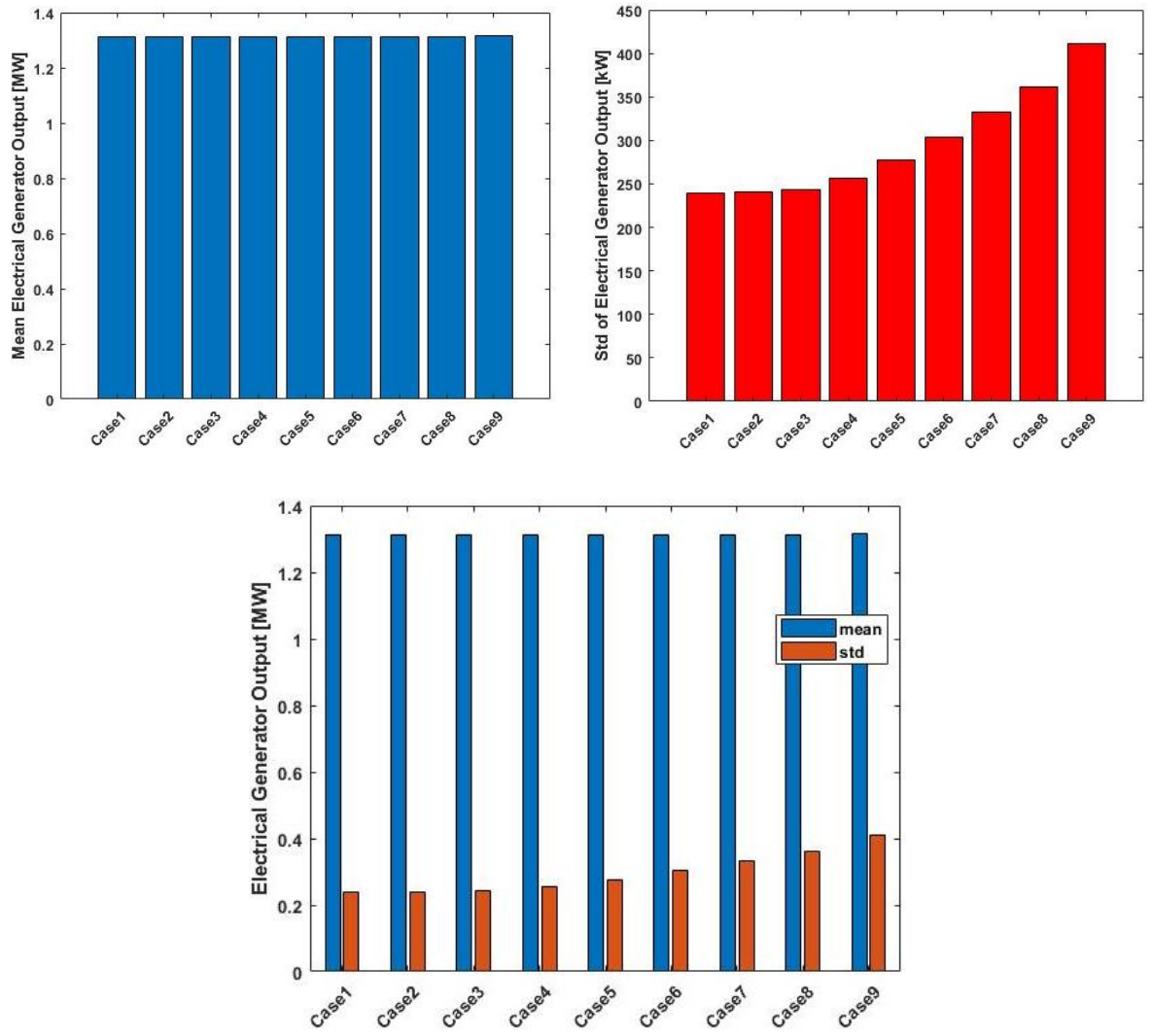

Figure 51. Mean and standard deviation of electrical generator output for different H_s and T_p in below-rated wind speed.

Figure 52 shows a dramatic growth in standard deviation of platform pitch from 0.22 degree for case1 compared to 1.49 degrees for case9. Moreover, mean platform pitch remains fairly static, changes from 1.564 to 1.524 degrees.

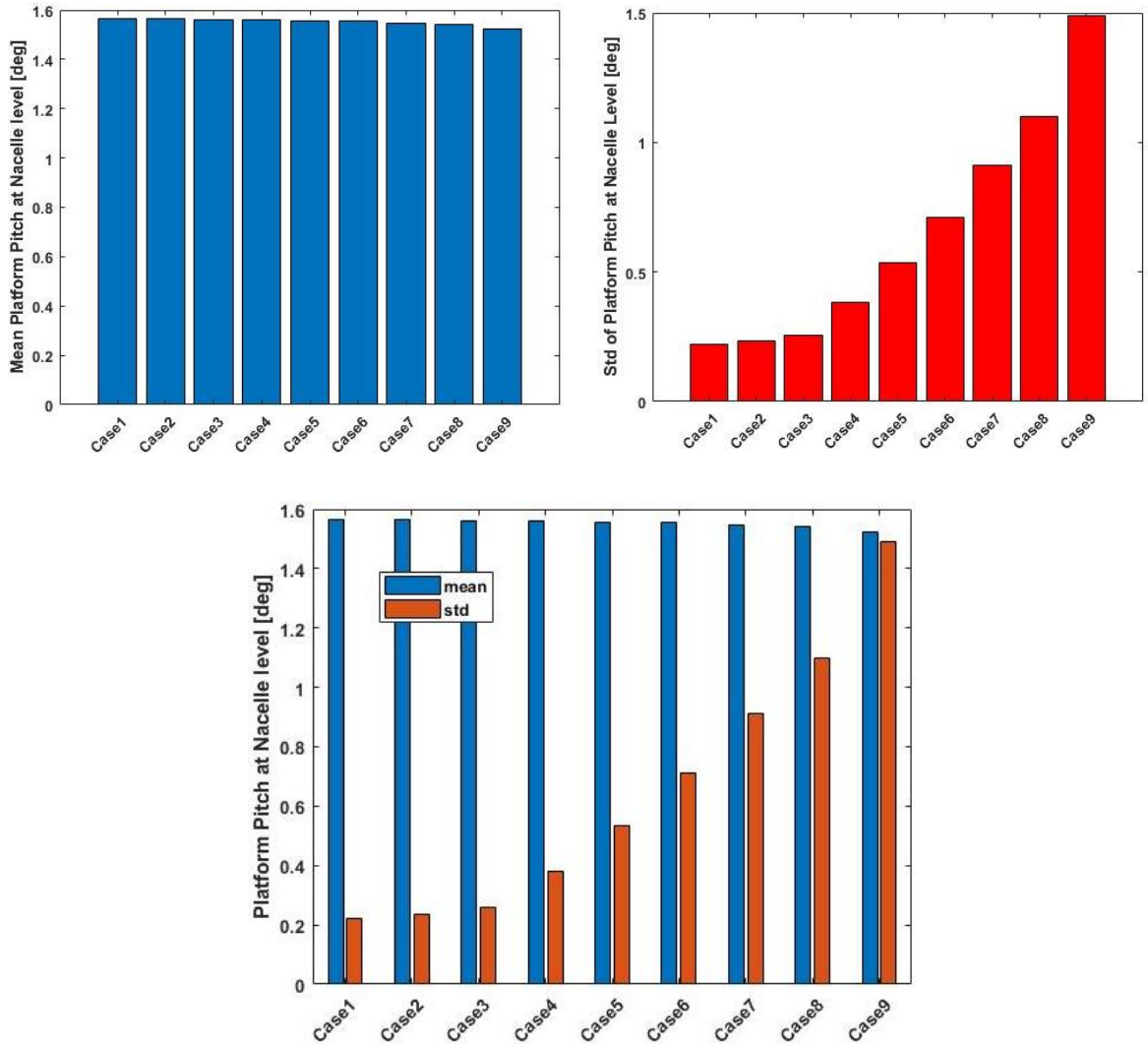

Figure 52. Mean and standard deviation of platform pitch for different H_s and T_p in below-rated wind speed.

While the mean tip out-of-plane deflection of one blade shows no change for case1, case2 and case3, the value falls slightly from 1.727 m for case3 to 1.697 m for case 9 illustrated in Figure 53. Furthermore, the standard deviation increases from 17.91 cm for case1 to 27.73 cm for case 9.

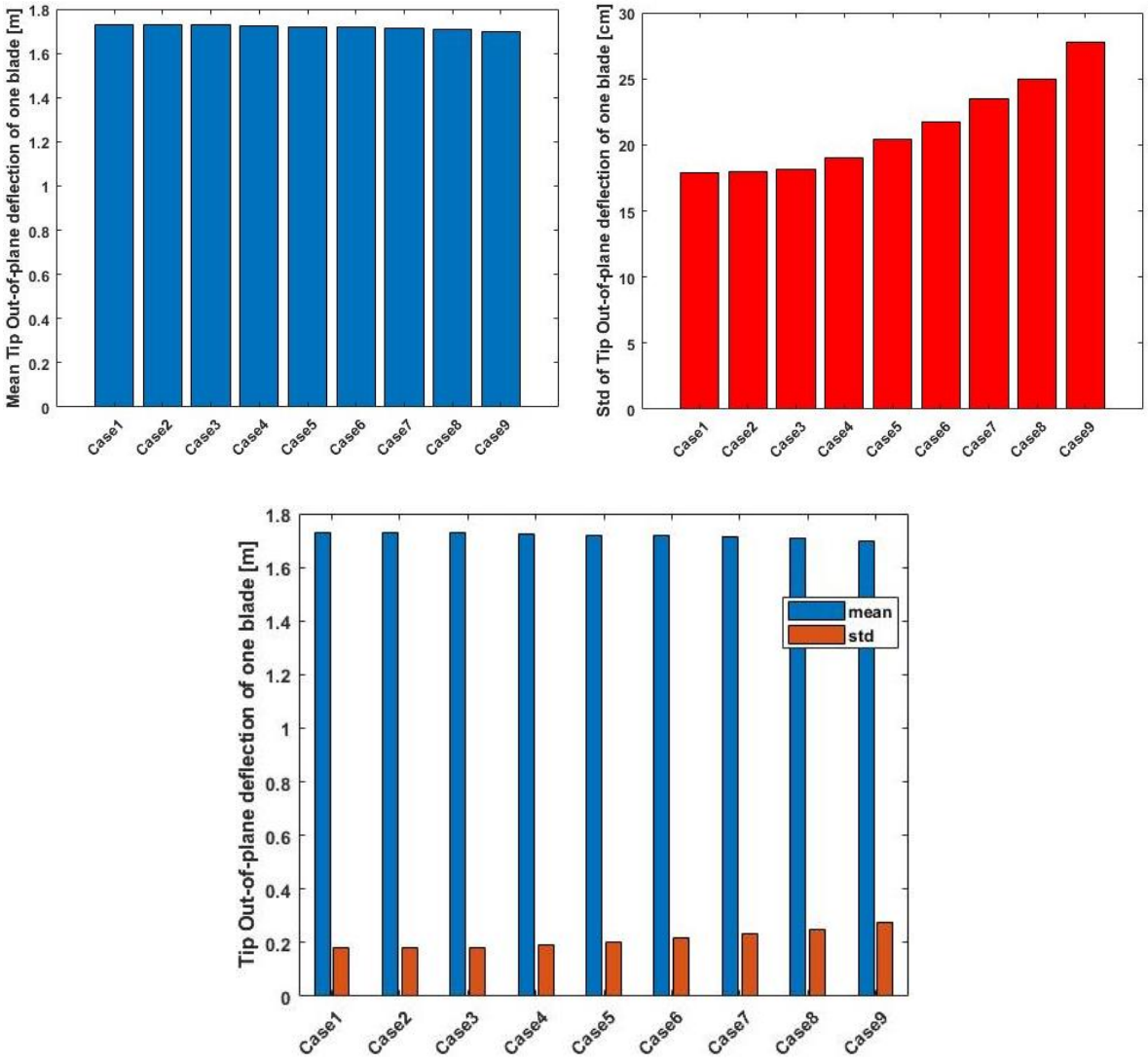

Figure 53. Mean and standard deviation of tip out-of-plane deflection of one blade for different H_s and T_p in below-rated wind speed.

2.1.1.2 Variation of turbulence intensity

Higher turbulence intensity produced higher standard deviations while mean values decreased gently in evaluated responses.

It is shown in Figure 54 that by increasing the turbulence intensity from 5% to 15%, the standard deviation of electrical generation output increases from 127.5 to 341 kW, while the mean electrical generation output slightly decreases from 1.339 to 1.291 MW.

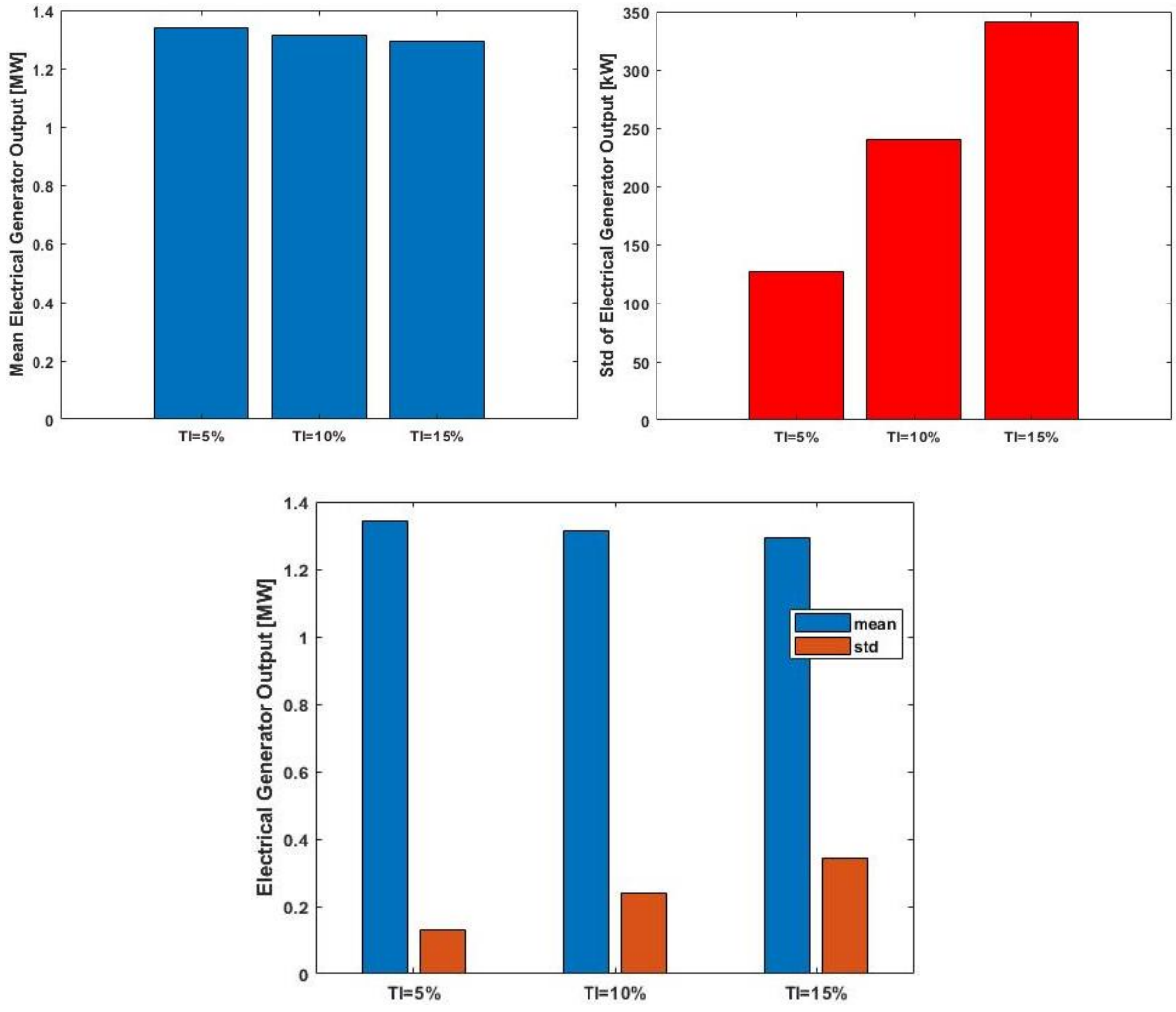

Figure 54. Mean and standard deviation of electrical generator output for three turbulence intensities in below-rated wind speed.

Figure 55 shows the same pattern as the previous figure, i.e. by increasing turbulence intensity, the mean value gradually drops while standard deviation rises steeply. The mean platform pitch falls from 1.595 to 1.529 degrees while standard deviation goes up from 0.1406 to 0.3394 degrees.

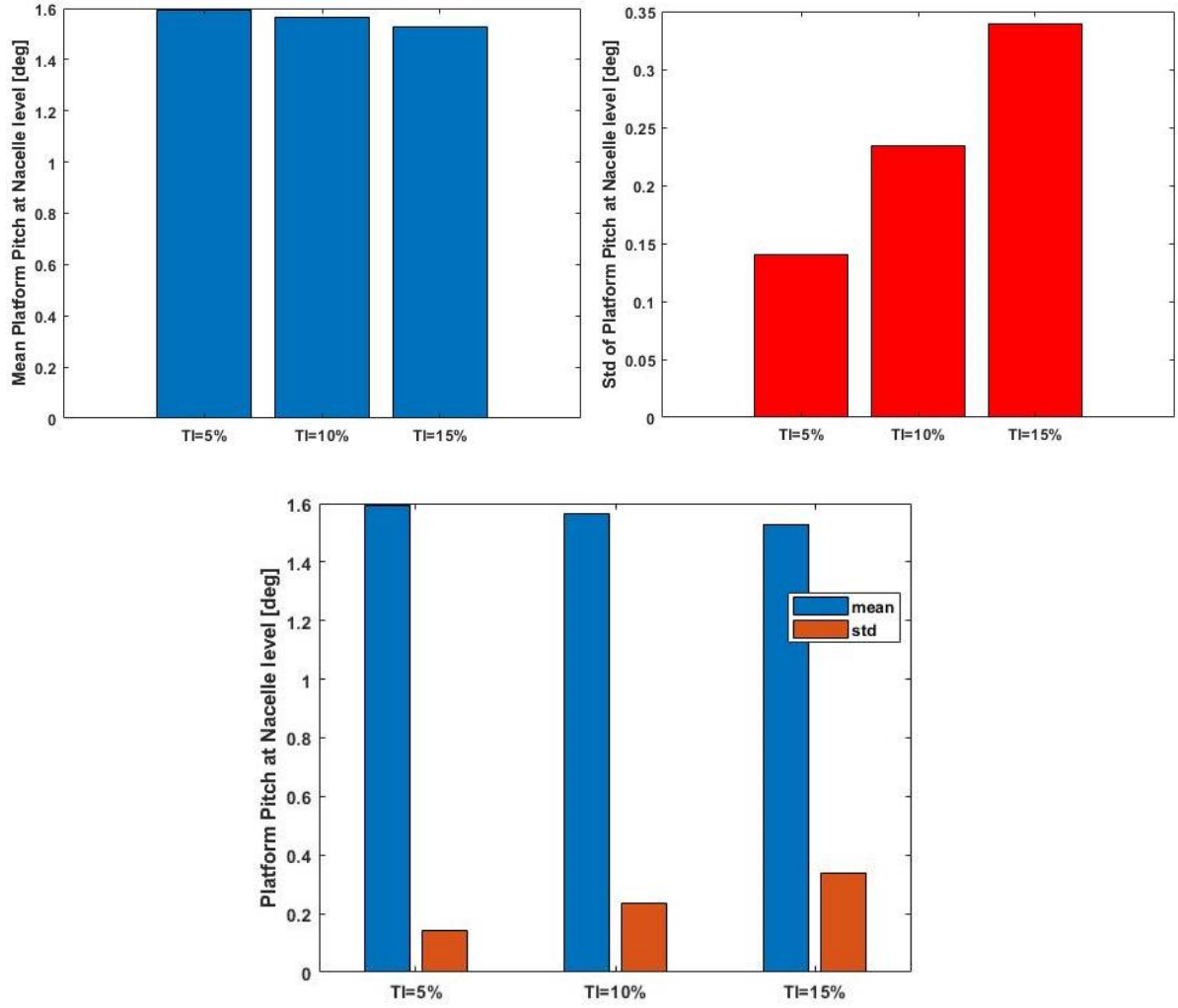

Figure 55. Mean and standard deviation of platform pitch for three turbulence intensities in below-rated wind speed.

Mean and standard deviation of tip out-of-plate deflection of one blade for 5%, 10% and 15% turbulence intensity are presented in Figure 56. The mean value decreases from 1.751 to 1.699 m and the standard deviation climbs from 11.63 to 24.24 cm.

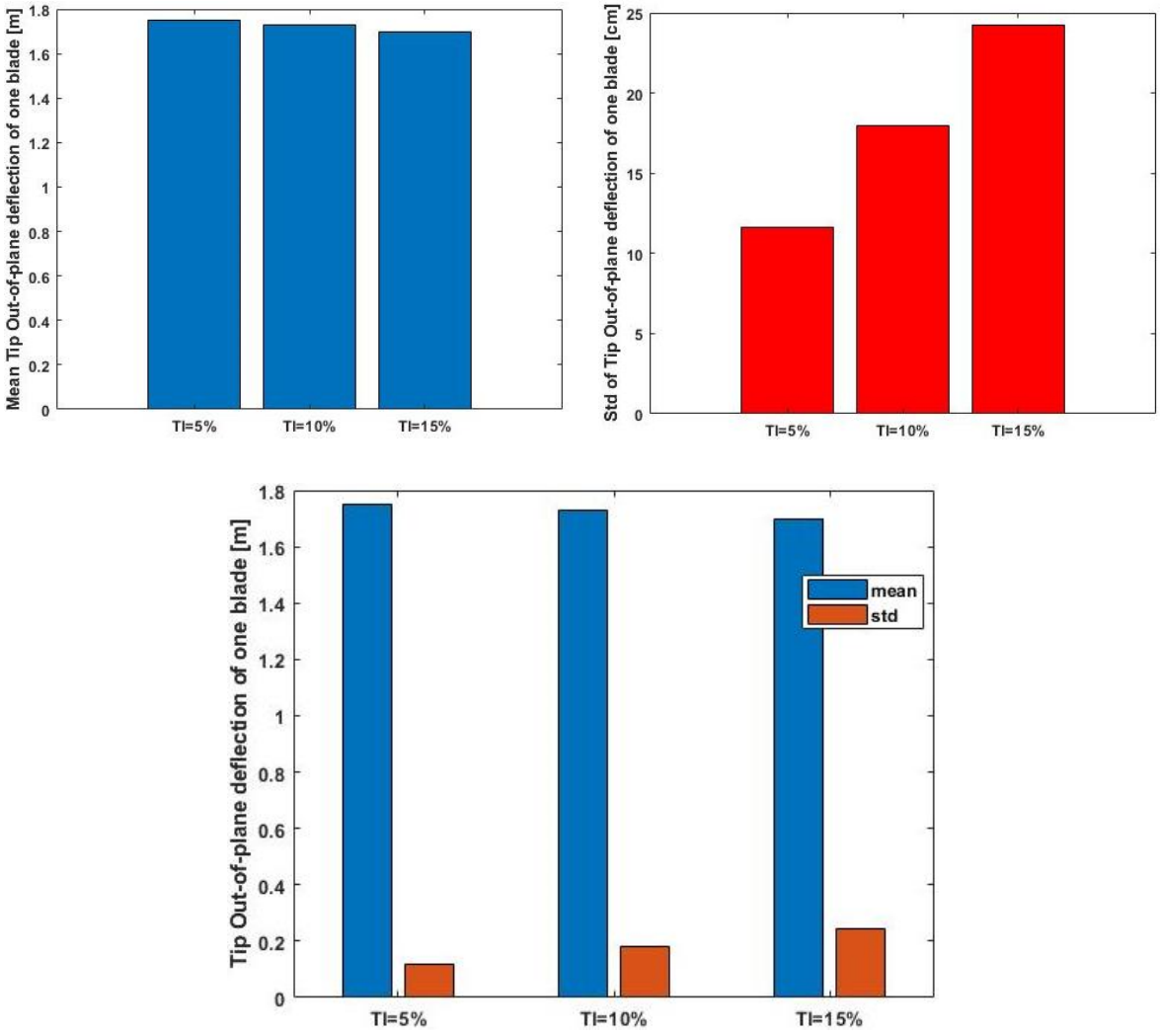

Figure 56. Mean and standard deviation of tip out-of-plane deflection of one blade for three turbulence intensities in below-rated wind speed.

2.1.1.3 Variation of alpha in wind shear profile power law

Varying α in wind shear profile power law showed no significant effect on both mean and standard deviation values of the responses.

Figure 57 illustrates that both mean and standard deviation of electrical generator output decline slightly by increasing alpha. The results show the mean value decreases from 1.334 to 1.310 MW and the standard deviation falls from 243 to 240.1 kW.

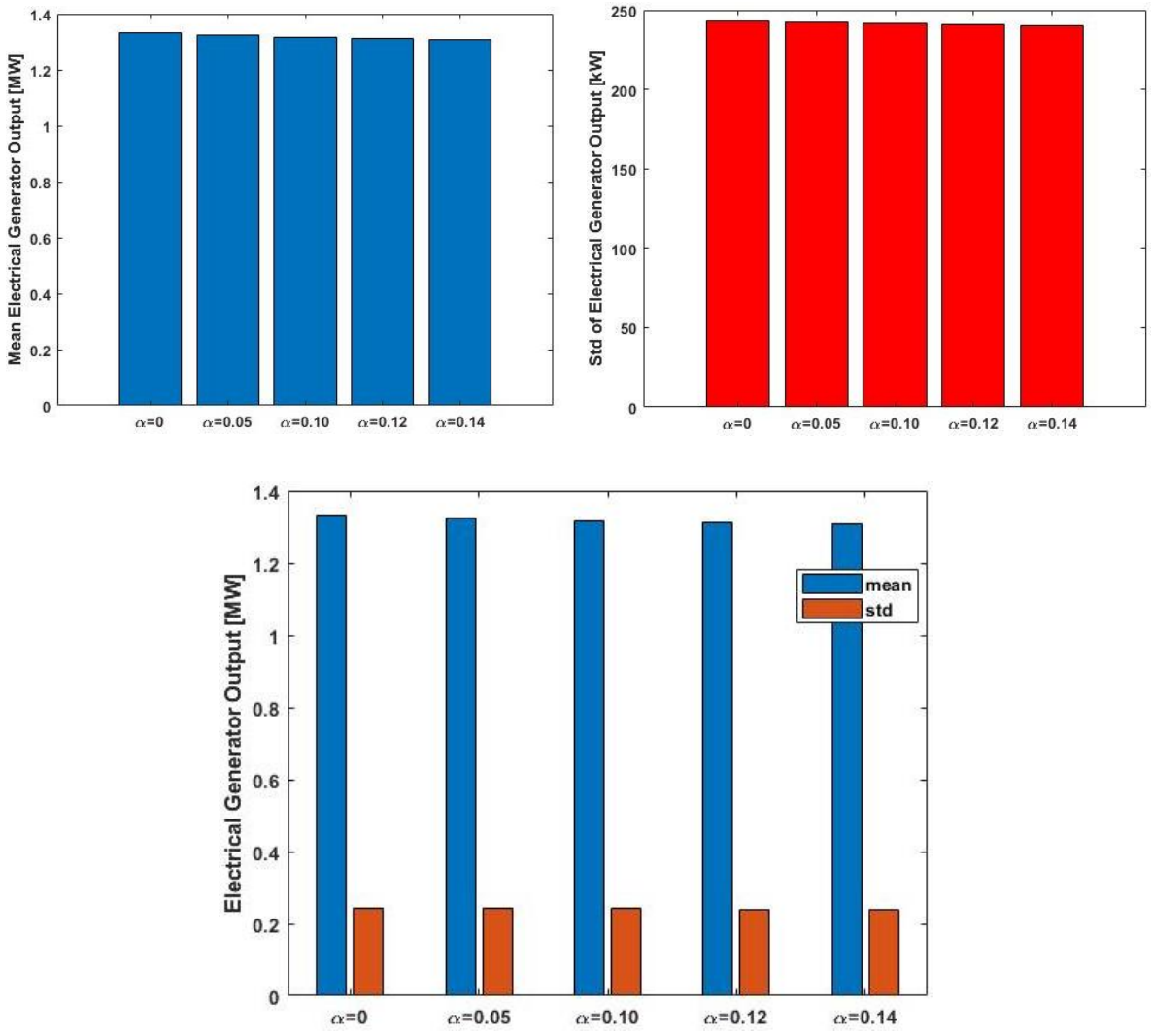

Figure 57. Mean and standard deviation of electrical generator output for five alphas in wind shear power law in below-rated wind speed.

The mean values of platform pitch for all alphas are the same, 1.563 degrees. However, the standard deviations barely decrease from 0.2352 to 0.2344 degrees. The results are shown in Figure 58.

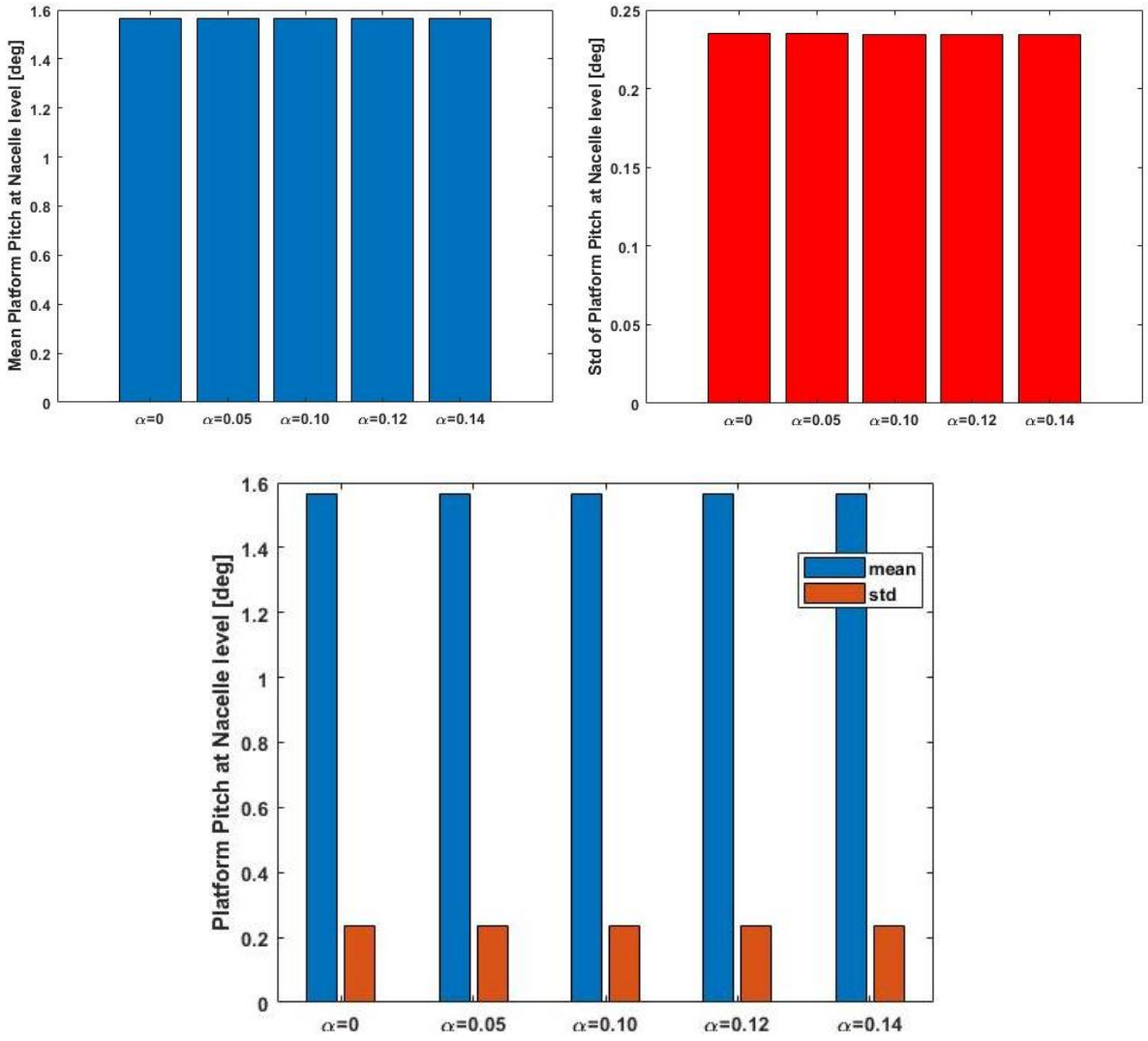

Figure 58. Mean and standard deviation of platform pitch for five alphas in wind shear power law in below-rated wind speed.

Figure 59 shows that mean of tip out-of-plane of one blade reduces gradually from 1.742m to 1.725m while alpha increases from 0 to 0.14. However, standard deviation of the response gently increases from 17.21 cm to 18.30 cm.

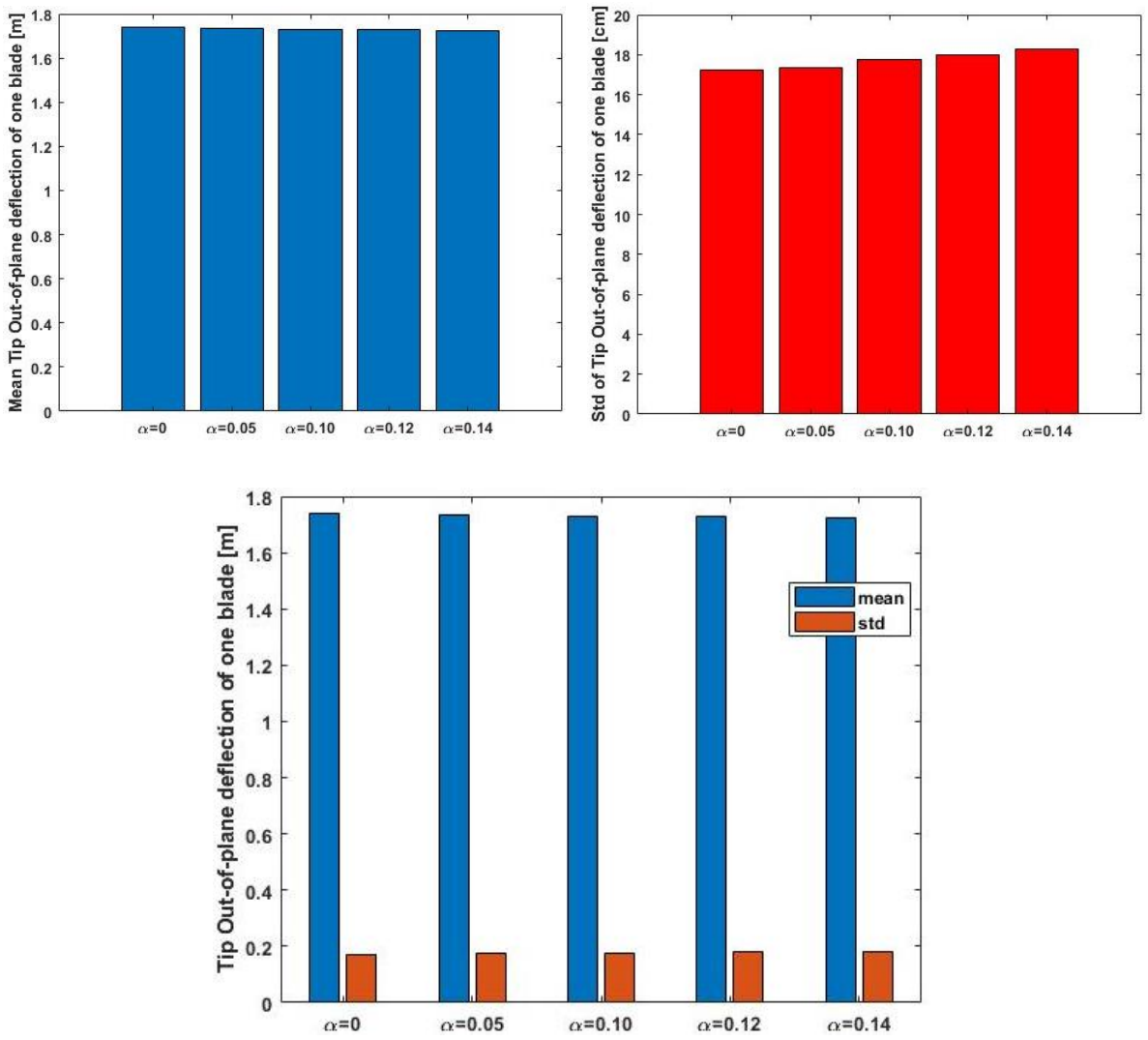

Figure 59. Mean and standard deviation of tip out-of-plane deflection of one blade for five alphas in wind shear power law in below-rated wind speed.

2.1.1.4 Variation of the spatial resolution of the numerical wind field

Both mean and standard variation values of the responses fluctuated by changing the spatial resolution of the numerical wind field.

Figure 60 shows mean electrical generator output fluctuates from 1.313 MW for case1 to 1.384 MW for case 2, 1.391 MW for case3 and 1.374 MW for case4. Moreover, the standard deviation of the response also shows the pattern of fluctuation with lowest value of 208 kW for case2 and highest value of 250 kW for case3.

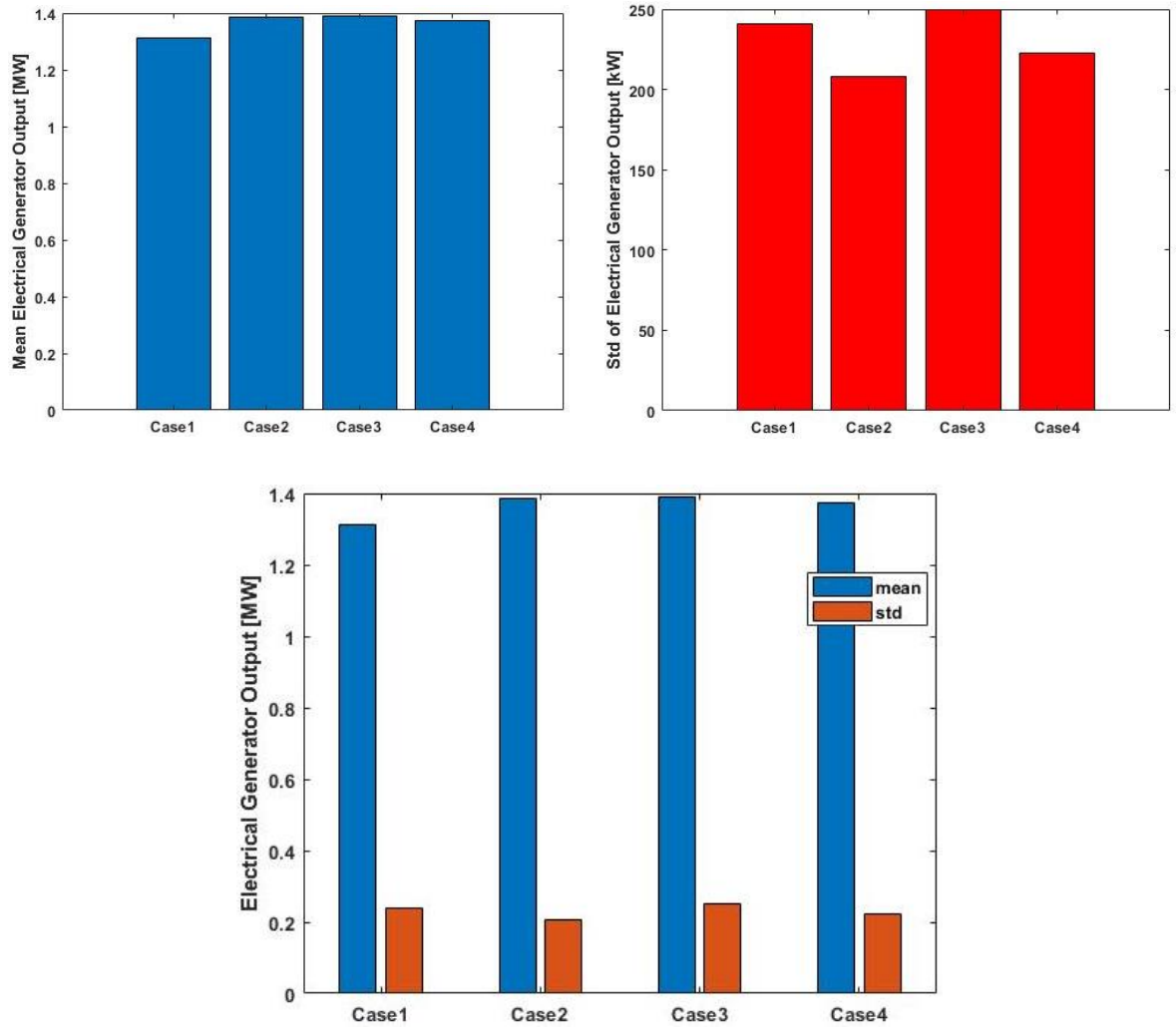

Figure 60. Mean and standard deviation of electrical generator output for four spatial resolutions in below-rated wind speed.

The results, shown in Figure 61, indicate that the variation of spatial resolutions have a slight effect on the platform pitch at nacelle level. The maximum and minimum of the mean values are 1.619 degrees for case3 and 1.563 degrees for case2 respectively. The standard deviations fluctuate from 0.2234 degrees for case2 to 0.2370 degrees for case4.

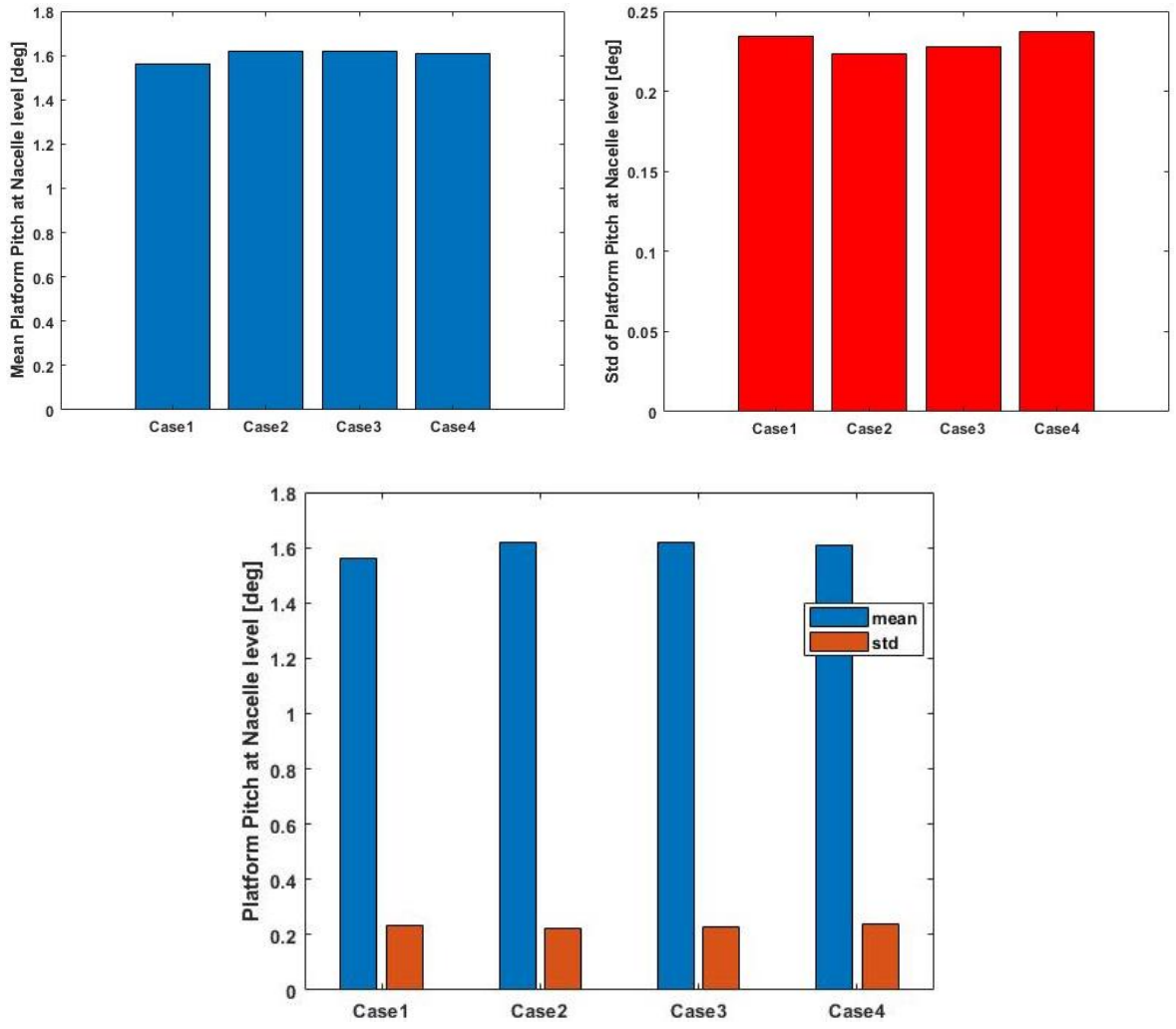

Figure 61. Mean and standard deviation of platform pitch for four spatial resolutions in below-rated wind speed.

Figure 62 shows a slight change in mean and standard deviation values of tip out-of-plane deflection of one blade. The mean value increases from 1.727 m for case2 to 1.769 m for case3 and then decreases to 1.763 m for case4. Furthermore, the highest standard deviation is 18.19 cm for case3 while the lowest standard deviation is 16.54 cm for case4.

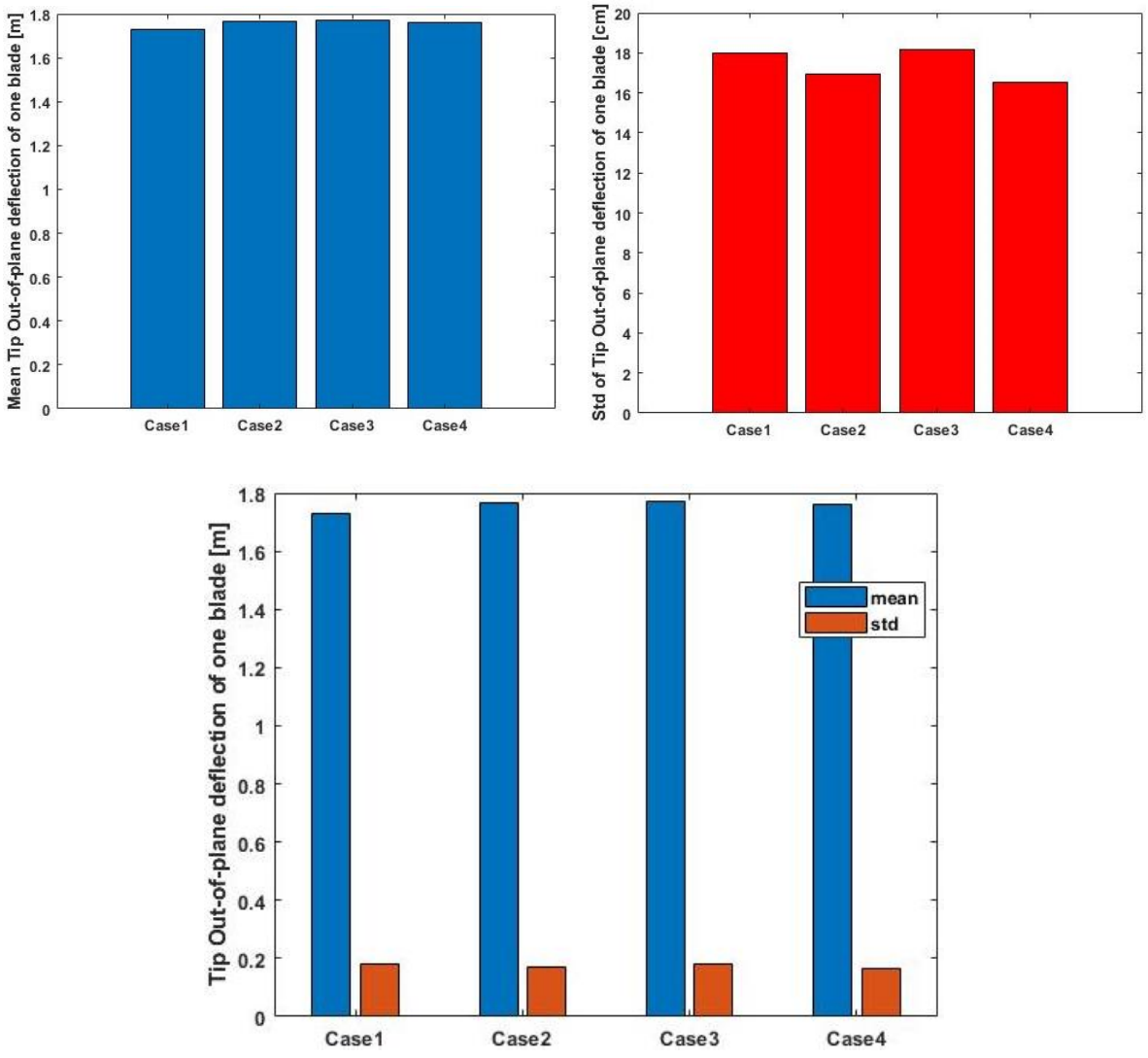

Figure 62. Mean and standard deviation of tip out-of-plane deflection of one blade for four spatial resolutions in below-rated wind speed.

2.1.2 Above-rated wind speed

2.1.2.1 Variation of wave characteristics

While mean values of the responses remained almost constant, standard deviation of the responses rapidly increased as significant wave height and wave peak period increased from case1 to case9.

The mean electrical generator output falls slightly from 2.3 MW for case1 to 2.281 MW for case9, illustrated in Figure 63. However, the standard deviation of electrical generator output increases dramatically from 11.07 for case1 to 112.3 kW for case9.

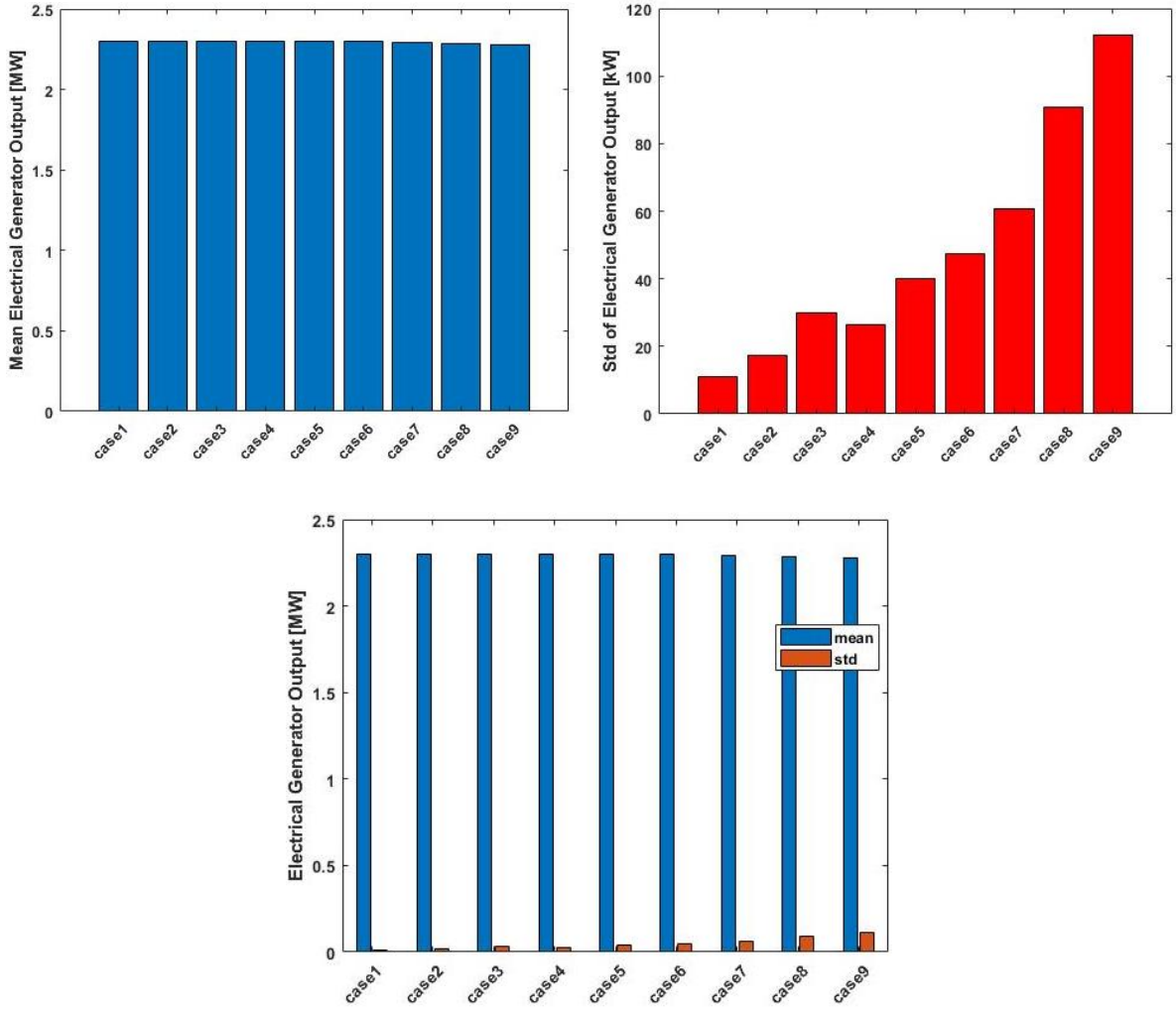

Figure 63. Standard deviation of electrical generator output for different H_s and T_p in above-rated wind speed.

As is illustrated by Figure 64, standard deviation of platform pitch rises rapidly from 0.28 to 1.68 degrees while mean value grows gradually from 1.29 to 1.36 degrees for case1 and case9 respectively.

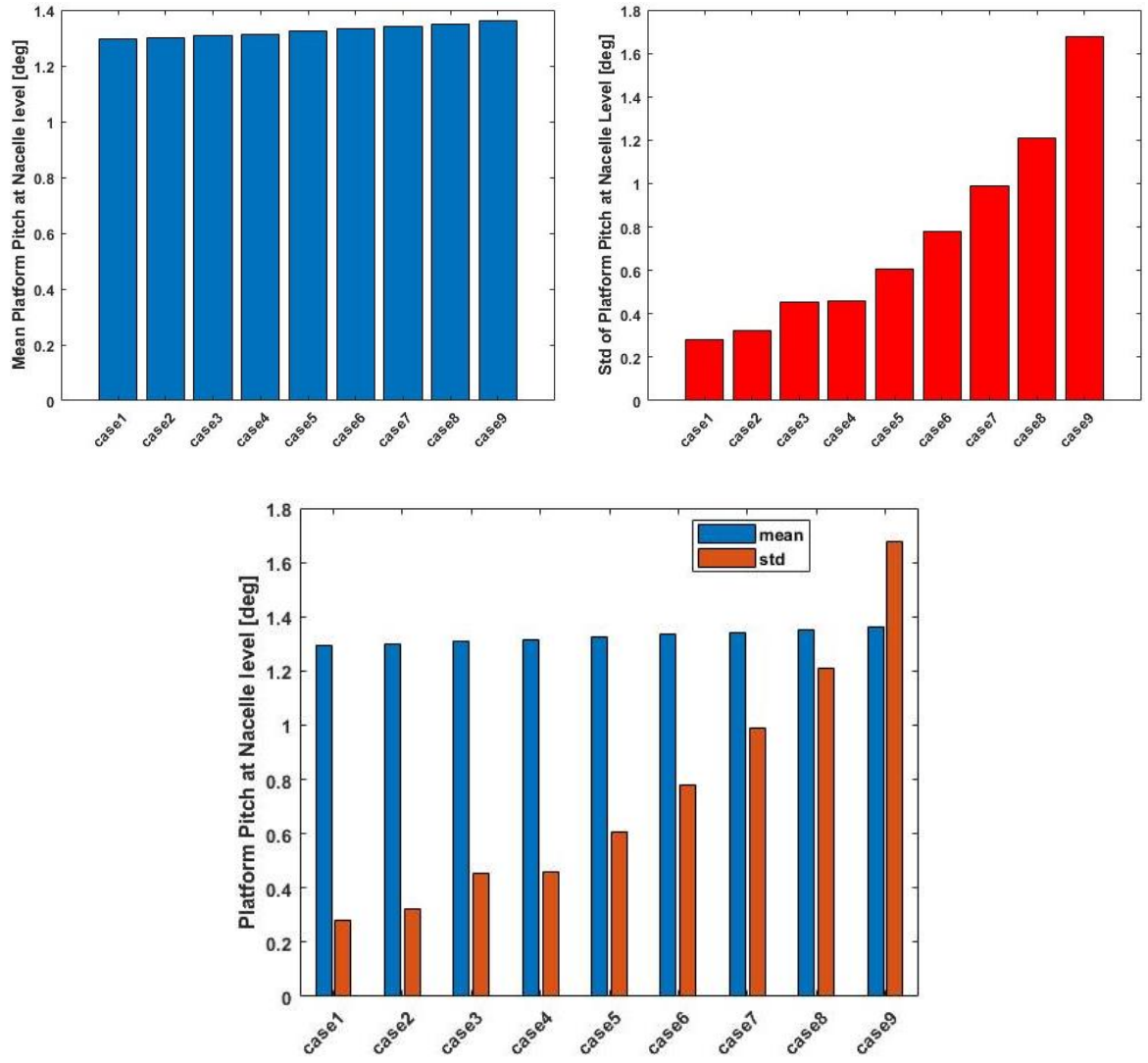

Figure 64. Standard deviation of platform pitch for different H_s and T_p in above-rated wind speed.

As it is shown by Figure 65, the mean tip out-of-plane deflection of one blade is almost stable, changes between 103.9 to 104.9 cm, while the change of standard deviation of tip out-of-plane deflection of one blade is 16.47 cm from case1 to case9, 37.93 and 54.4 cm respectively.

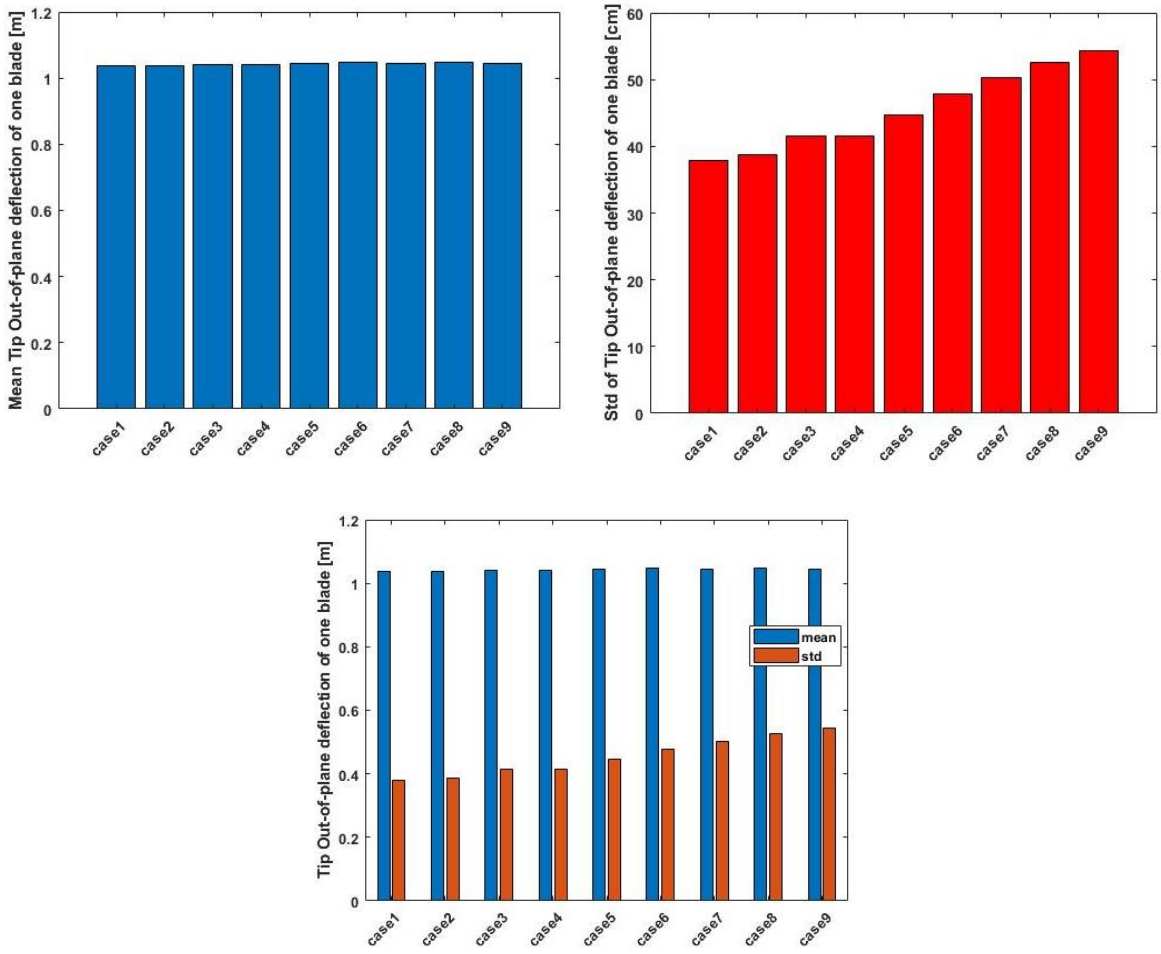

Figure 65. Standard deviation of tip out-of-plane deflection of one blade for different H_s and T_p in above-rated wind speed.

2.1.2.2 Variation of turbulence intensity

By increasing turbulence intensity, the standard deviation of the responses grew significantly, and mean value of the responses changed gently.

Figure 66 depicts that while turbulence intensity increases from 5% to 15%, the standard deviation of electrical generator output rapidly rises from 11.25 to 68.51 kW and mean value slightly reduces from 2.3 to 2.29 MW.

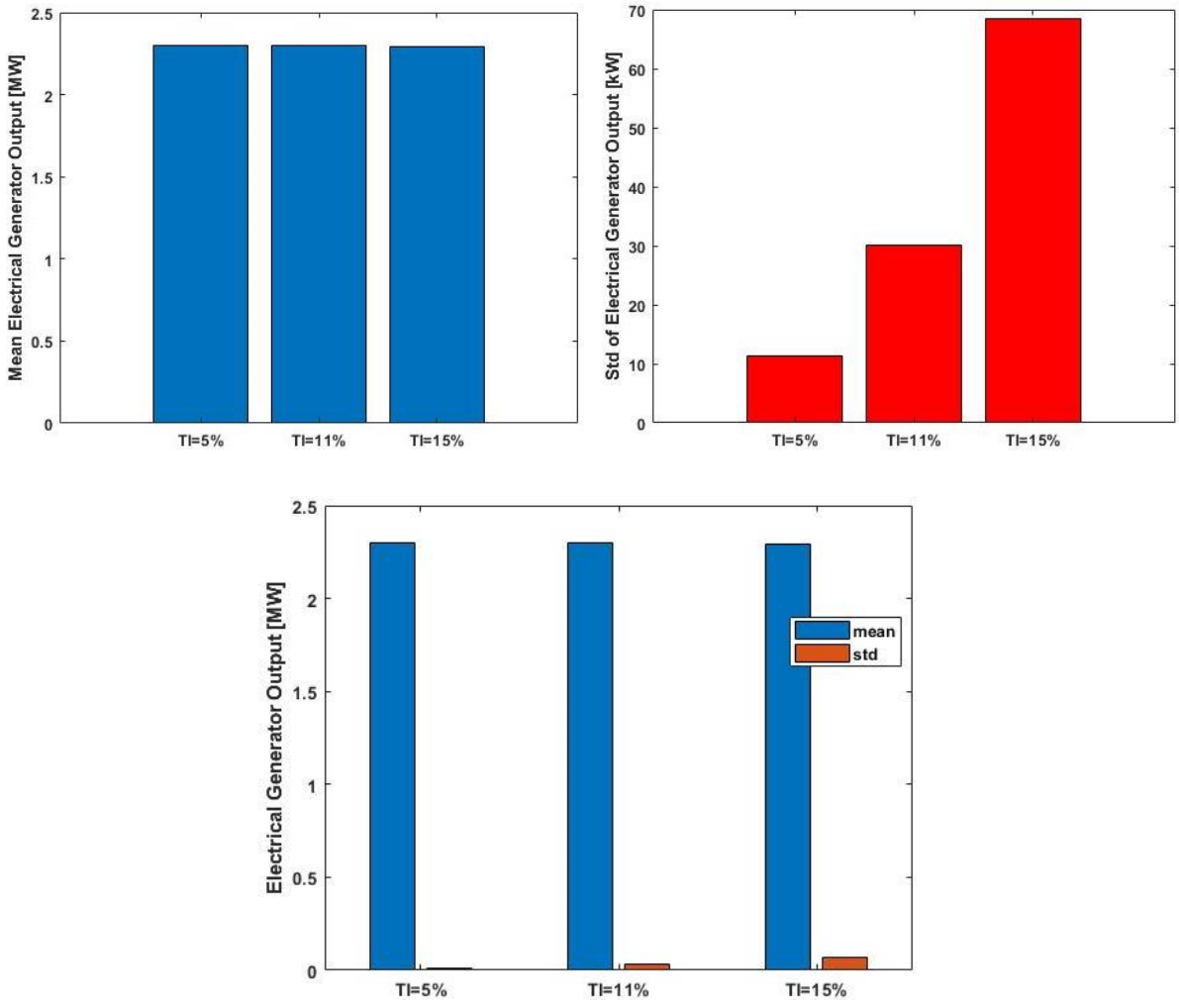

Figure 66. Mean and standard deviation of electrical generator output for three turbulence intensities in above-rated wind speed.

It can be seen from Figure 67 that standard deviation of platform pitch is 0.37, 0.45 and 0.55 degree for turbulence intensity of 5%, 11% and 15% respectively. Moreover, the mean value of platform pitch changes from 1.295 degrees for TI=5% to 1.31 degrees for TI=11% and 1.325 degrees for TI=15%.

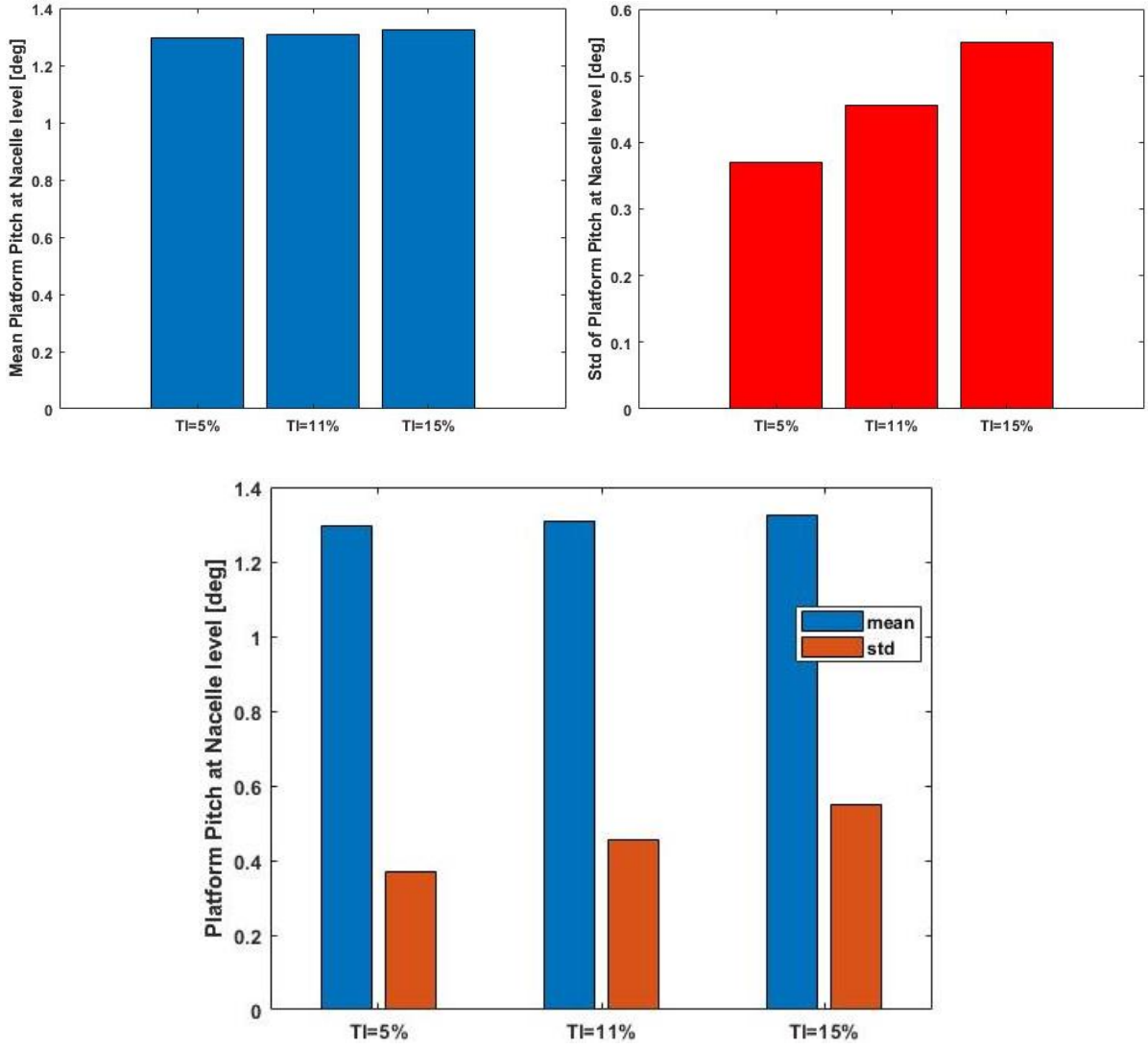

Figure 67. Mean and standard deviation of platform pitch for three turbulence intensities in above-rated wind speed.

The mean and standard deviation of tip out-of-plane deflection of one blade for turbulence intensity of 5% are 101.5 cm and 26.51 cm, for turbulence intensity of 11% are 104.2 cm and 41.62 cm, and for turbulence intensity of 15% are 106.9 cm and 53.18 cm respectively, presented in Figure 68.

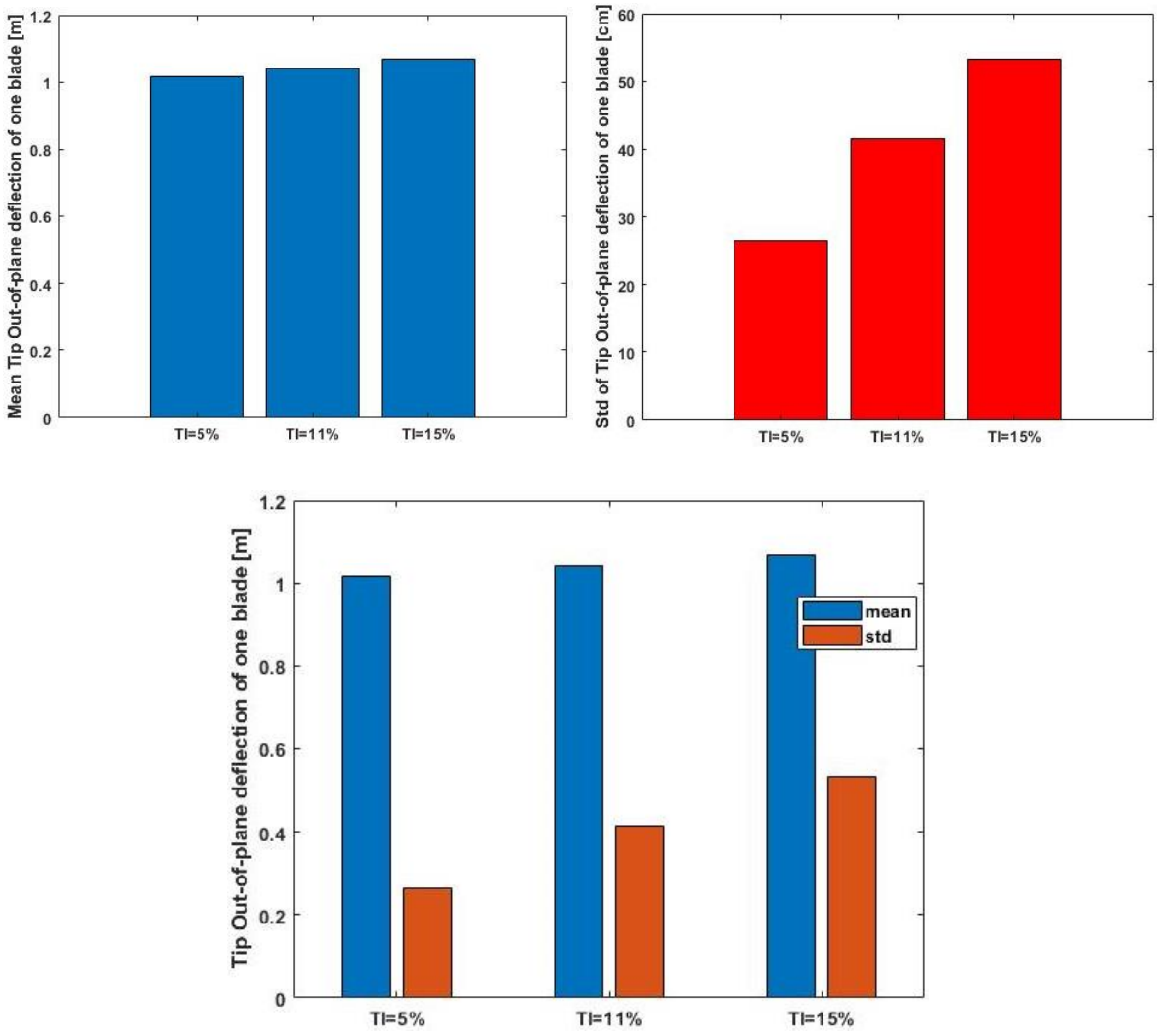

Figure 68. Mean and standard deviation of tip out-of-plane deflection of one blade for three turbulence intensities in above-rated wind speed.

2.1.2.3 Variation of alpha in wind shear profile power law

The studies showed that the effect of alteration of alpha in wind shear profile is negligible in both mean and standard deviation of the investigated responses.

Figure 69 depicts that mean value of electrical generator output remains constant while the standard deviation increases slightly. The mean value is 2.298 MW when alpha is 0, 0.05 and 0.1, while the mean value decreases 1 kW to 2.297 MW when alpha is 0.12 and 0.14. Moreover, the data also show that the standard deviation grows about 2 kW when alpha changes from 0 to 0.14. The standard deviation is 28.52, 29.41 and 30.8 kW when alpha is 0, 0.1 and 0.14 respectively.

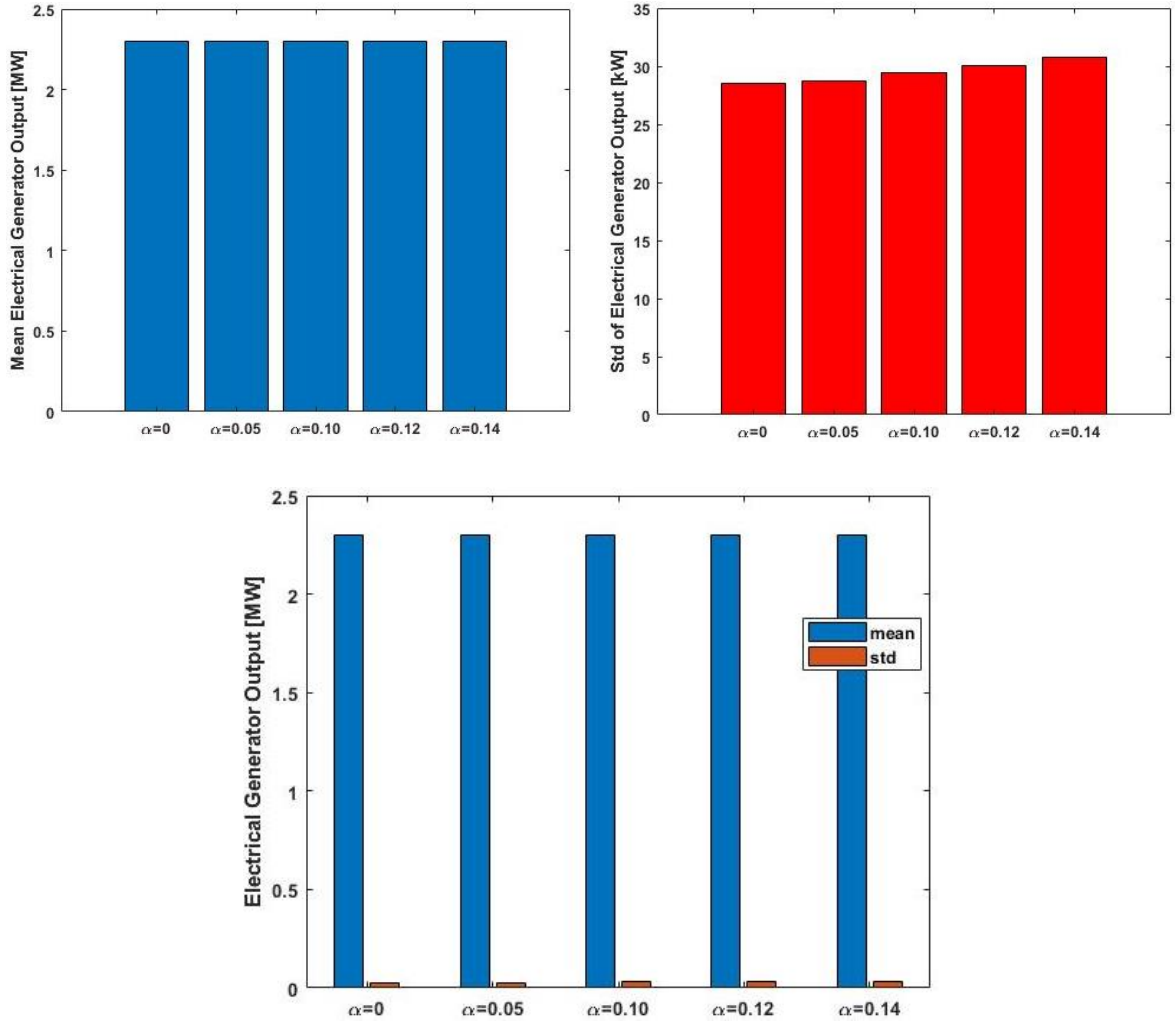

Figure 69. Mean and standard deviation of electrical generator output for five alphas in wind shear power law in above-rated wind speed.

Mean platform pitch rises steadily from 1.267 degrees to 1.315 degrees when alpha increases from 0 to 0.14 respectively, shown in Figure 70. However, the standard deviation is pretty constant in 0.45 degree for all alphas. Minimum and maximum standard deviation are 0.4541 for α=0 and 0.4557 for α=0.14 respectively.

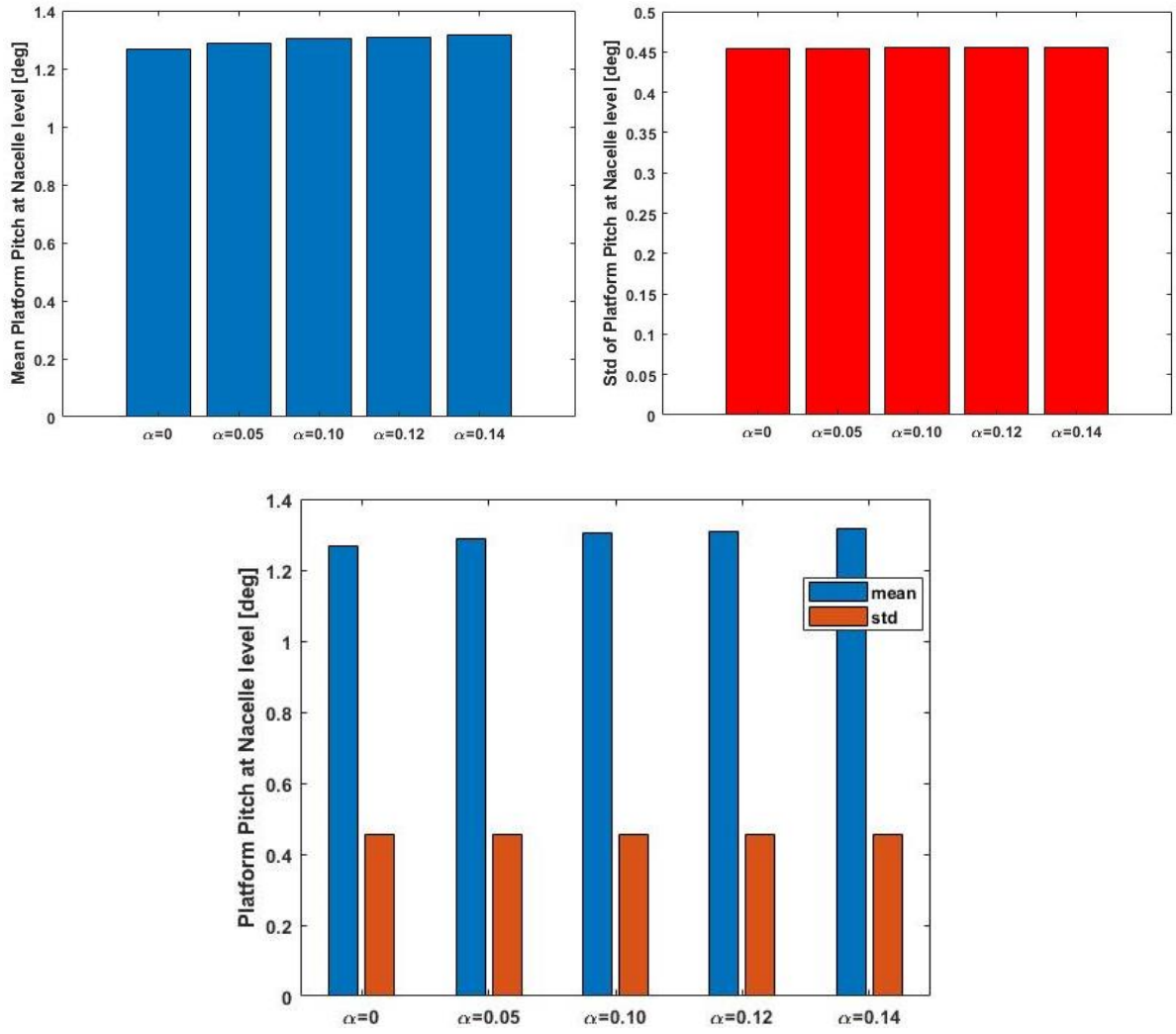

Figure 70. Mean and standard deviation of platform pitch for five alphas in wind shear power law in above-rated wind speed.

Figure 71 proves that the standard deviation of tip out-of-plane deflection of one blade increases gently from 38.85 cm to 42.56 cm by increasing of alpha from 0 to 0.14 while the mean value remains constant at approximately 104 cm, with minimum value of 103.7 and maximum value of 104.2.

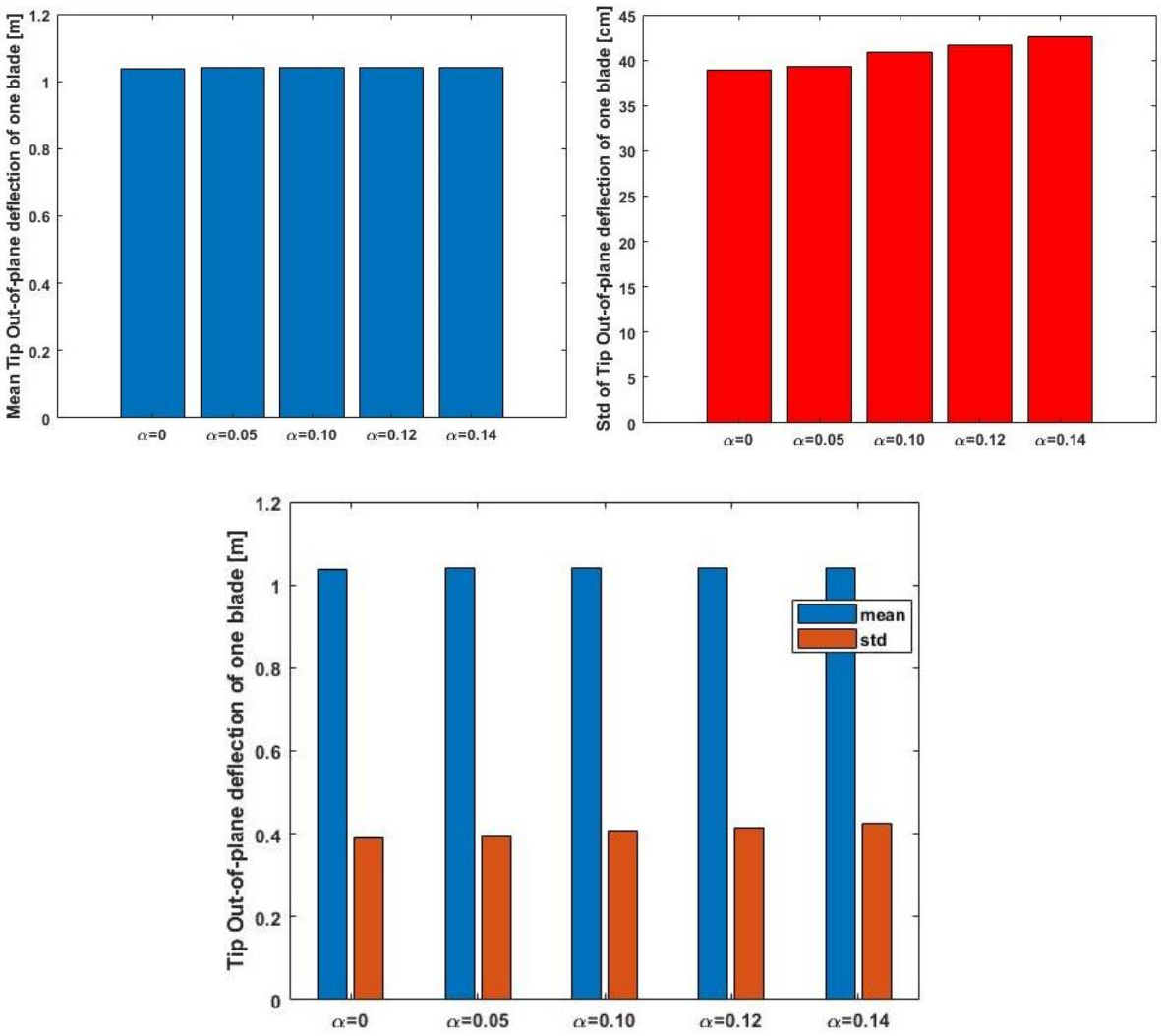

Figure 71. Mean and standard deviation of tip out-of-plane deflection of one blade for five alphas in wind shear power law in above-rated wind speed.

2.1.2.4 Variation of the spatial resolution of the numerical wind field

The results showed minor effect of variation of the spatial resolution on the studied responses.

Figure 72 illustrates a fluctuation in the standard deviation of electrical generator output between 20.26 kW for case3 and 30.02 kW for case1, while mean value changes slightly between 2.297 MW for case1 and 2.299 MW for case2 and case3.

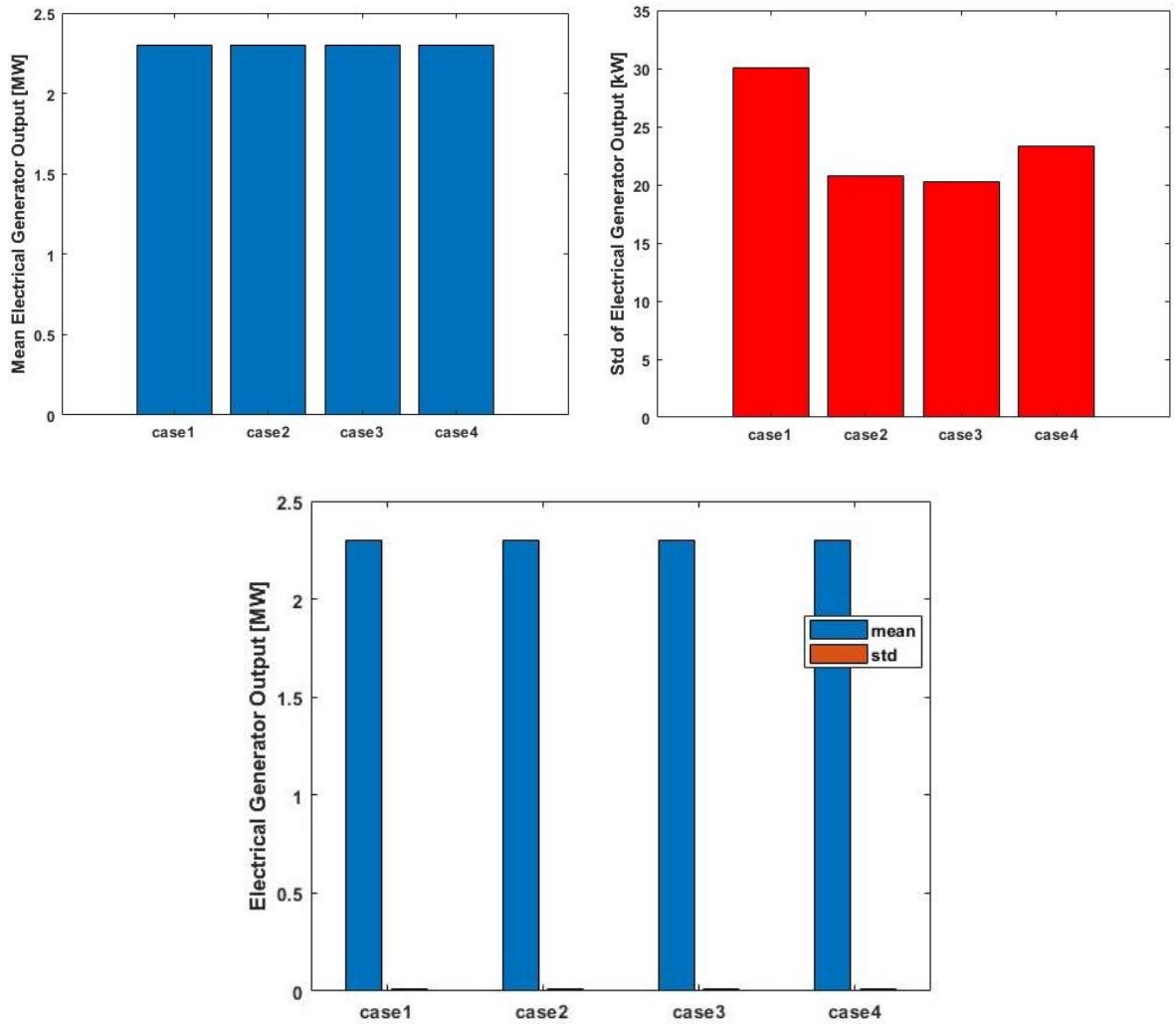

Figure 72. Mean and standard deviation of electrical generator output for four spatial resolutions in above-rated wind speed.

Figure 73 indicates that standard deviation of platform pitch first decreases from 0.4556 for case1 to 0.436 degree for case3 and then increases to 0.4677 degree for case4. Furthermore, the mean value is 1.31 degrees for case1, falls to 1.275 degrees for case2 and then rises to 1.282 degrees and 1.291 degrees for case 3 and case4 respectively.

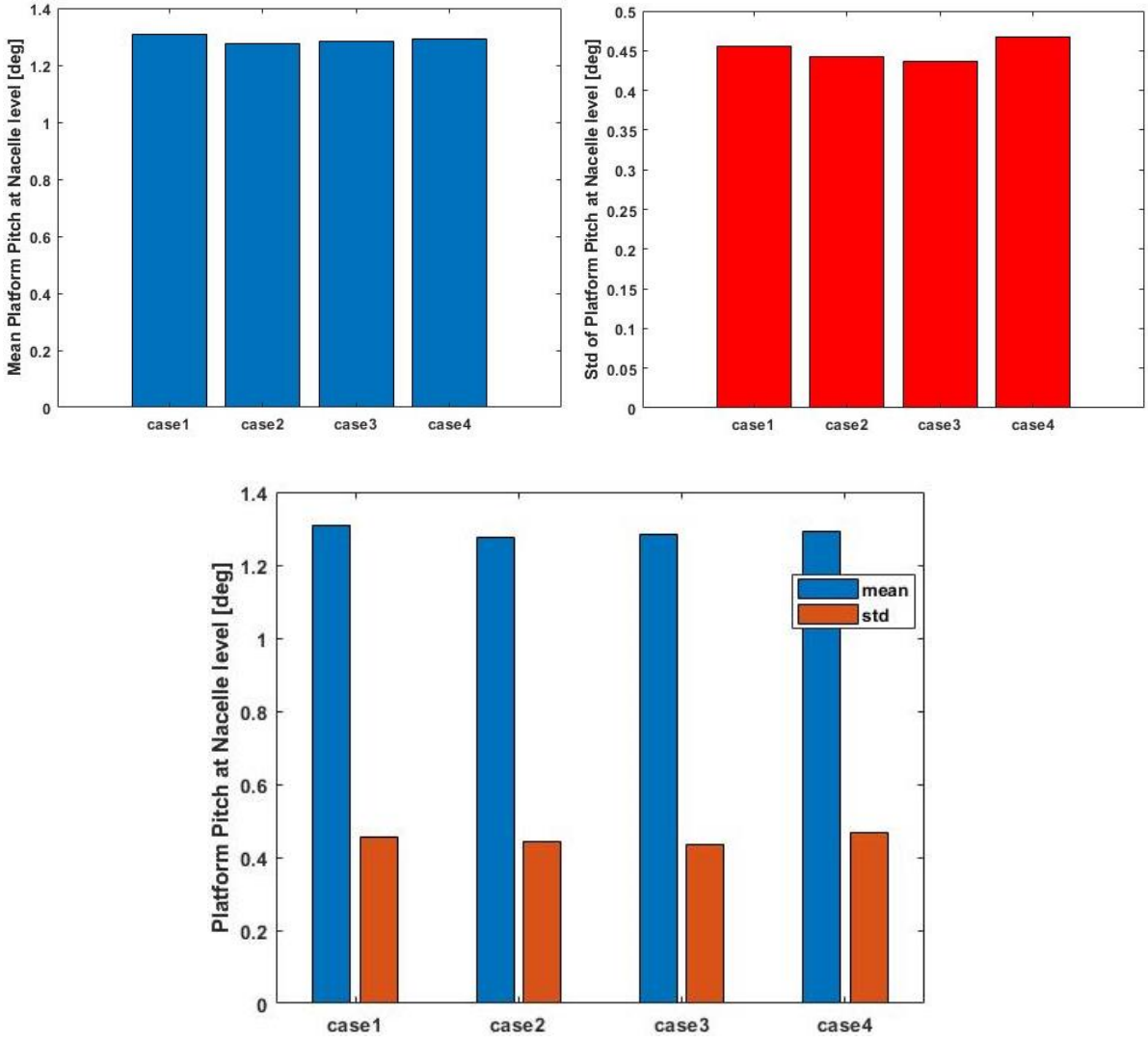

Figure 73. Mean and standard deviation of platform pitch for four spatial resolutions in above-rated wind speed.

It can be seen from Figure 74 that both mean and standard deviation of tip out-of-plane deflection of one blade change slightly with variation of the spatial resolution of the numerical wind field. The mean and standard deviation are 104.2 cm and 41.62 cm for case1, 99.12 cm and 39.61 cm for case2, 99.4 cm and 40 cm for case3 and 100.6 cm and 38.35 cm for case4.

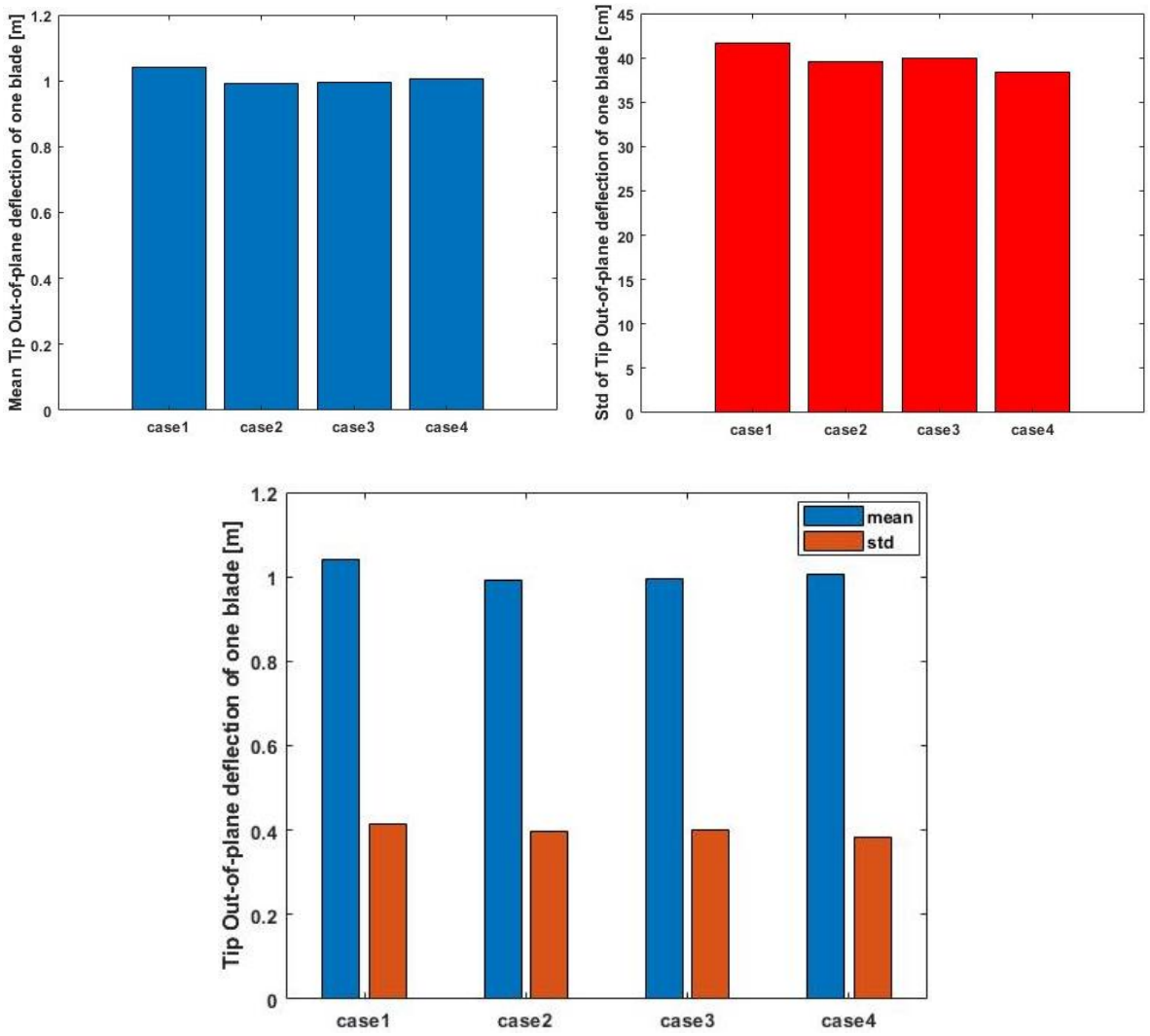

Figure 74. Mean and standard deviation of tip out-of-plane deflection of one blade for four spatial resolutions in above-rated wind speed.

2.2 OC3-Hywind results

2.2.1 Below-rated wind speed

2.2.1.1 Variation of wave characteristics

The results showed the standard deviation of the studied responses rose by higher wave characteristics while the mean value of the responses remained quite constant.

Mean mechanical power has a range between 4.41 MW for case1 and 4.433 MW for case7, presented in Figure 75. However, the standard deviation grows rapidly from 659.2 kW for case1 to 890.6 kW for case9.

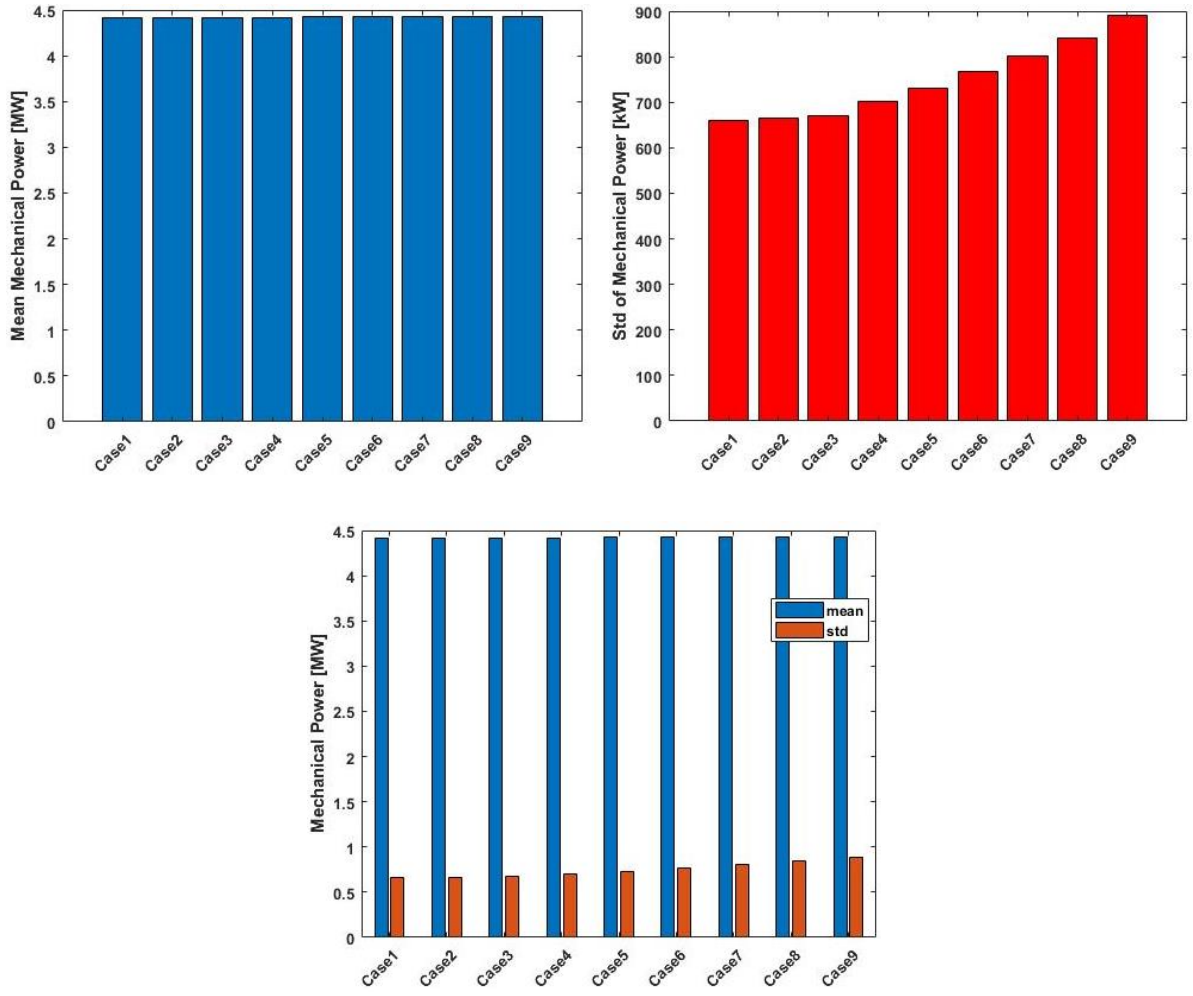

Figure 75. Mean and standard deviation of mechanical power for different $\mathbf{H_s}$ and $\mathbf{T_p}$ in below-rated wind speed.

Standard deviation of platform pitch rises about 100% from case1 and case9, illustrated in Figure 76. The standard deviation is 0.5157 degree for case1 and grows to 1.023 degrees for case9. The mean platform pitch changes only 0.282 degree, from 4.968 degrees for case1 to 4.686 degrees for case9.

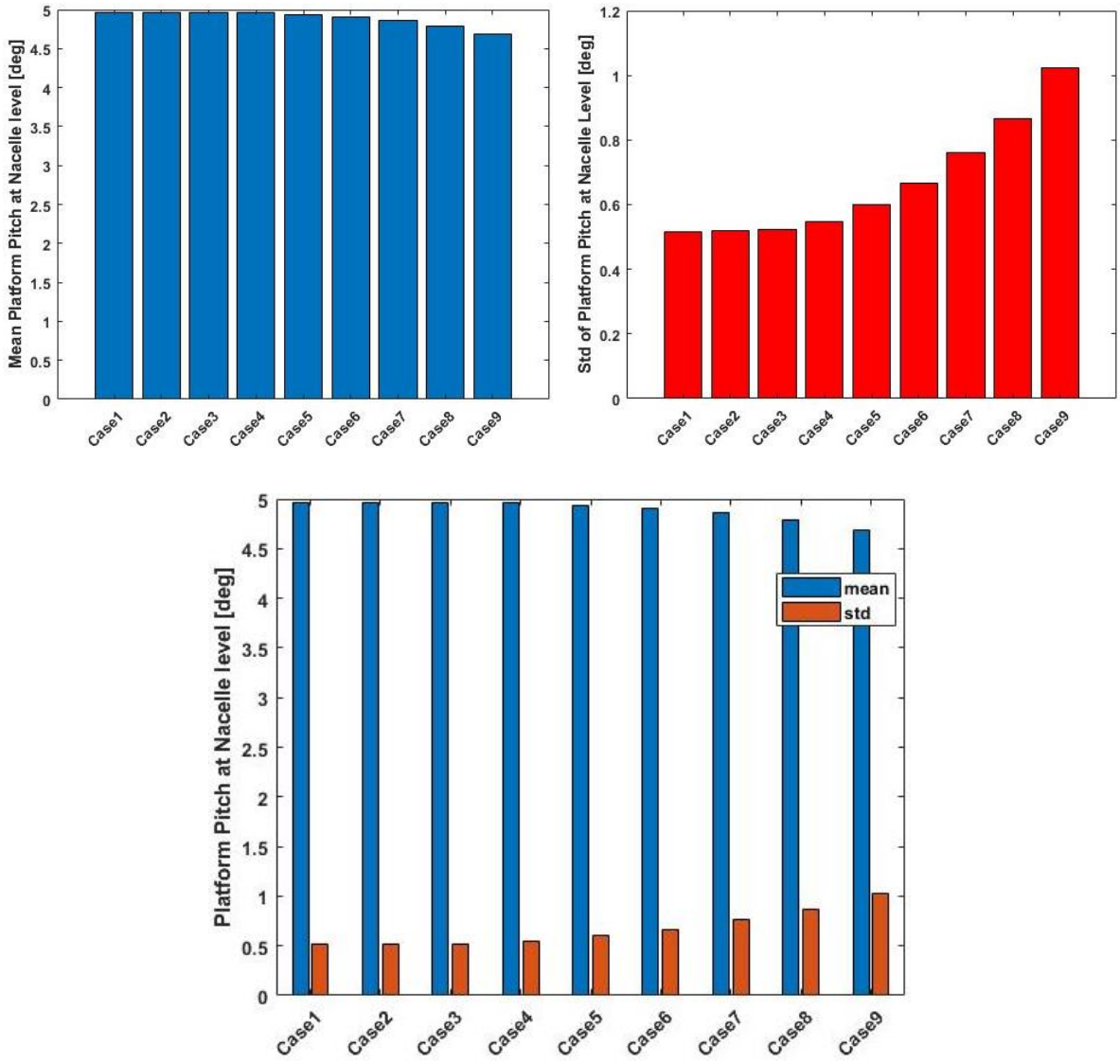

Figure 76. Mean and standard deviation of platform pitch for different $\mathbf{H_s}$ and $\mathbf{T_p}$ in below-rated wind speed.

As is shown by Figure 77, mean tip out-of-plane deflection of one blade declines slightly from 5.197 m for case1 to 4.905 m for case9 while the standard deviation goes up sharply from 57.19 cm for case1 to 109.2 cm for case9.

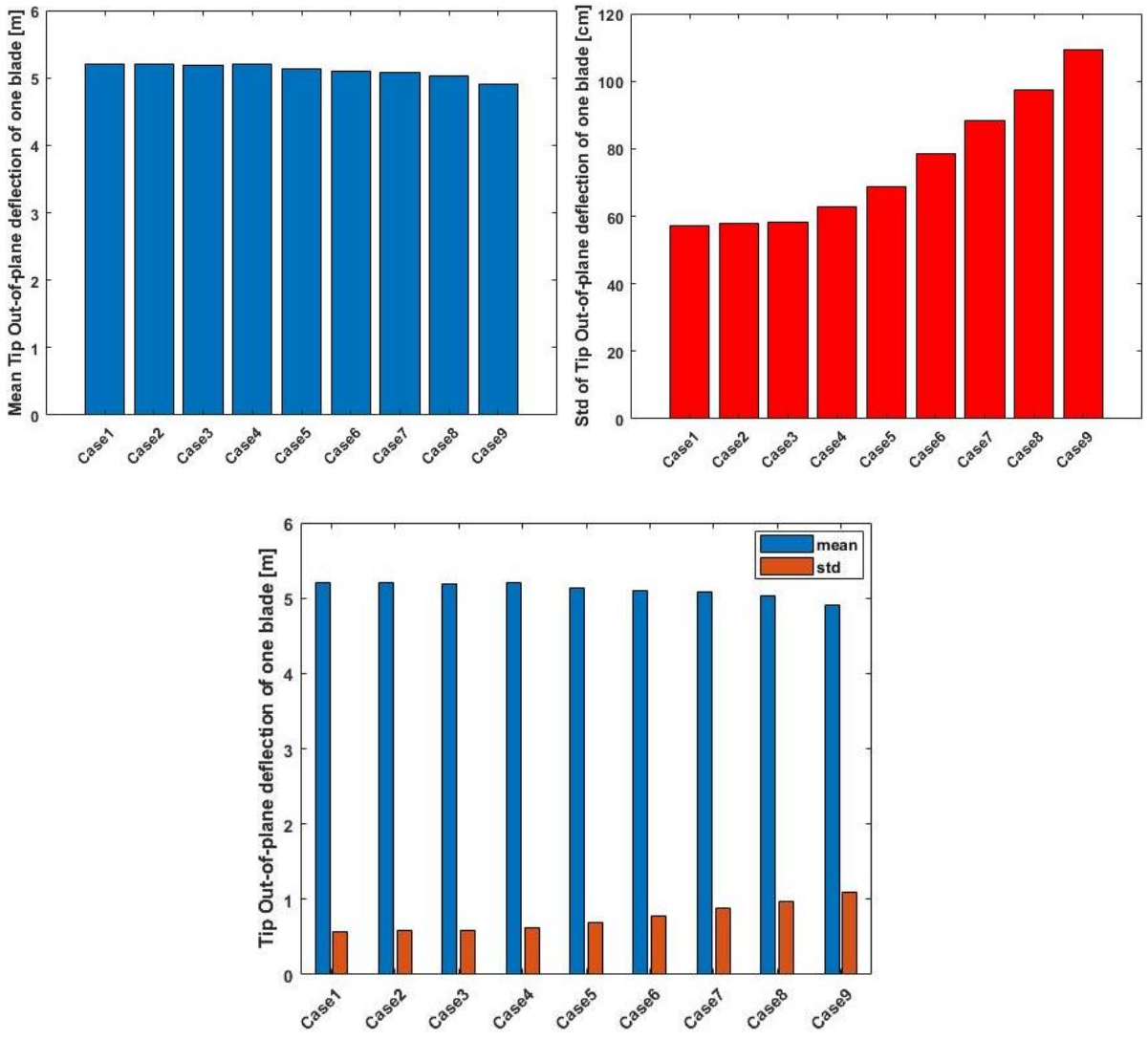

Figure 77. Mean and standard deviation of tip out-of-plane deflection of one blade for different $\mathbf{H_s}$ and $\mathbf{T_p}$ in below-rated wind speed.

2.2.1.2 Variation of turbulence intensity

While the mean value of the investigated responses dropped gradually, the standard deviation of the responses rose significantly when the turbulence intensity increased from 5% to 15%.

From Figure 78 it is clear the decline of mean mechanical power from 4.544 MW when TI=5% to 4.411 MW when TI=10% and 4.252 MW when TI=15%. The standard deviation grows though by increasing turbulence intensity. The standard deviation is 401.7 kW, 663.9 kW and 859.8 kW when turbulence intensity equals to 5%, 10% and 15% respectively.

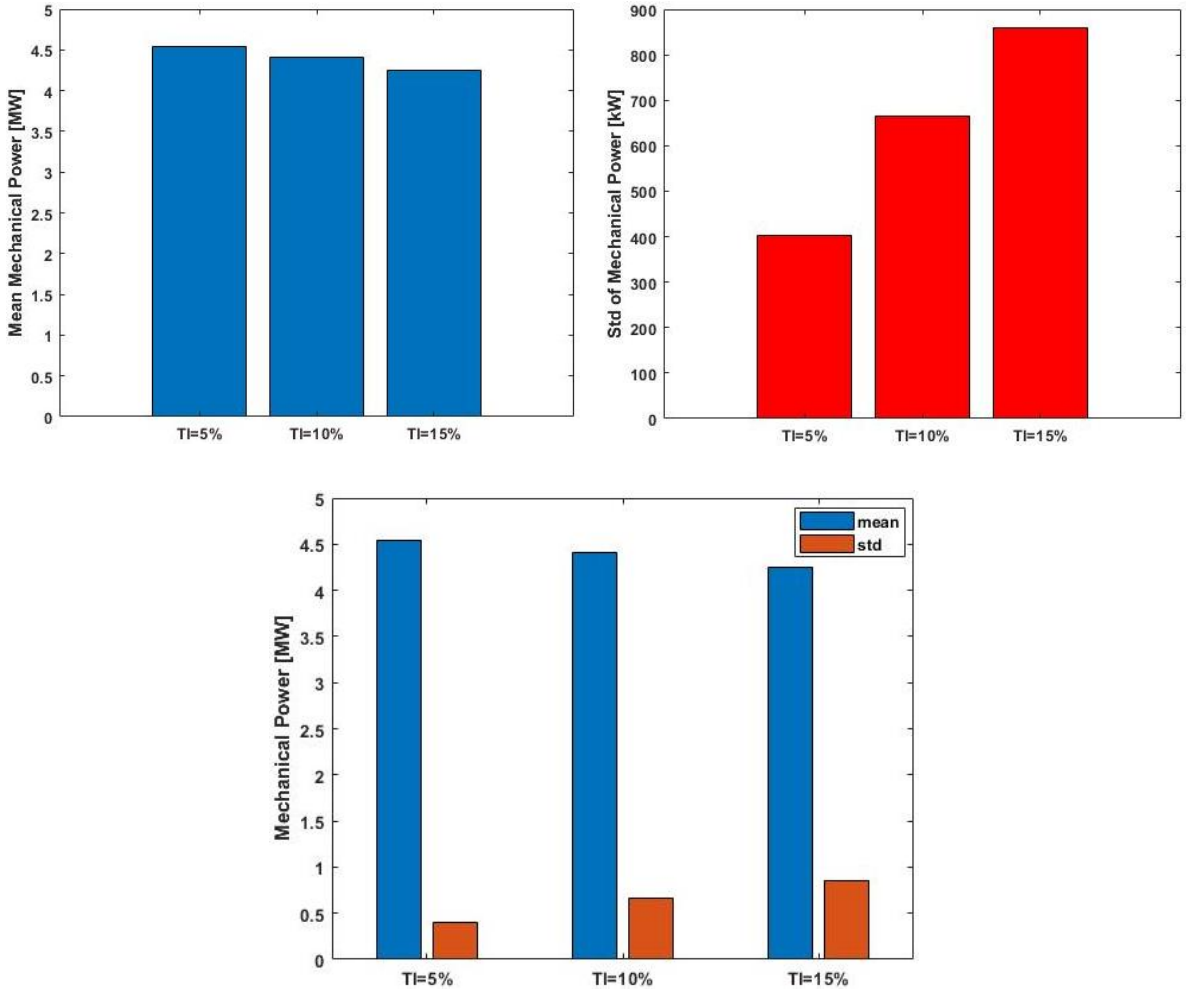

Figure 78. Mean and standard deviation of mechanical power for three turbulence intensities in below-rated wind speed.

As can be seen from Figure 79, the standard deviation of platform pitch goes up from 0.282 degree for TI=5% to 0.5195 degree for TI=10% and 0.7967 degree for TI=15%. In contrast, the mean value drops when turbulence intensity increases. The mean value is 5.203, 4.967 and 4.673 when turbulence intensity equals to 5%, 10% and 15% respectively.

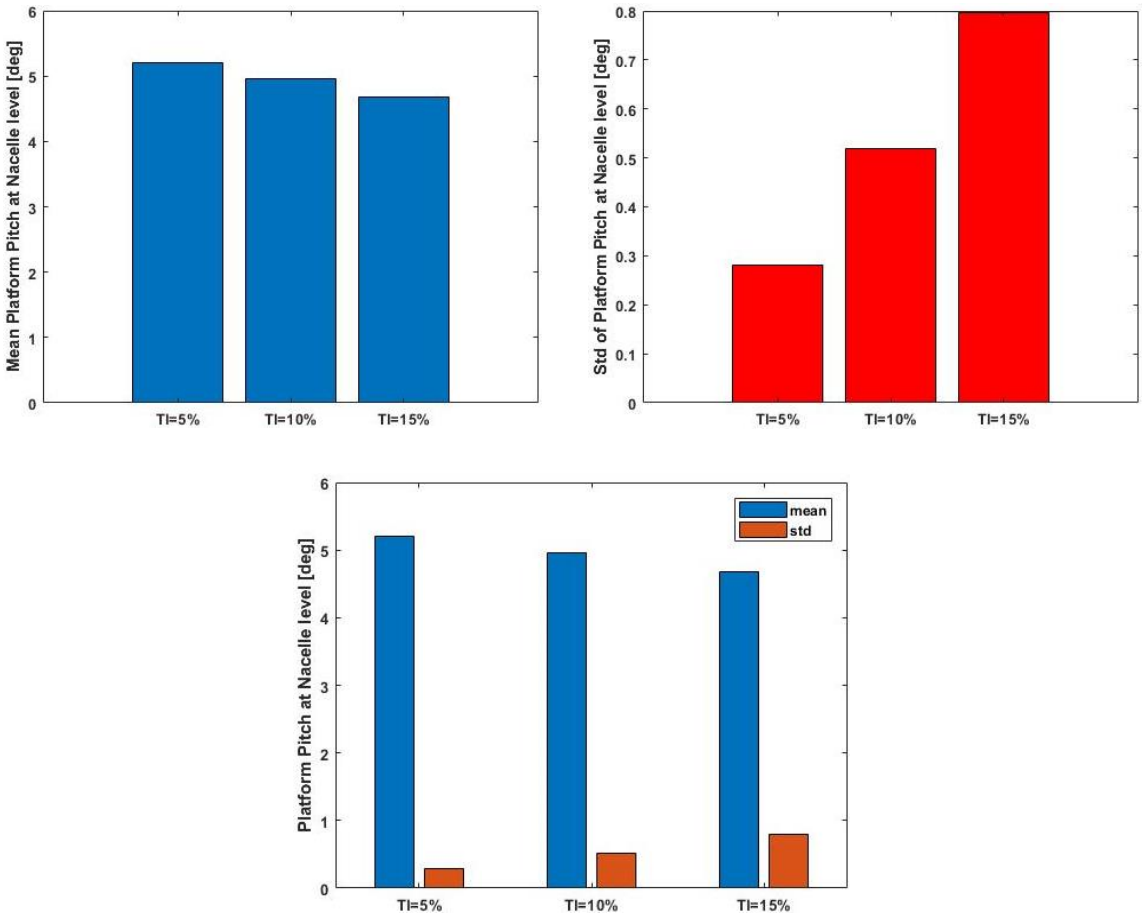

Figure 79. Mean and standard deviation of platform pitch for three turbulence intensities in below-rated wind speed.

Figure 80 illustrates that by increasing turbulence intensity from 5% to 10% and 15%, mean tip out-of-plane deflection for one blade decreases from 5.437 m to 5.202 m and 4.895 m and the standard deviation increases from 32.06 cm to 57.73 and 84.3 cm respectively.

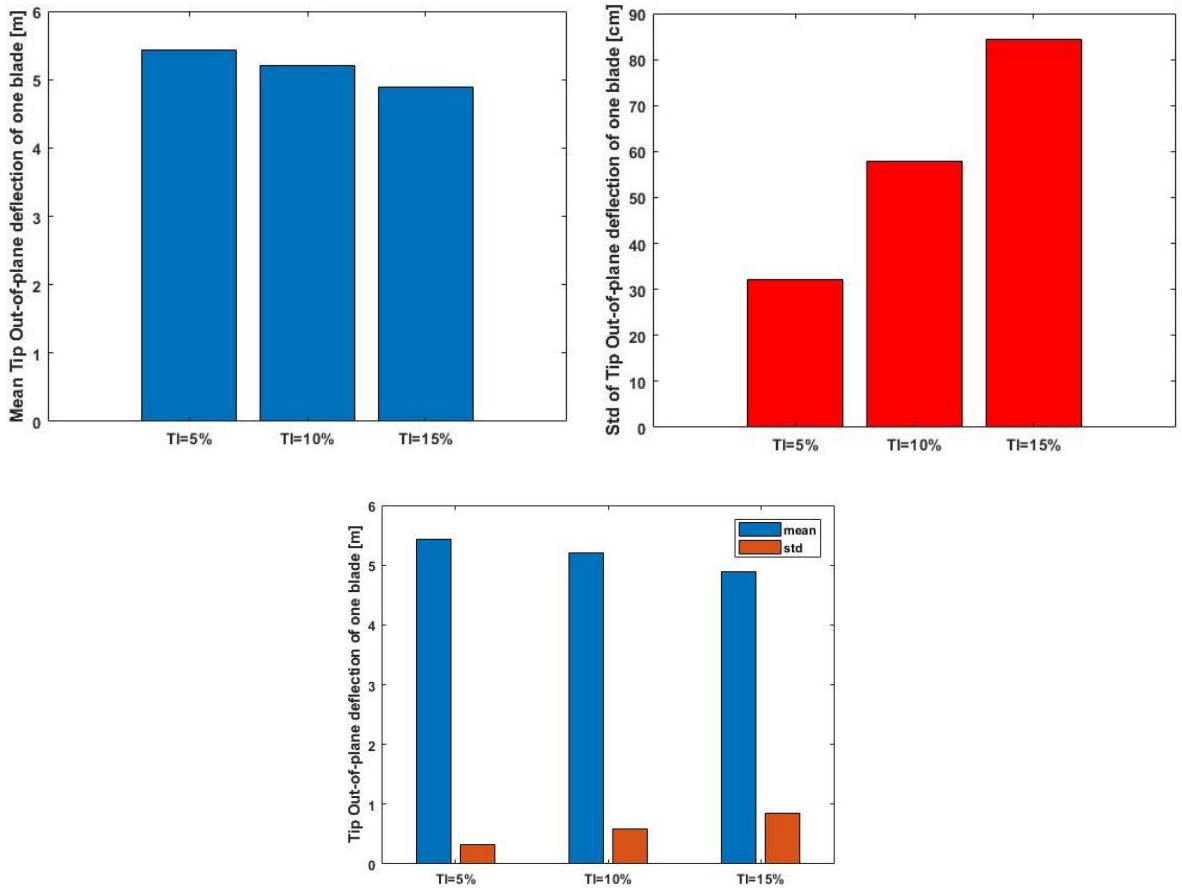

Figure 80. Mean and standard deviation of tip out-of-plane deflection of one blade for three turbulence intensities in below-rated wind speed.

2.2.1.3 Variation of alpha in wind shear profile power law

The variation of alpha in wind shear profile power law has a slight effect on both mean and standard deviation of the responses.

Figure 81 indicates that the maximum mean and standard deviation of mechanical power are 4.491 MW for α=0 and 665.4 kW for α=0.14 respectively. Furthermore, the minimum mean and standard deviation of mechanical power are 4.4 MW for α=0.14 and 643.6 kW for α=0 respectively.

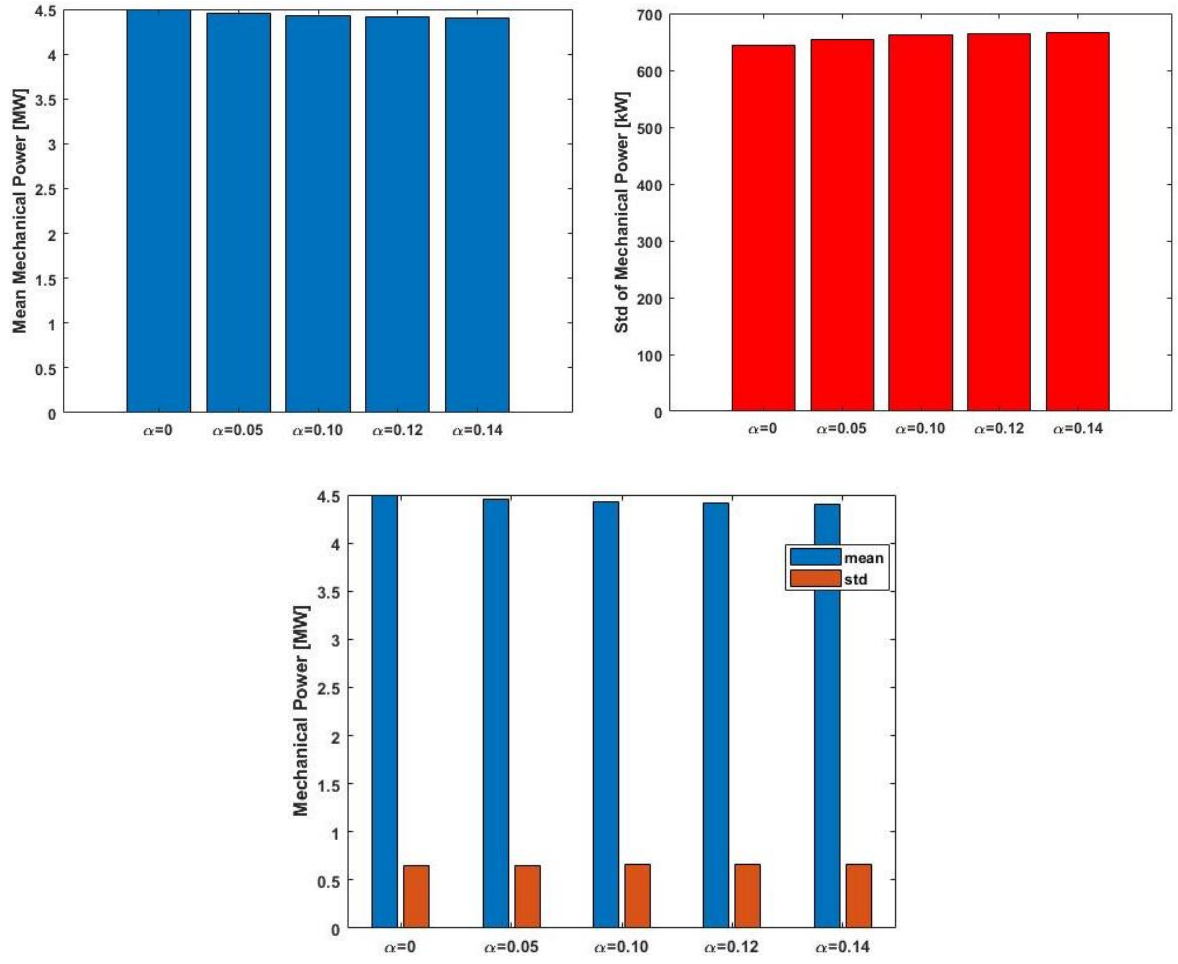

Figure 81. Mean and standard deviation of mechanical power for five alphas in wind shear power law in below-rated wind speed.

As can be seen from Figure 82, both mean and standard deviation of platform pitch are quite constant. The maximum and minimum of the mean value are 4.972 degrees for α=0.14 and 4.918 degrees for α=0 respectively. However, the maximum and minimum of the standard deviation are 0.5241 degree for α=0 and 0.5176 degree for α=0.14 respectively.

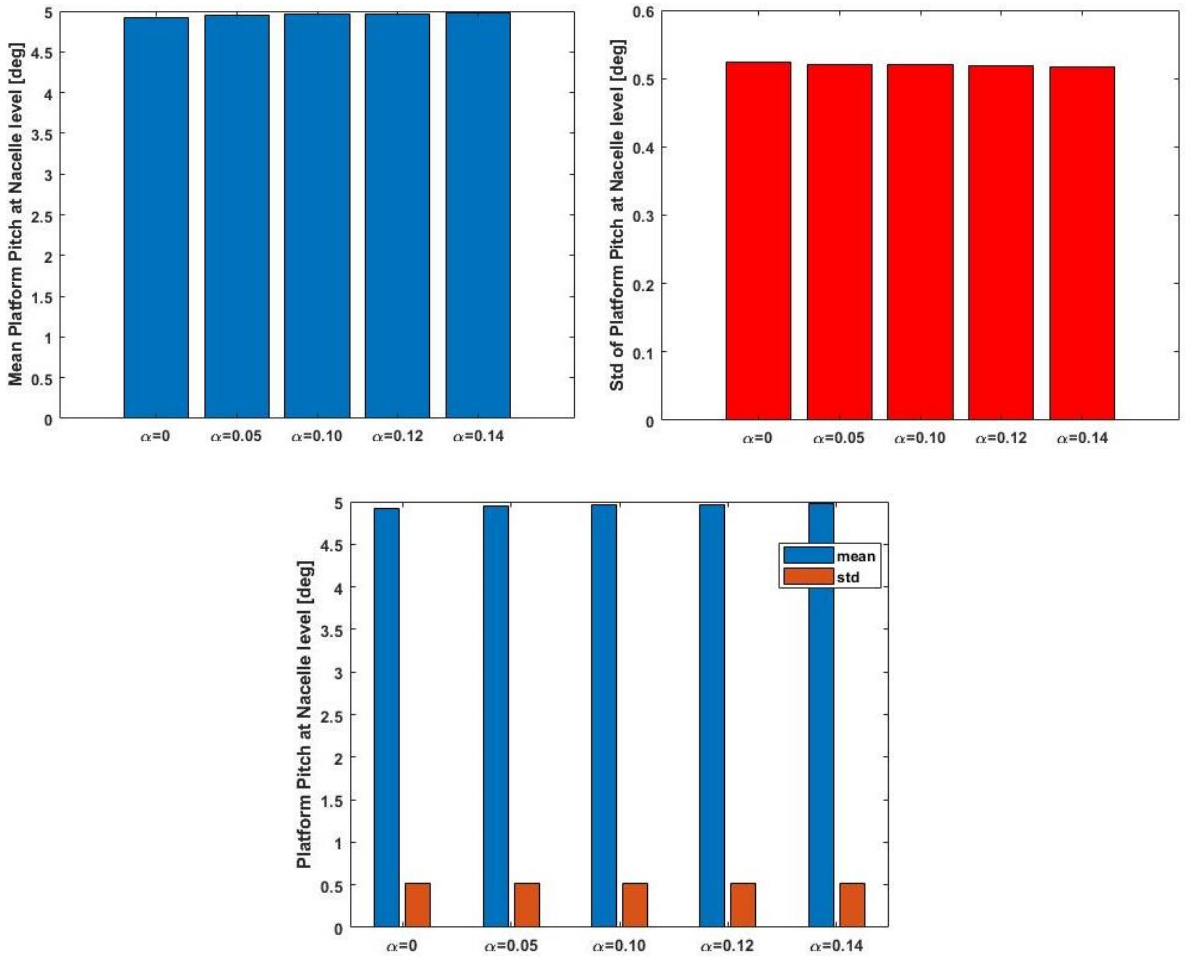

Figure 82. Mean and standard deviation of platform pitch for five alphas in wind shear power law in below-rated wind speed.

The mean tip out-of-plane deflection of one blade changes from 5.197 m for α=0.14 to 5.217 m for α=0.05, presented in Figure 83. It can be seen from the data that the maximum mean value, 5.217 m, and minimum standard deviation, 55.32 cm, occur when α=0.05. Moreover, the standard deviation is 56.92 cm for α=0, falls to 55.32 cm for α=0.05 and increases to 59.23 cm for α=0.14.

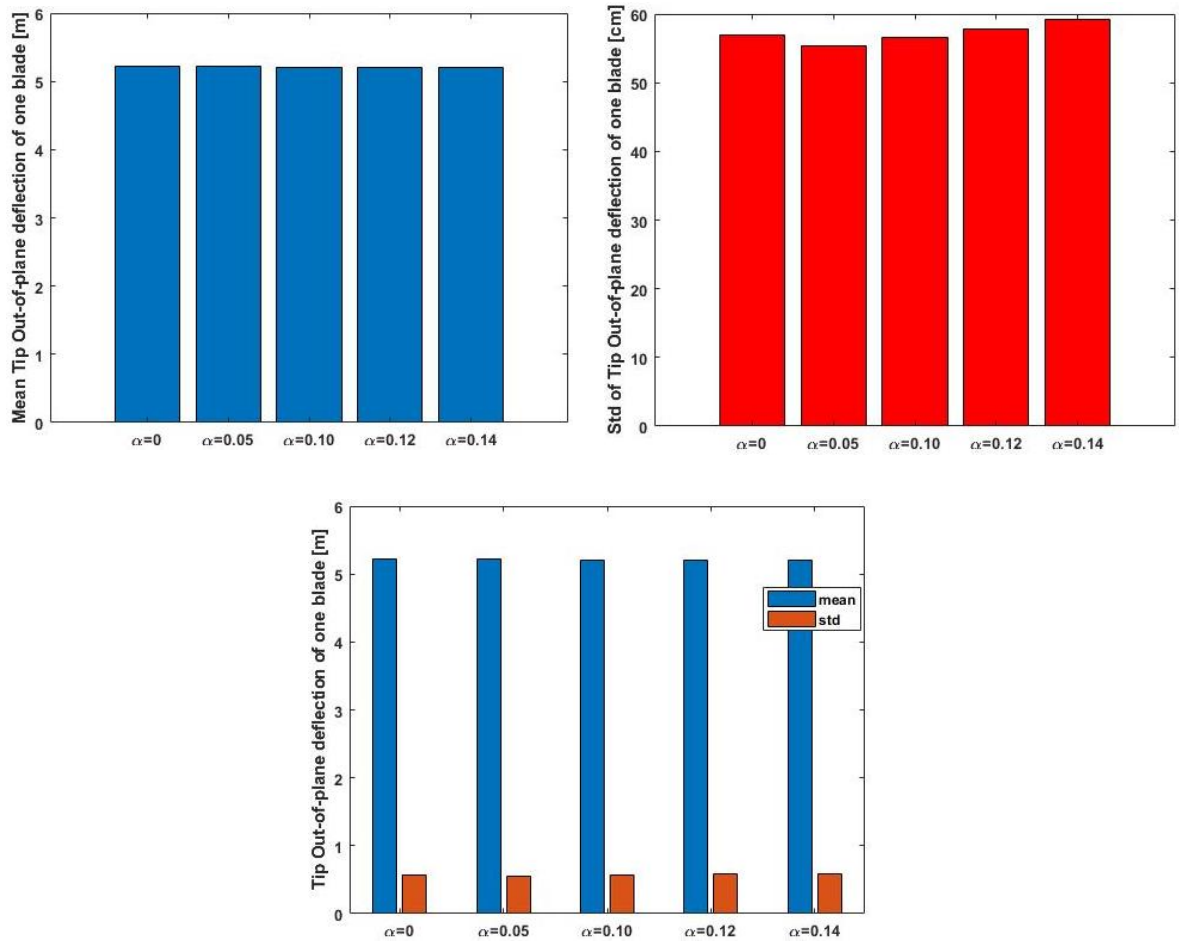

Figure 83. Mean and standard deviation of tip out-of-plane deflection of one blade for five alphas in wind shear power law in below-rated wind speed.

2.2.1.4 Variation of the spatial resolution of the numerical wind field

The results indicate fluctuation in the studied responses of the structure with respect to the variation of spatial resolution of the numerical wind field.

As presented by Figure 84, mean mechanical power is 4.411 MW, 4.661 MW, 4.573 MW and 4.602 MW for case1, case2, case3 and case4 respectively. The standard deviation fluctuates more widely, the analysis shows the standard deviation is 663.9 kW, 563.3 kW, 664 kW and 614.6 kW for case1, case2, case3 and case4 respectively.

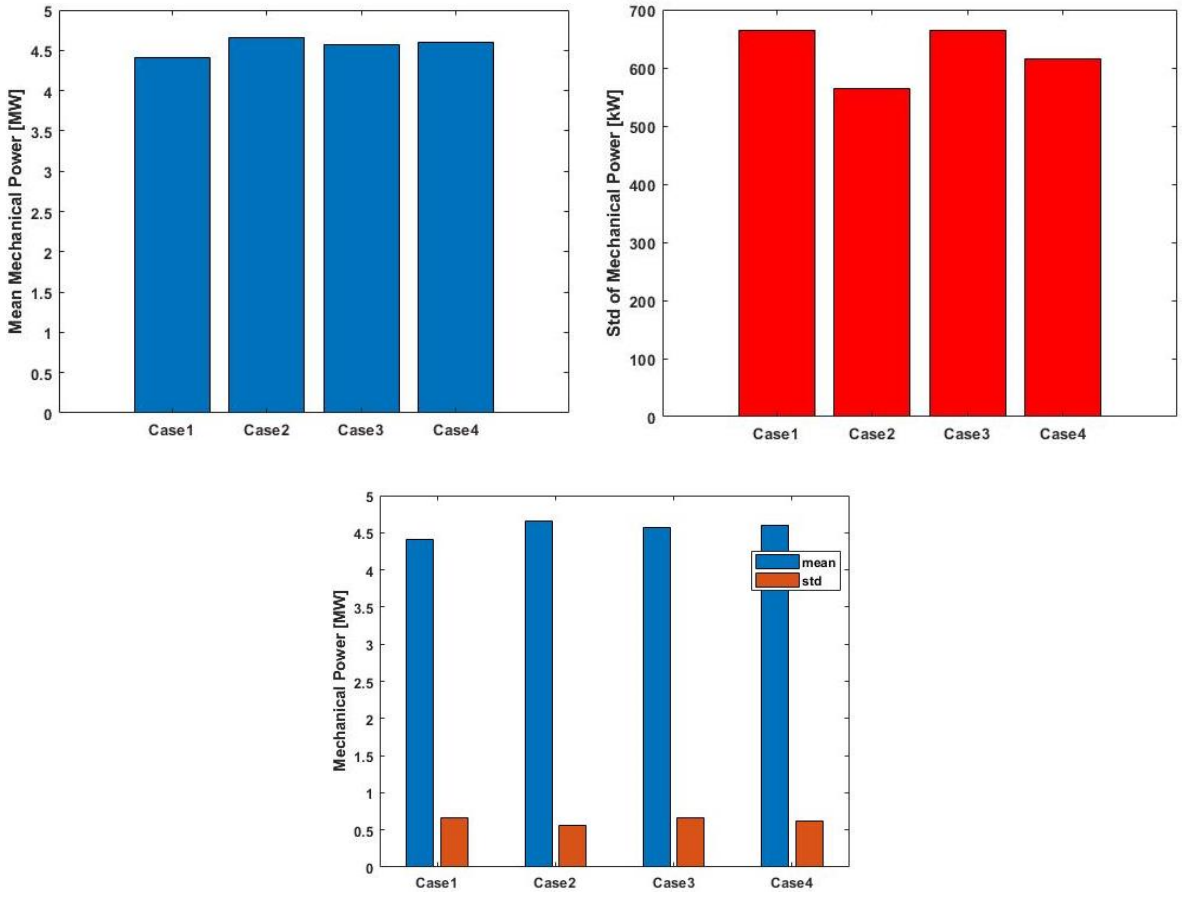

Figure 84. Mean and standard deviation of mechanical power for four spatial resolutions in below-rated wind speed.

Figure 85 shows mean platform pitch is in its maximum value, 5.118 degrees, for case2 while the standard deviation is in its maximum value, 0.6419 degree, for case3. Both mean and standard deviation values are in their minimum values for case1 where mean value is 4.967 degrees and the standard value is 0.5195 degree.

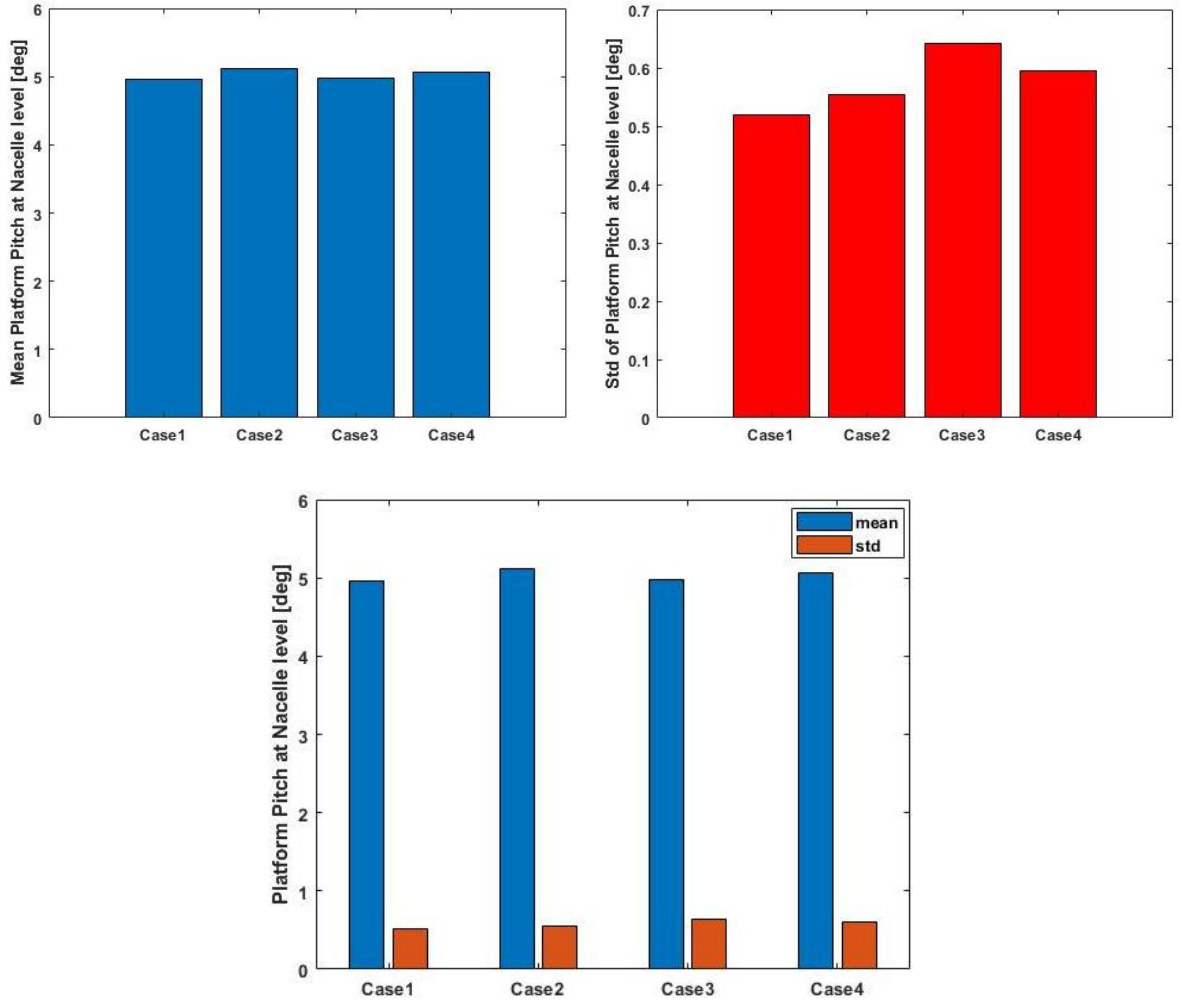

Figure 85. Mean and standard deviation of platform pitch for four spatial resolutions in below-rated wind speed.

Mean tip out-of-plane deflection of one blade, shown in Figure 86, goes up and down. The mean value is 5.202 m, 5.316 m, 5.141 m and 5.262 m for case1, case2, case3 and case4 respectively. The standard deviation grows from 57.73 cm for case1 to 63.41 cm for case3 and then falls to 56.73 cm for case4.

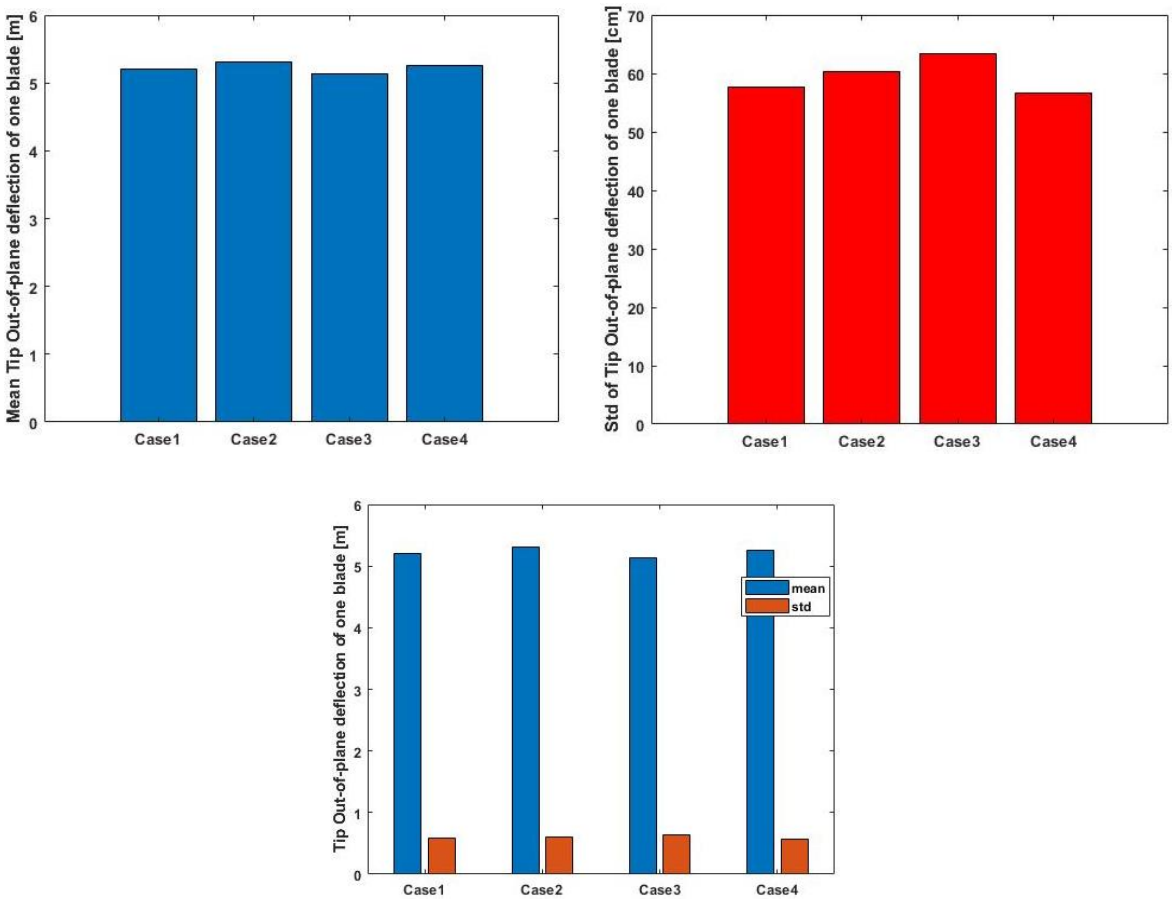

Figure 86. Mean and standard deviation of tip out-of-plane deflection of one blade for four spatial resolutions in below-rated wind speed.

2.2.2 Above-rated wind speed

2.2.2.1 Variation of wave characteristics

The analyses showed by increasing significant wave heights and wave peak periods, standard deviation of the investigated responses increased while the mean values remained quite steady.

Figure 87 depicts that mean mechanical power decreases slightly from 5.195 MW for case1 to 5.140 MW for case9 by increasing wave characteristics. However, the standard deviation rises rapidly from 140 kW for case1 to 213.8 kW for case9.

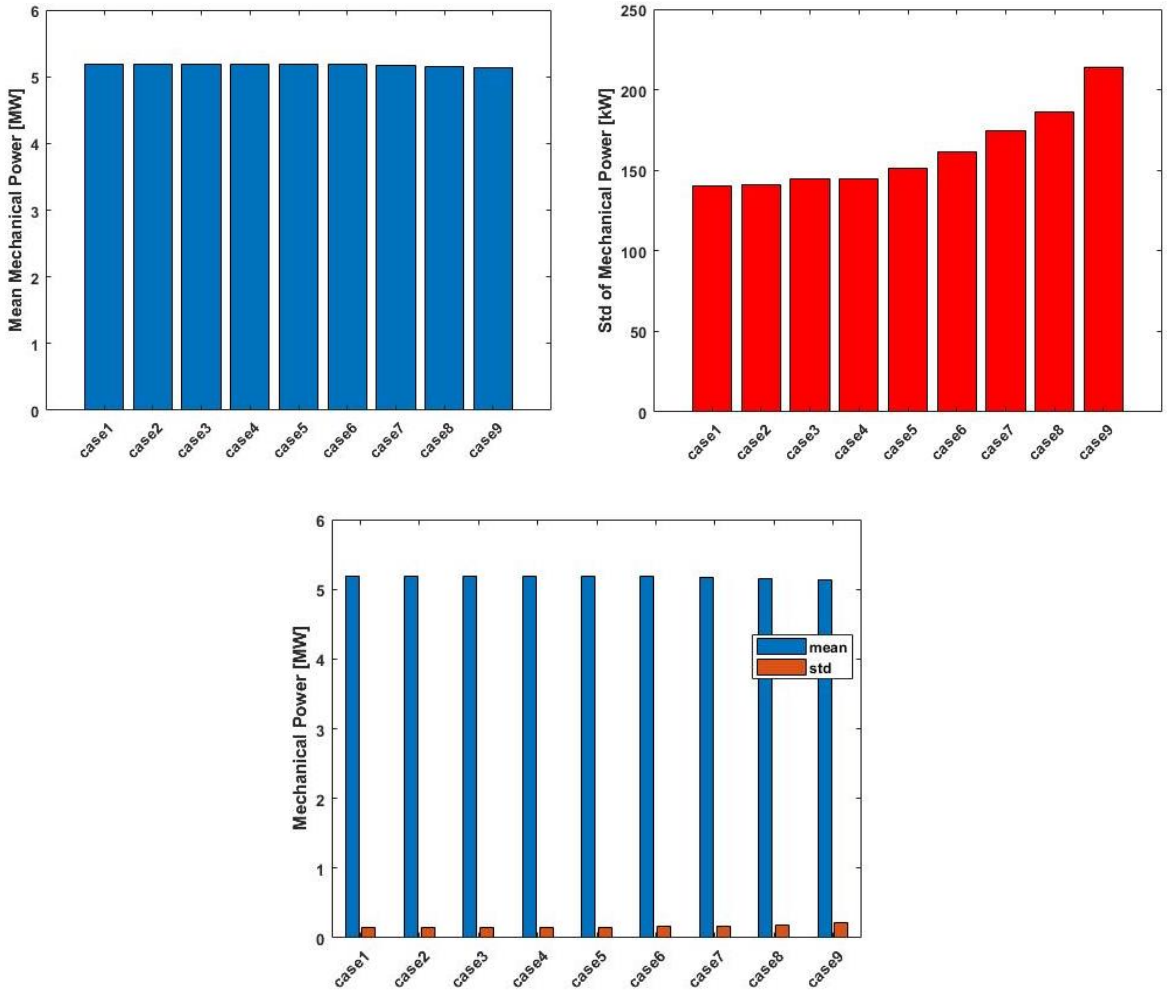

Figure 87. Mean and standard deviation of mechanical power for different $\mathbf{H_s}$ and $\mathbf{T_p}$ in above-rated wind speed.

Figure 88 shows that the mean platform pitch is quite constant over various wave characteristics, for instance maximum and minimum of mean platform pitch are 2.765 degrees for case5 and 2.736 degrees for case9 respectively. The standard deviation of platform pitch changes widely from 0.5735 degree for case1 to 1.107 degree for case9.

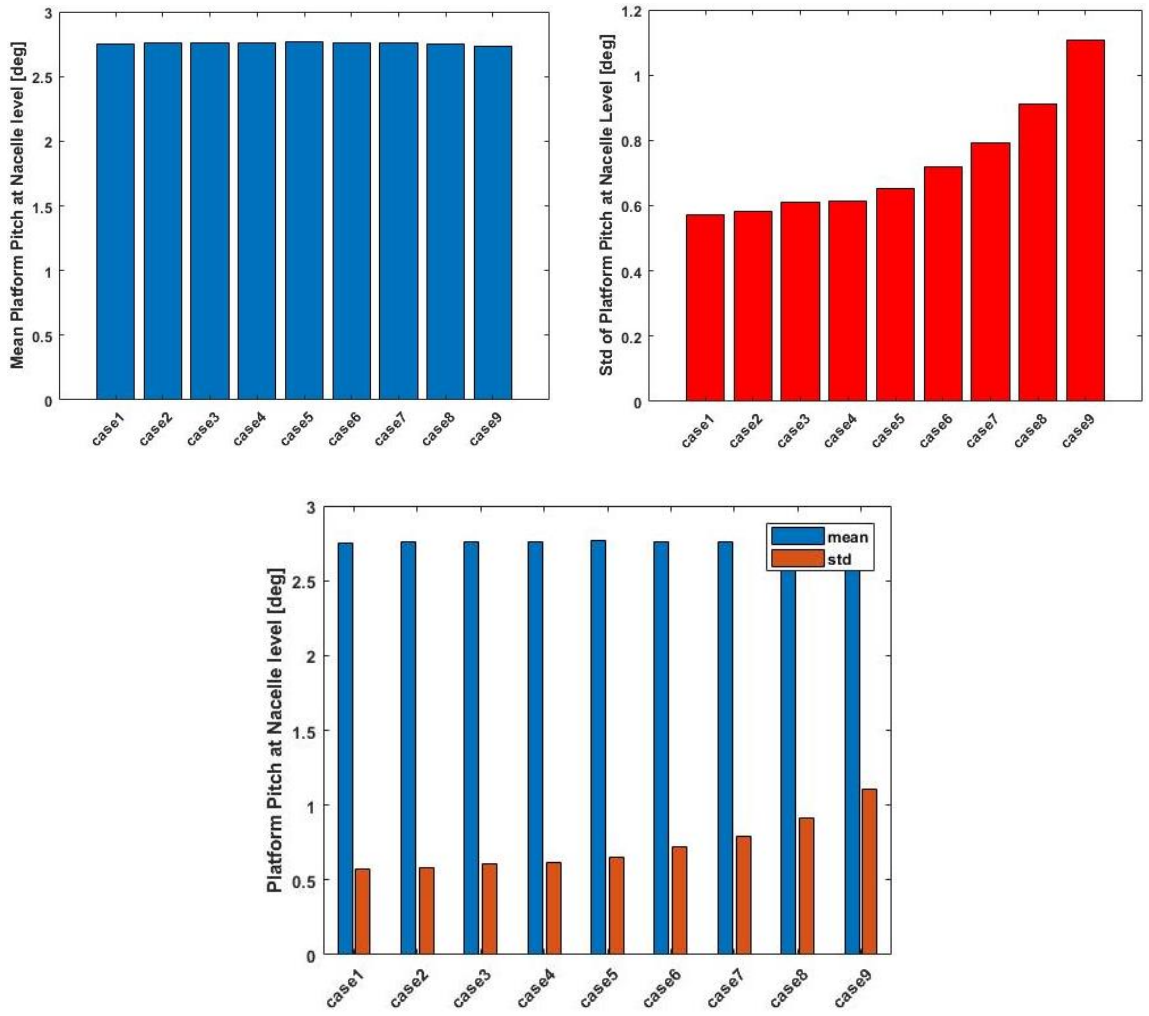

Figure 88. Mean and standard deviation of platform pitch for different $\mathbf{H_s}$ and $\mathbf{T_p}$ in above-rated wind speed.

The variation of mean tip out-of-plane deflection of one blade is narrower than two other studied responses, illustrated in Figure 89. The maximum standard deviation is 136.4 cm for case9 and the minimum standard deviation is 107.3 cm for case1. The mean values go up and down slightly. The mean value is 1.403 m for case1, falls to 1.391 m for case3, increases to 1.431 m for case4, again decreases to 1.331 m for case8 and finally rises to 1.339 m for case9. Moreover, it can be seen from Figure 89 that the standard deviation is higher than the mean value in case9, 1.364 m and 1.339 m respectively.

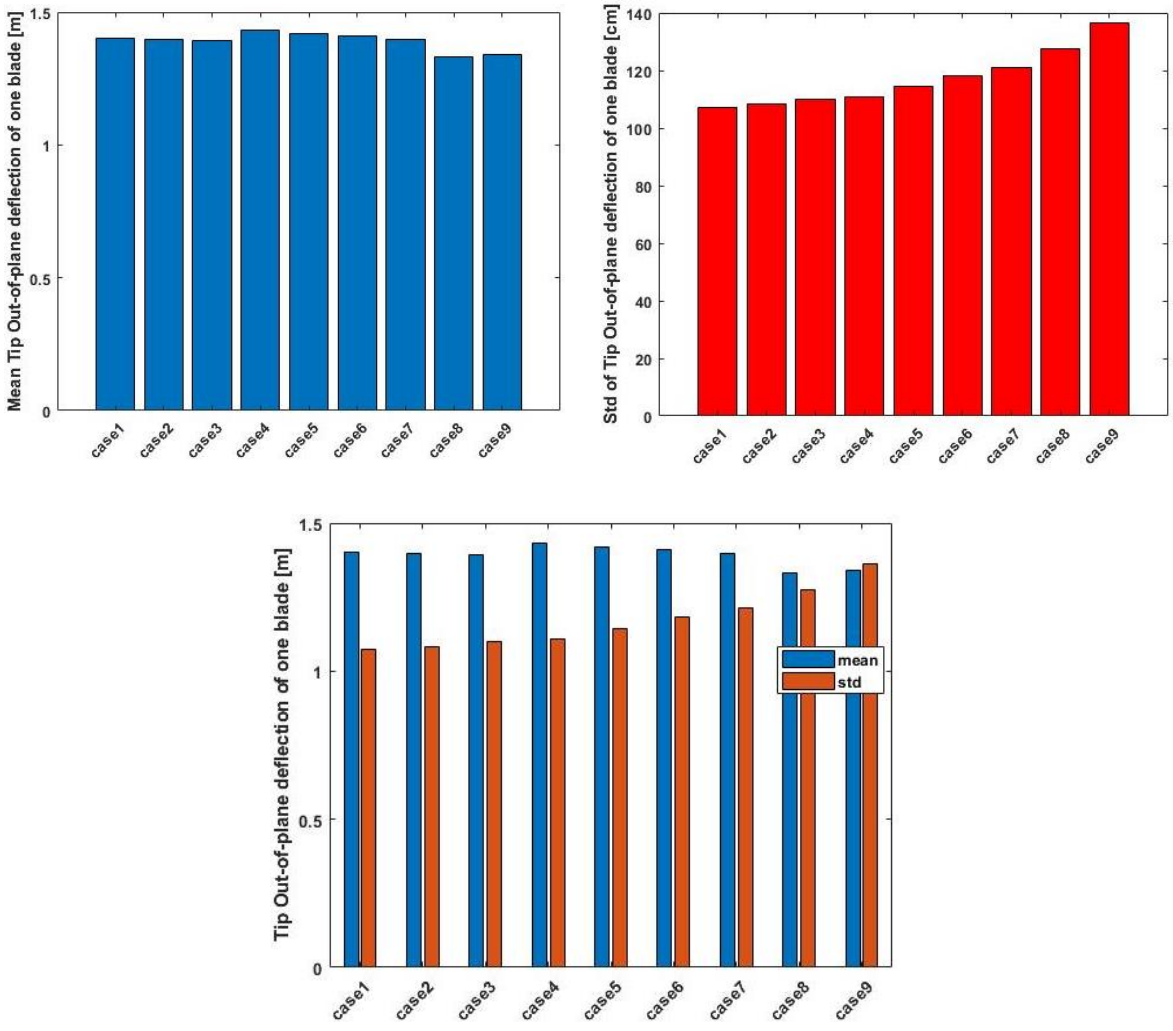

Figure 89. Mean and standard deviation of tip out-of-plane deflection of one blade for different $\mathbf{H_s}$ and $\mathbf{T_p}$ in above-rated wind speed.

2.2.2.2 Variation of turbulence intensity

The mean mechanical power reduces only 87 kW when turbulence intensity increases from 5% to 15%, illustrated in Figure 90. The mean value is 5.241 MW for TI=5%, 5.190 MW for TI=11% and 5.154 MW for TI=15%. The standard deviation of mechanical power however rises significantly by increasing turbulence intensity. The standard deviation is 74.63 kW for TI=5%, 144.4 kW for TI=11% and 195.8 kW for TI=15%.

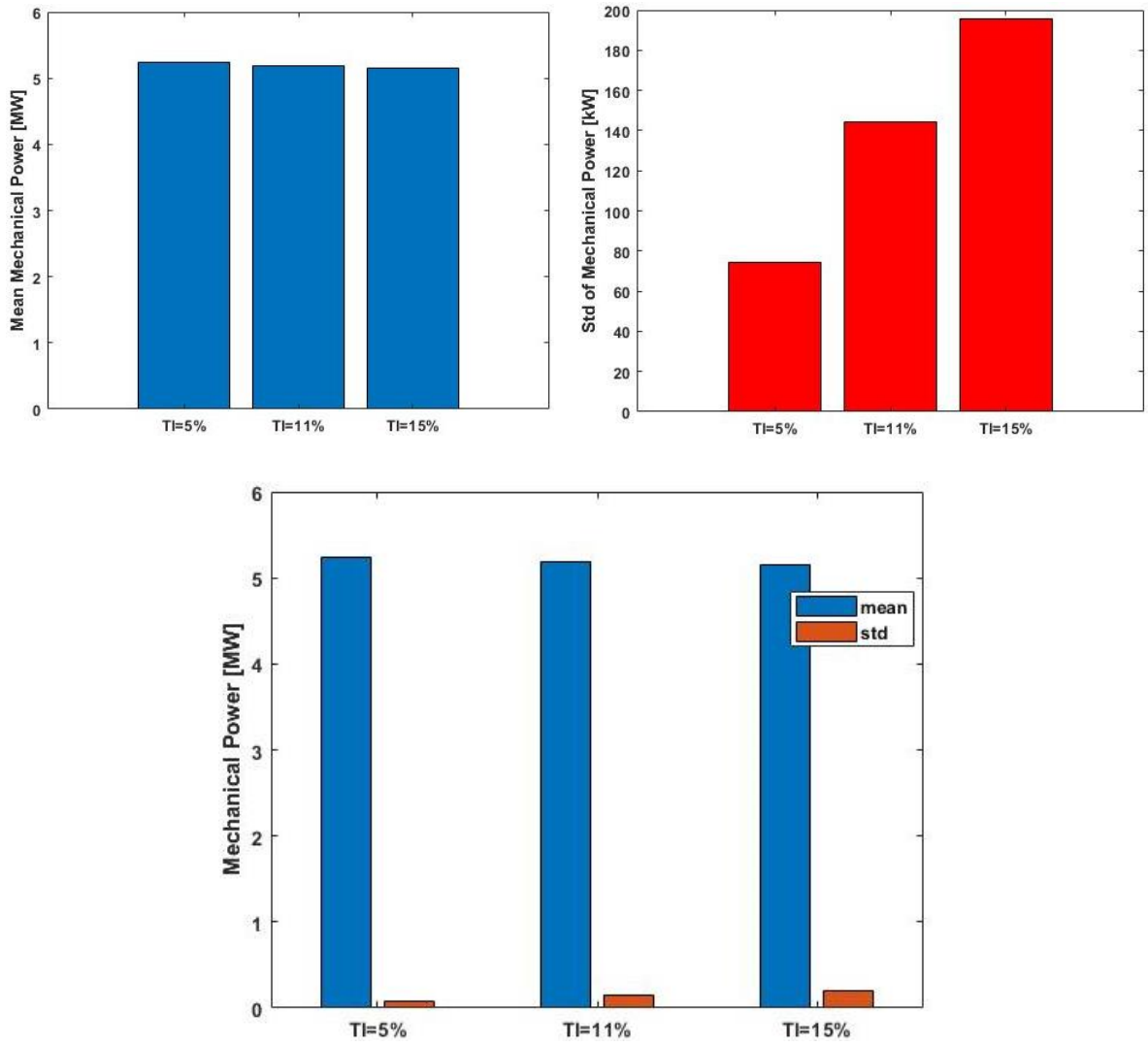

Figure 90. Mean and standard deviation of mechanical power for three turbulence intensities in above-rated wind speed.

Figure 91 illustrates that the standard deviation of platform pitch changes widely from 0.3396 degree for TI=5% to 0.6109 degree for TI=5% and 0.8310 degree for TI=15%. The mean value drops about 0.1 degree when turbulence intensity grows 10%. The value is 2.810 degree for TI=5%, 2.759 degrees for TI=11% and 2.706 degrees for TI=15%.

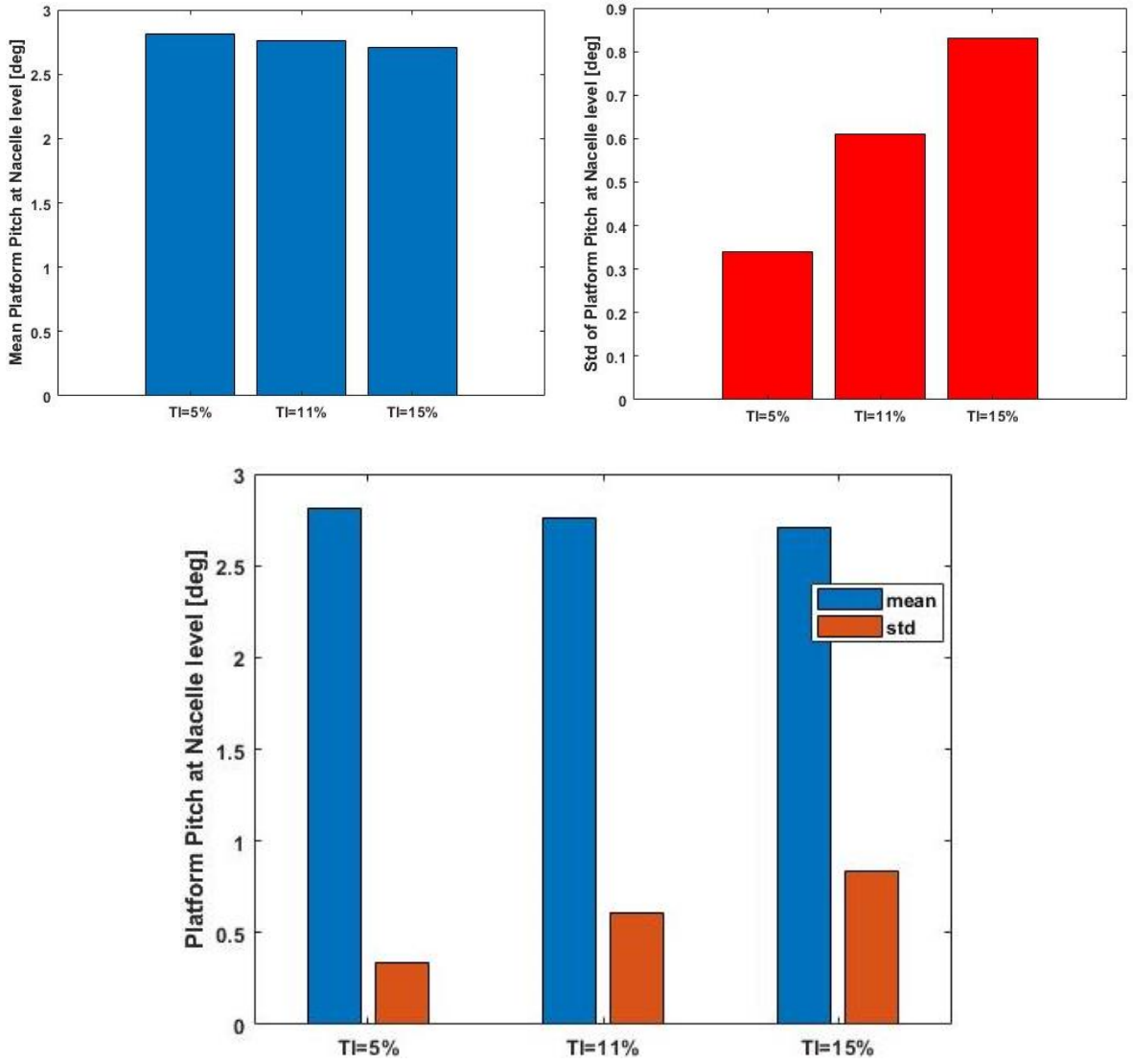

Figure 91. Mean and standard deviation of platform pitch for three turbulence intensities in above-rated wind speed.

Figure 92 shows the same pattern as previous responses by increasing turbulence intensity, i.e. the mean tip out-of-plane deflection of one blade decreases slightly, and the standard deviation increases widely. The mean value and standard deviation of tip out-of-plane deflection of one blade are 1.452 m and 77.02 cm, 1.391 m and 110.2 cm, 1.361 m and 137.9 cm for turbulence intensity of 5%, 11% and 15% respectively.

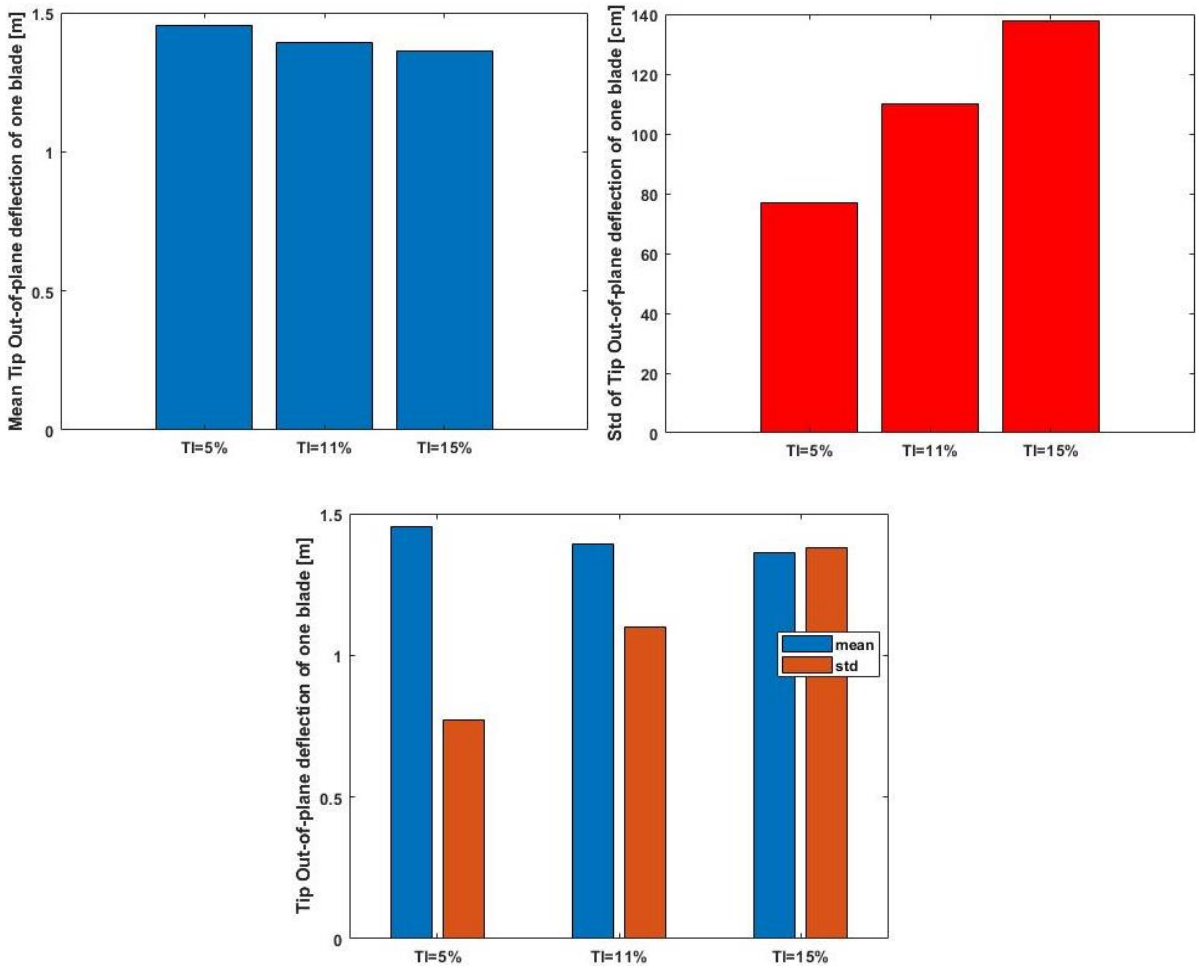

Figure 92. Mean and standard deviation of tip out-of-plane deflection of one blade for three turbulence intensities in above-rated wind speed.

2.2.2.3 Variation of alpha in wind shear profile power law

Variation of alpha in wind shear profile power low influenced standard deviation of tip out-of-plane deflection of one blade, i.e. the standard deviation rose by increasing alpha. However, the effect of variation of alpha was rarely observed in other mean and standard deviation of responses.

The mean and standard deviation of mechanical power remain almost unchanged by variation of alpha, presented in Figure 93. The mean value is 5.191 MW when alpha is 0, 0.05 and 0.1, and decreases to 5.190 MW when alpha is 0.12 and 0.14. The standard deviation is 142.9 kW for α=0, 143.7 kW for α=0.05, 144.2 kW for α=0.1, 144.4 kW for α=0.12 and 144.6 kW for α=0.14.

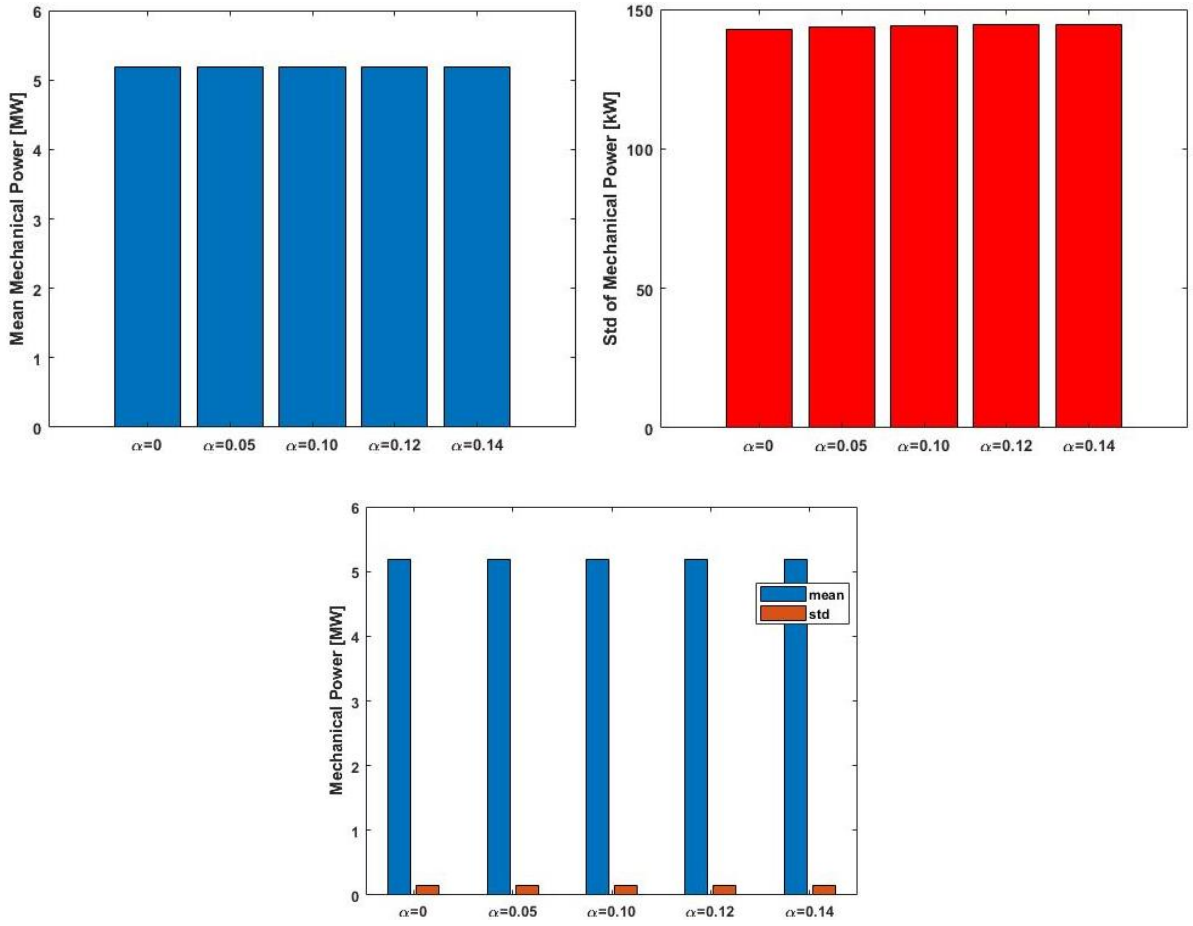

Figure 93. Mean and standard deviation of mechanical power for five alphas in wind shear power law in above-rated wind speed.

Variation of alpha has more effect on mean platform pitch than the standard deviation of the response, shown in Figure 94. The minimum and maximum mean value are 2.633 degrees when α=0 and 2.774 degrees when α=0.14 respectively. The standard deviation is almost constant, 0.6 degree, with minimum of 0.6036 degree when α=0 and maximum of 0.6117 degree when α=0.14.

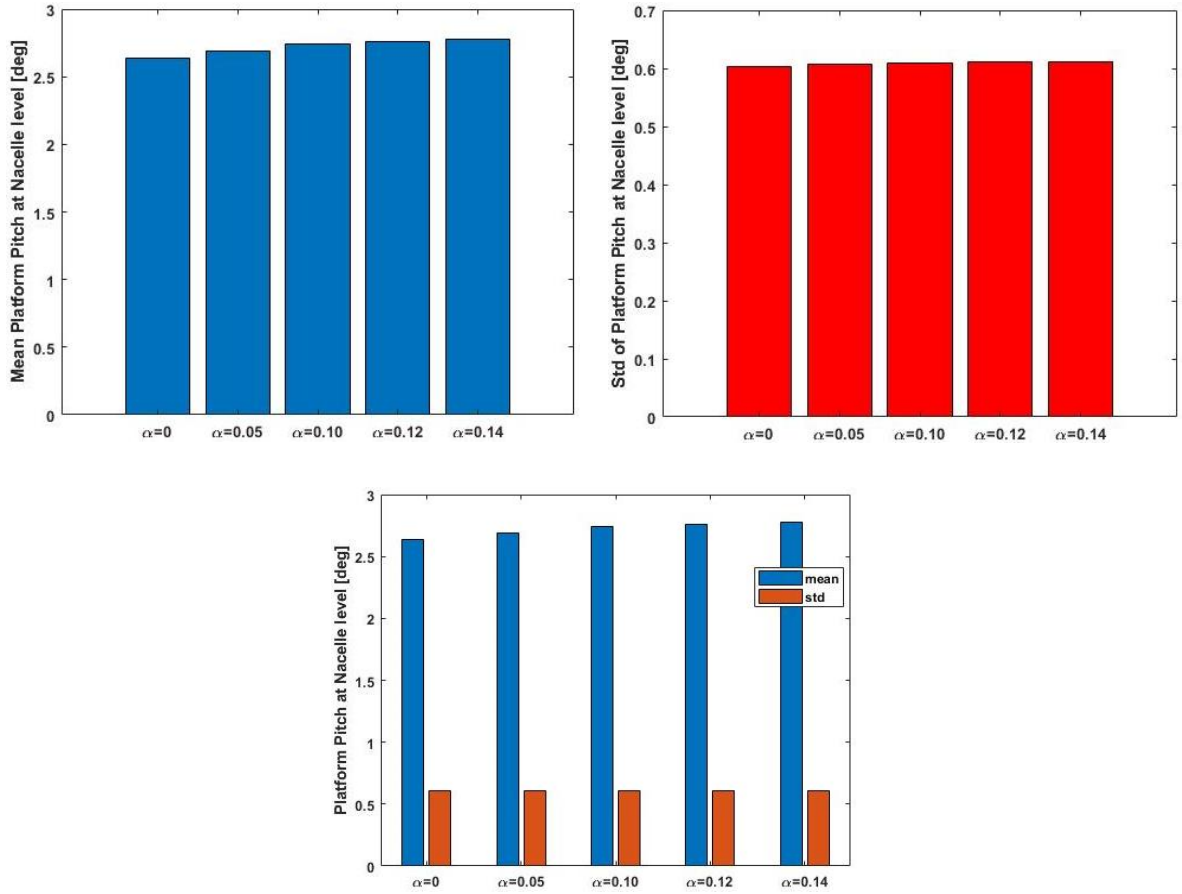

Figure 94. Mean and standard deviation of platform pitch for five alphas in wind shear power law in above-rated wind speed.

By variation of alpha, the difference between maximum and minimum of the mean tip out-of-plane deflection of one blade is 2.1 cm while the difference between maximum and minimum of the standard deviation is 21 cm, illustrated in Figure 95. The mean value falls from 1.405 m when α=0 to 1.384 m when α=0.14. However, the standard deviation grows from 94.7 cm when α=0 to 115.7 cm when α=0.14.

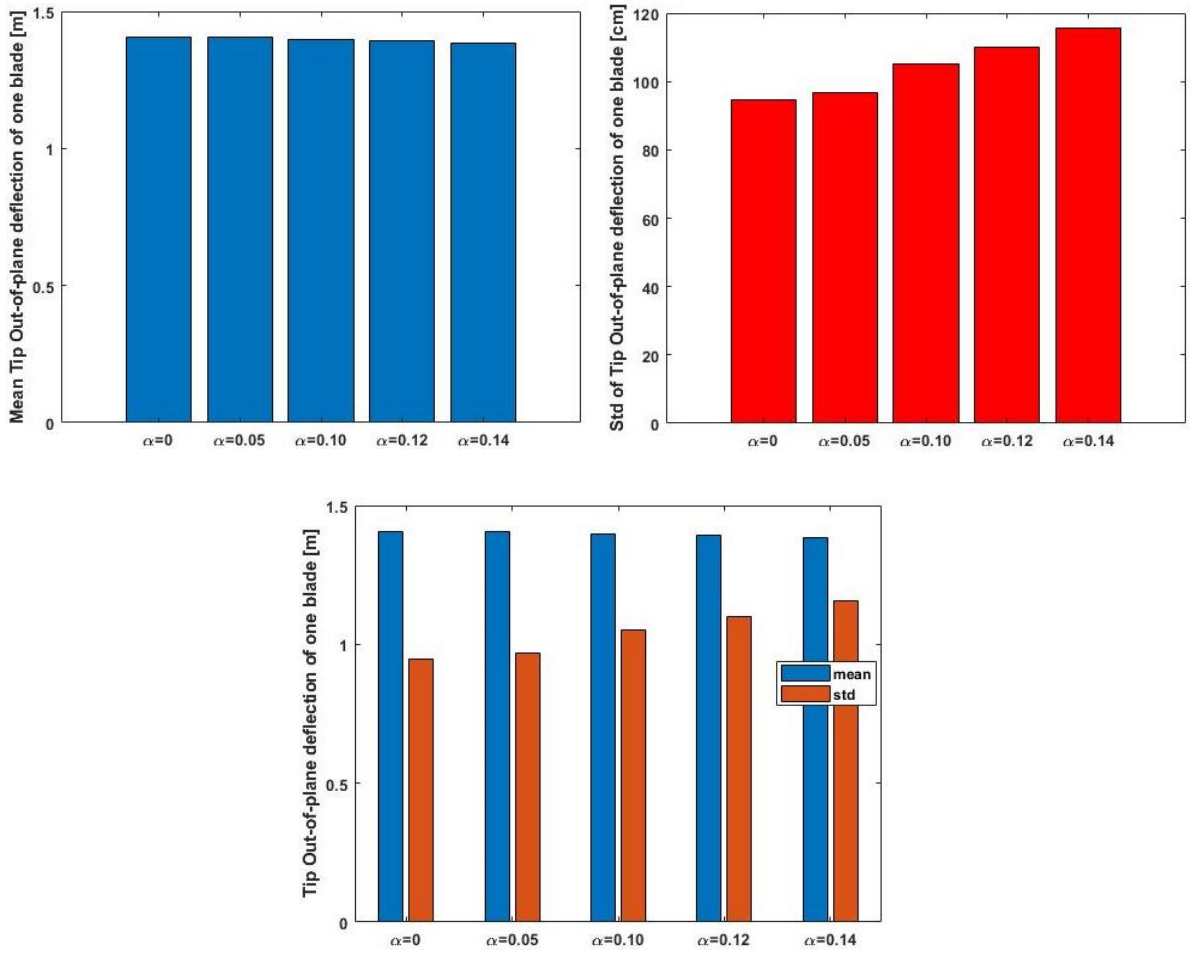

Figure 95. Mean and standard deviation of tip out-of-plane deflection of one blade for five alphas in wind shear power law in above-rated wind speed.

2.2.2.4 Variation of the spatial resolution of the numerical wind field

By variation of spatial resolution of the numerical wind field, the standard deviation of the studied responses showed fluctuations, although the mean values remained almost stable.

As can be seen from Figure 96, mean mechanical power shows almost constant value for different cases, 5.190 MW for case1 and case4, 5.188 MW for case2 and 5.187 MW for case3. The standard deviation shows more variation over different cases, goes up from 144.4 kW for case1 to 162.4 kW for case2 and goes down to 160.7 for case3 and 143.8 kW for case4.

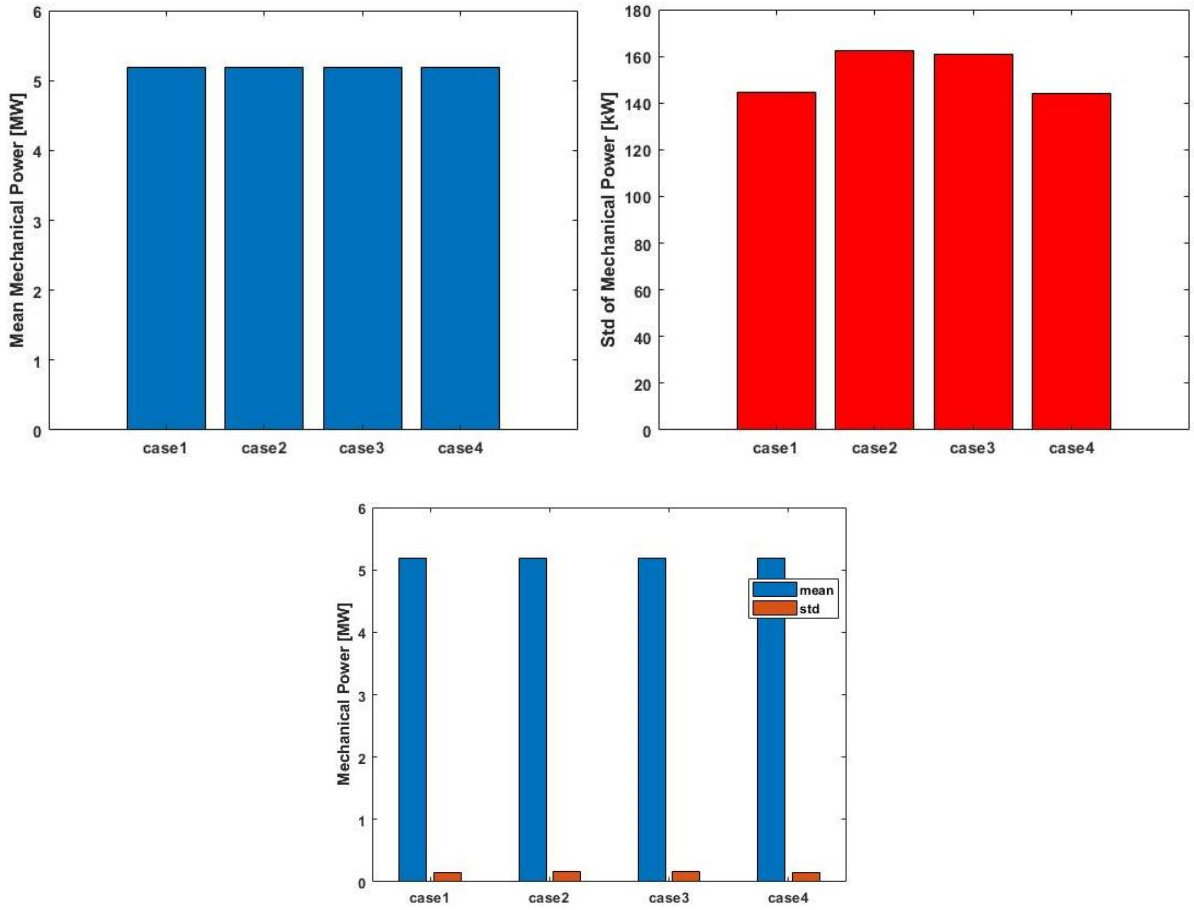

Figure 96. Mean and standard deviation of mechanical power for four spatial resolutions in above-rated wind speed.

Figure 97 indicates the mean platform pitch is almost 2.7 degrees over different cases, with 2.759 degree for case1 as maximum value and 2.712 degrees for case2 as minimum value. The

standard deviation fluctuates more and changes from 0.5673 degree for case3 as maximum value to 0.6248 degree for case4 as minimum value.

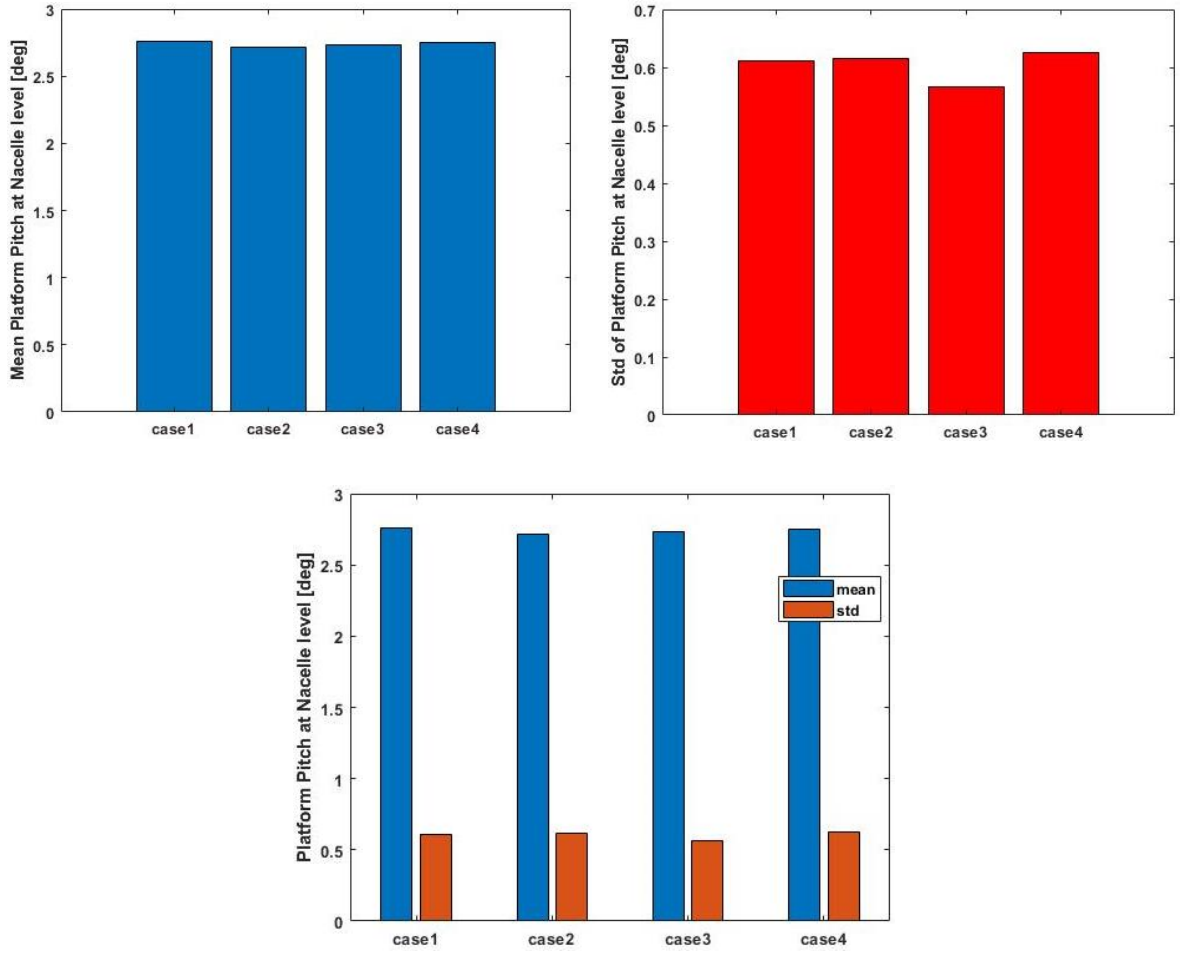

Figure 97. Mean and standard deviation of platform pitch for four spatial resolutions in above-rated wind speed.

As is illustrated by Figure 98, mean tip out-of-plane deflection of one blade is in its maximum, 1.391 m, for case1 while the minimum value, 1.293 m, occurs in case2. The mean value is 1.321 m and 1.315 m for case3 and case4 respectively. The results also show that the standard

deviation changes slightly over different cases. The standard deviation is 110.2 cm for csae1, 111 cm for case2, 107.7 cm for case3 and 107.5 cm for case4.

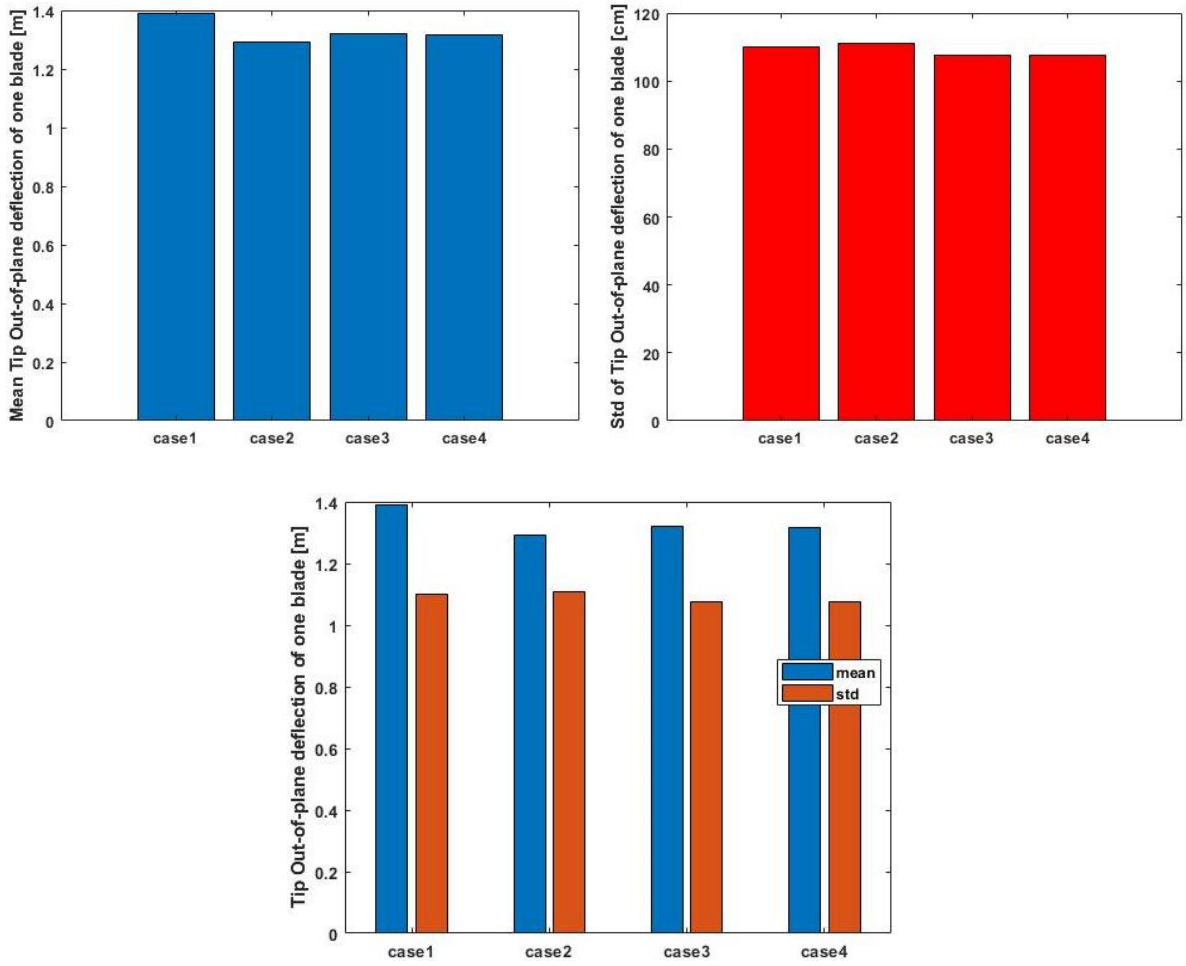

Figure 98. Mean and standard deviation of tip out-of-plane deflection of one blade for four spatial resolutions in above-rated wind speed.